Mechanisms of Fast Axonal Transport Impairment by the HIV Glycoprotein gp120

BY

SARAH BERTH
B.A. Northwestern University, 2004

THESIS

Submitted as partial fulfillment of the requirements
for the degree of Doctor of Philosophy in Neuroscience
in the Graduate College of the
University of Illinois at Chicago, 2015

Chicago, Illinois

Defense Committee:

Mark Rasenick, Chair
Scott Brady, Advisor
Larry Tobacman
Gerardo Morfini
Tom Hope, Northwestern University

Contribution of Authors

Chapter I is an introduction, my hypothesis, and specific aims for my thesis. Chapter II is a literature review that places my dissertation question in the context of the larger field and highlights the significance of my research question. Chapter III represents the materials and methods for my dissertation, and Chapter IV includes the results. Parts of a published manuscript encompassing Specific Aim 1 (Berth, S., Morfini, G., Sarma T., Caicedo, H., Brady, S.T. (2015) Internalization and Axonal Transport of the HIV Glycoprotein gp120. *ASN Neuro* 7(1): pii: 1759091414568186) of which I was the primary author and major driver of the research are included in Chapter II-V (see Figures 1-9). My research mentors Dr. Scott Brady and Dr. Gerardo Morfini contributed to the writing of the manuscript. Dr. Tulika Sarma aided with training on confocal microscopy and development of microfluidic devices. Dr. Hugo Caicedo designed and fabricated the microfluidic devices. I anticipate publishing a second paper using data from my Specific Aim 2 (Figures 10-15), which are unpublished data. For these experiments, Ms. Hajwa Kim assisted with statistical analysis, and Dr. Yuka Atagi assisted with the microtubule binding assay. Chapter V and VI represent my synthesis of the research presented in this thesis/dissertation and my overarching conclusions. The future directions of this field and this research question are discussed.

TABLE OF CONTENTS

TABLE OF CONTENTS (continued)

TABLE OF CONTENTS (continued)

LIST OF TABLES

LIST OF FIGURES

LIST OF FIGURES (continued)

LIST OF ABBREVIATIONS

069A	MW01-2-069A-SRM
AD	Alzheimer's Disease
AIDS	Acquired Immunodeficiency Syndrome
ALS	Amyotrophic Lateral Sclerosis
AMP-PNP	Adenylyl imidodiphosphate
ANI	Asymptomatic Neurocognitive Impairment
ANOVA	Analysis of Variance
APP	Amyloid Precursor Protein
ATC	Axonal Terminal Compartment
ATN	Acute Toxic Neuropathy
ATP	Adenosine Triphosphate
BBB	Blood Brain Barrier
cART	Combination Anti-retroviral Treatment
CD	Methyl-β-cyclodextrin
CDK-5	Cyclin-Dependent Kinase 5
CDyn	Cytoplasmic Dynein
CK1	Casein Kinase 1
CK2	Casein Kinase 2
CMT	Charcot-Marie-Tooth disease
CNS	Central Nervous System
CTxB	Cholera Toxin B
ddI	Didanosine
DHC	Dynein Heavy Chain
DIC	Dynein Intermediate Chain
DLC	Dynein Light Chain
DM	Diabetes Mellitus
DSP	Distal Sensory Polyneuropathy
DRG	Dorsal Root Ganglion
EEA1	Early Endosome Antigen 1
FAT	Fast Axonal Transport
FIV	Feline Immunodeficiency Virus
GFAP	Glial Fibrillary Acidic Protein
GPCR	G-Protein Coupled Receptor
GSK-3β	Glycogen Synthase Kinase 3- β
HAD	Human Immunodeficiency Virus Associated Dementia
HAND	Human Immunodeficiency Virus Associated Neurocognitive Disorders
h.i.	Heat Inactivated
HIV	Human Immunodeficiency Virus
HSD	Honest Significance Test
HSP	Hereditary Spastic Paraplegia
HSPG	Heparan Sulfate Proteoglycans

LIST OF ABBREVIATIONS (continued)

IFN-γ	Interferon-γ
IgG	Immunoglobulin G
IL	Interleukin
Iκ B	Inhibitor of Kappa B
IKK	Inhibitor of Kappa B Kinase
JNK	c-Jun N-terminal Kinase
KHC	Kinesin Heavy Chain
KLC	Kinesin Light Chain
LAMP2	Lysosome-Associated Membrane Protein-2
LC	Light Chain
LIC	Light Intermediate Chain
LRP	Lipoprotein Related Protein
LTP	Long Term Potentiation
MAP2	Microtubule-Associated Protein-2
MAP2K	Mitogen Activated Protein Kinase Kinase
MAP3K	Mitogen Activated Protein Kinase Kinase Kinase
MLK	Mixed Lineage Kinase
MND	Mild Neurocognitive Disorder
MBO	Membrane Bounded Organelle
MPP+	1-Methyl-4-Phenylpryidinium
NEMO	NF-κB Essential Modulator
NF-κB	Nuclear Factor k-light chain-enhancer of activated B cells
NGF	Nerve Growth Factor
NMDA	*N*-methyl-D-aspartate
NMDAR	*N*-methyl-D-aspartate Receptor
NRTI	Nucleoside Reverse Transcriptase Inhibitor
OA	Okadaic Acid
p38 MAPK	p38 Mitogen Activated Protein Kinase
PD	Parkinson's Disease
PDMS	Polydimethylsiloxane
PKC	Protein Kinase C
PKR	RNA-Activated Protein Kinase
PNS	Peripheral Nervous System
PP1	Protein Phosphatase 1
PrP	Prion Protein
PS1	Presenilin 1
RANTES	Regulated and Normal T cell Expressed and Secreted
rhNGF	recombinant human Nerve Growth Factor
SAPK	Stress-Activated Protein Kinases
SDC	Somatodendritic Compartment

LIST OF ABBREVIATIONS (continued)

SIV	Simian Immunodeficiency Virus
SSRI	Selective Serotonin Reuptake Inhibitor
SOD1	Superoxide dismutase 1
TAK-1	Transforming Growth Factor-β-Activated Kinase -1
TNF-α	Tumor Necrosis Factor-α
TUNEL	Terminal deoxynucleotidyl transferase-mediated dUTP Nick-End Labeling
Trk	Tropomyosin Receptor Kinase
VEC-DIC	Video Enhanced Contrast-Differential Interference Contrast

SUMMARY

Over 1 million people in the United States are infected by Human Immunodeficiency Virus (HIV; CDC, 2012), a virus that attacks the immune system with devastating consequences. The development of combination anti-retroviral therapy (cART) has changed the prognosis of HIV from a death sentence to a chronic illness that must be managed. However, HIV patients still suffer from a wealth of complications. Despite tight control of viral load by cART, close to 30% of HIV patients develop distal sensory neuropathy (DSP), a neuropathy that is marked by excruciating pain. The mechanism for the development of DSP is still little understood, and there is a lack of effective treatments.

DSP is a dying-back neuropathy that primarily targets unmyelinated axons of dorsal root ganglion (DRG) neurons, with axonal degeneration that proceeds distally to proximally. Another characteristic of DSP is its progressive nature, with a gradual, late onset. These features of DSP are characteristic features of dying-back neuropathies caused by impaired fast axonal transport (FAT). Neurons, especially those with long axons such as sensory and motor neurons in the peripheral nervous system (PNS), are highly dependent on FAT to transport proteins that are synthesized in cell bodies to their needed locations in the axons. Inhibition of FAT through aberrant phosphoregulation has been linked to a number of progressive dying-back neuropathies, suggesting an underlying mechanism for a class of these neuropathies, termed “dysferopathies”

(Morfini et al., 2007; Morfini et al., 2009).

Might DSP be a dysferopathy as well? The experiments in this dissertation were undertaken to address this question. Although the mechanism for DSP remains little understood, the HIV glycoprotein gp120, which is overproduced and shed, is neurotoxic to DRG neurons (Li et al., 2005; Mocchetti et al., 2012). Experiments were designed to evaluate whether the mechanism of gp120's neurotoxicity might involve FAT.

First, we examined whether F11 cells, rat DRG neurons hybridized with mouse neuroblastoma cells, internalized gp120. Gp120 was internalized in a time-dependent manner that was partially independent of gp120 binding to its coreceptor CXCR4. Immunocytochemical and pharmacological experiments indicated that gp120 is not internalized through the common endolysosomal pathway. Rather, results from experiments here indicate that gp120 was mainly internalized in a cholesterol-dependent manner through lipid rafts, with a minor fraction being internalized by fluid phase pinocytosis. Experiments using compartmentalized microfluidic chambers revealed that after internalization, gp120 is retrogradely transported from DRG axons to their cell bodies, but not in the opposite direction. These studies define mechanisms of gp120 internalization in the PNS and reveal that extracellular gp120 is retrogradely transported along DRG axons.

With these results, we examined whether intra-axonal gp120 might alter FAT regulation. Perfusing gp120 into squid axoplasm severely inhibited both anterograde and retrograde FAT. Two divergent gp120 strains were perfused and

exhibited similar impairments, demonstrating that this action of gp120 is conserved across strains. Co-perfusing gp120 with various kinase inhibitors mapped out the signaling pathways that gp120 activates to impair FAT. The results suggested that gp120 activated the mitogen activated protein kinase kinase kinase (MAP3K) Tak-1. This led to activation of the downstream targets: protein phosphatase 1 (PP1), Inhibitor Kappa Kinase (IKK)-2, p38 mitogen activated protein kinase (MAPK) and c-Jun N-terminal kinase (JNK). While it is known that p38 MAPK and JNK can directly phosphorylate kinesin to inhibit FAT (Morfini et al., 2006; Morfini, 2013 (submitted)), Tak-1-mediated activation of PP1 and IKK-2 represents a novel regulatory signaling pathway for FAT. Microtubule binding assays indicated that a mechanism for gp120-induced impairment of FAT might also involve release of cytoplasmic dynein (CDyn) from microtubules. These results define a novel mechanism for gp120-induced neurotoxicity through inhibition of FAT and explain the progressive, dying-back axonal degeneration in DSP.

CHAPTER 1

INTRODUCTION

The most common neurological complication of HIV infection is sensory neuropathy, with close to 30% of HIV patients developing sensory neuropathies during the course of their disease (Ellis et al., 2010; Evans et al., 2011; Anziska et al., 2012; Ghosh et al., 2012). Of these, the most common form of sensory neuropathy is distal sensory neuropathy (DSP; Schifitto et al., 2005), which is directly attributed to HIV infection. DSP is characterized by progressive distal to proximal dying-back degeneration of unmyelinated axons from dorsal root ganglion (DRG) neurons, causing debilitating pain (Keswani et al., 2002). Patients suffer from a lack of treatment options (Phillips et al., 2010), and the mechanism for DSP remains uncertain. However, a significant body of research has documented the neurotoxicity of the HIV glycoprotein gp120 (Brenneman et al., 1988; Toggas et al., 1994; Lannuzel et al., 1995; Meucci and Miller, 1996; Hesselgesser et al., 1998; Meucci et al., 1998; Singh et al., 2005; Kaul et al., 2007; Bachis et al., 2009), which is overproduced and shed (Schneider et al., 1986). These observations suggest that gp120 might play a direct role in causing DSP.

DRG neurons are highly polarized with long axons, making them critically dependent on fast axonal transport (FAT) of proteins synthesized in the cell body for axonal maintenance and health. In fact, the dying-back axonal degeneration seen in DSP is the same pattern of degeneration seen in "dysferopathies," dying-back neuropathies that are linked by the common mechanism of dysregulation of

phosphotransferase signaling pathways that control FAT (Morfini et al., 2009).

The experiments in this dissertation are designed to address whether a direct mechanism of gp120 neurotoxicity gp120 might be through intra-axonal gp120 interfering with signaling pathways that regulate FAT. *I propose that gp120 is internalized by DRG neurons, leading to impairment of FAT through abnormal activation of intra-axonal kinases and phosphatases.* This will be addressed using the following specific aims:

Aim 1: To evaluate the mechanisms of internalization and intracellular location of gp120.

Previous studies of gp120 neurotoxicity has focused on the extracellular binding of gp120 to neurons to cause pathology; however, another possibility is that intraneuronal gp120 can be toxic. *I propose that gp120 is internalized by DRG neurons and released into the axoplasm.* The experiments in this aim determine the mechanism of gp120 internalization and characterize its intracellular actions. Mechanisms of gp120 internalization were evaluated by immunofluorescence studies that quantitated and examined the specificity of gp120 internalization. Additionally, the endocytic pathway through which gp120 was internalized was defined through colocalization studies. Further, compartmentalized microfluidic chambers were used to identify the location of gp120 internalization into DRG neurons, and to examine axonal trafficking of gp120. *I found that gp120 internalization was specific and partially dependent on binding to its co-receptor CXCR4. Also, gp120 was internalized through lipid rafts, with a minor fraction internalized through fluid phase pinocytosis.*

Additionally, gp120 was internalized in the axon and transported to cell body. Understanding the mechanisms of intracellular actions of gp120 will provide a basis for future development of treatment targets.

Aim 2: To identify intra-axonal signaling pathways underlying gp120-induced alterations in FAT.

The remarkable polarity, length and architecture of DRG neurons result in a critical dependence on the precise regulation of FAT. It is established that FAT is controlled through the activities of various kinases and phosphatases in the axon; dysregulation of FAT leads to axonal degeneration in a dying-back pattern (Morfini et al., 2009). *I propose that gp120 alters signaling cascades for regulation of FAT, leading to inhibition of FAT and axonal degeneration.* Preliminary evidence demonstrated a profound impairment of FAT by gp120. The upstream signaling cascades induced by gp120 to impair FAT were identified and their downstream effects on FAT were studied using both squid axoplasm motility assays and biochemistry assays. Microtubule binding of kinesin and dynein in response to gp120 treatment was assessed. *We found that gp120 affects a signaling pathway that activates the kinase transforming growth factor-β-activated kinase-1 (Tak-1), leading to downstream activation of c-Jun N-terminal Kinase (JNK) and p38 Mitogen Activated Protein Kinase (p38) as well as protein phosphatase 1 (PP1) and Inhibitor of Kappa B Kinase (IKK). Each of these downstream kinases can affect FAT either directly or indirectly.* These studies characterize mechanisms through which gp120 affects intra-axonal signaling pathways and disturbs the precise enzymatic regulation of FAT.

CHAPTER II

LITERATURE REVIEW

Berth, S., Morfini, G., Sarma T., Caicedo, H., Brady, S.T. (2015) Internalization and Axonal Transport of the HIV Glycoprotein gp120. ASN Neuro 7(1): pii: 1759091414568186

1. Human Immunodeficiency Virus

1.1 Human Immunodeficiency Virus Overview

The human immunodeficiency virus (HIV) is a lentivirus that causes compromised immune systems and opportunistic infections. Untreated, HIV infection eventually leads to Acquired Immune Deficiency Syndrome (AIDS), which is characterized by severe damage to the immune system. HIV infection is a global epidemic, with over 34 million people infected by HIV (WHO/UNAIDS/UNICEF, 2011). In the United States alone, over 1 million inhabitants have HIV infections (CDC, 2012). Despite significant progress in managing the disease, HIV remains incurable and a major public health challenge.

AIDS was first recognized in the United States in 1981 (Greene, 2007). In 1983 and 1984, it was discovered that AIDS is caused by infection by the human immunodeficiency virus (HIV) (Barre-Sinoussi et al., 1983; Gallo et al., 1983; Gallo et al., 1984; Popovic et al., 1984; Schupbach et al., 1984), a retrovirus that is a member of the lentivirus family. HIV is primarily transmitted through sexual contact, but can also be transmitted perinatally and through blood products. HIV directly infects cells of the immune system, including CD4+ T cells, macrophages and dendritic cells, ultimately leading to death of the CD4+ T cells. When the CD4+ count gets below 200/μL, the HIV infection has progressed to AIDS.

HIV is a single-stranded, positive sense, enveloped RNA virus. To infect cells, the envelope glycoprotein gp120 binds to CD4 (Kwong et al., 1998). This triggers a conformational change in gp120 that induces the binding of gp120 to its co-receptors CXCR4 or CCR5 (Kwong et al., 1998) allowing entry of HIV into the cell. Although HIV internalization is generally thought to occur through direct fusion with the plasma membrane (Stein et al., 1987; Blumenthal et al., 2012), recently it was demonstrated with time-resolved imaging of single HIV molecules that HIV undergoes endocytosis and then fuses with endosomes to enter cells (Miyauchi et al., 2009). In fact, other studies have found that HIV undergoes clathrin-mediated endocytosis (Daecke et al., 2005; Bosch et al., 2008) or enters cells through lipid rafts and fluid phase pinocytosis (Liu et al., 2002). Although this remains controversial, it is likely that HIV can use multiple mechanisms to enter cells. Once inside the cell, HIV reverse transcribes its RNA into double-stranding DNA and then the DNA is imported into the cell nucleus where it is integrated into the host genome (Greene and Peterlin, 2002). Once integrated, HIV can either be latent or be transcribed to produce new virus particles (Greene and Peterlin, 2002).

In 1996, combination antiretroviral therapy (cART) for HIV was introduced, transforming HIV from a lethal infection into a chronic disease. Although cART can drastically reduce the amount of HIV in the plasma to undetectable levels, it cannot eradicate HIV (Blankson et al., 2002). This is due to the fact that latently infected cells maintain reservoirs of HIV in lymphoid organs, the CNS and the genitourinary tract (Blankson et al., 2002). Despite the development of successful strategies for managing HIV infections, some HIV-

related pathologies persist and generate quality of life issues for patients.

1.2 Animal Models of Human Immunodeficiency Virus

HIV infection is specific to humans and some primates, which poses a challenge to study in the laboratory. Although chimpanzees can be infected with HIV, they rarely progress to AIDS, making them useful mainly for vaccine studies (Nath et al., 2000). However, several animal models have been used to overcome this specificity. For example, some non-human primates and cats are susceptible to Simian Immunodeficiency Virus (SIV) and Feline Immunodeficiency Virus (FIV), respectively. Both SIV and FIV are lentiviruses that are similar to the HIV virus; they also cause AIDS-like disease and replicate neuropathological changes seen in AIDS (Maung et al., 2012). Chimeric SIV-HIV viruses have also been created in an attempt to develop an even better primate model (Ambrose et al., 2007). However, primate models are not always feasible for studying cell and molecular mechanisms of HIV-related pathologies due to expense and ethical concerns.

Although rodents are not susceptible to HIV or HIV-like viruses, they can be manipulated to model HIV. For example, several transgenic mouse lines and even a transgenic rat line have been created that express the HIV full genome or certain HIV proteins that model aspects of HIV or AIDS (Toggas et al., 1994; Hanna et al., 1998; Michaud et al., 2001; Reid et al., 2001). Other tools to examine HIV in mice include chimera mutants in which gp120 was replaced with gp80 from the murine leukemia virus to induce infection (Potash et al., 2005), in addition to mouse strains reconstituted with human hematopoetic systems to

allow HIV infection (Van Duyne et al., 2009; Dash et al., 2011). Alternatively, injection, perfusion or expression of a single HIV protein may also be useful to determine the individual contributions of each protein to disease (Maung et al., 2012).

1.3 Human Immunodeficiency Virus Interactions with the Nervous System

Although HIV does not productively infect neurons, it has interactions with both the central nervous system (CNS) and peripheral nervous system (PNS). To enter the central nervous system, HIV uses a mechanism termed "Trojan Horse" to cross the blood brain barrier (BBB; Peluso et al., 1985; Haase, 1986). HIV-infected leukocytes can enter the brain through the bloodstream. Since the virus persists inside the leukocytes, it evades recognition and can pass undetected across the BBB (Haase, 1986). Other pathways have been proposed such as cell-free virus entry into the brain as well as transmission by infected endothelial cells; however, these do not appear to be major pathways for entry of HIV into the CNS (Kramer-Hammerle et al., 2005). Neuroinvasion occurs early in HIV infection; HIV has been found within several areas of the brain after only 15 days of infection (Davis et al., 1992). The primary cells in the brain that are infected by HIV are of mesodermal lineage (i.e. perivascular macrophages and parenchymal microglia), with some evidence for restricted infection of astrocytes (Kramer-Hammerle et al., 2005). Productive infection of neurons and oligodendrocytes remains controversial (Kramer-Hammerle et al., 2005), but is

likely to be limited in scope.

In the PNS, HIV is found predominantly in infected macrophages and satellite cells that surround dorsal root ganglion neurons (Brannagan et al., 1997), although low levels of HIV have been detected within the DRG neurons of HIV patients with neuropathy (Brannagan et al., 1997) and AIDS patients (Nagano et al., 1996) (Yoshioka et al., 1994).

2. Neurological complications of Human Immunodeficiency Virus

HIV infection leads to a host of neurological complications. While cART has decreased some of these complications, others remain prevalent among HIV patients, including both CNS and PNS pathologies. In addition to loss of quality of life, neurological complications also increase the risk of mortality (Vivithanaporn et al., 2010), making these complications an important focus of study.

2.1 Neurological Complications in the Central Nervous System

With the introduction of cART, the incidence rate of a host of neurological complications such as toxoplasmosis, progressive multifocal leukoencephalopathy, cryptococcal meningitis and CNS lymphoma has drastically been reduced (Clifford, 2008). The incidence of HIV-associated dementia (HAD), a severe form of HIV-associated neurocognitive disorders (HAND), has also decreased dramatically since cART (McArthur, 2004). However, milder forms of HAND, including asymptomatic neurocognitive

impairment (ANI) and mild neurocognitive disorder (MND), continue to be common among HIV patients at a rate similar to that seen before cART (Clifford, 2008; Heaton et al., 2010). Neurological impairment was observed in at least 50% of HIV patients in the CHARTER study (Clifford, 2008). ANI is defined as inferior performance in at least two domains of neuropsychological testing, without impact on daily living (Antinori et al., 2007). In addition to poor performance in neuropsychological testing, MND patients also report cognitive decline that interferes to a minor degree with daily function (Antinori et al., 2007). MND patients may also have motor impairments (McArthur et al., 2005). HAD represents moderate to severe dementia, with marked impairment in daily living (Antinori et al., 2007). Although prior to development of cART the dementia in HAND was primarily subcortical, now patients are beginning to show more learning and memory deficits, suggesting a shift in the brain regions that are targeted in HAND (Kranick and Nath, 2012).

It is thought that the continued high prevalence of HAND may be due to inadequate CNS penetration by anti-retroviral drugs, so the main focus with treatment is to use anti-retroviral drugs that have improved access to the CNS (Kranick and Nath, 2012). There has been limited success with other adjunctive therapy (Tan and McArthur, 2012), although attention has begun to be turned to psychiatric medicine such as selective serotonin reuptake inhibitors (SSRI) and glycogen synthase kinase-3 β (GSK3-β) inhibitors (Ances et al., 2008). In addition, the drug regimen itself may have secondary effects that have yet to be recognized. Larger trials will be needed to determine if SSRI's and GSK3-β inhibitors are effective in HAND treatment (Ances et al., 2008).

2.2 Neurological Complications in the Peripheral Nervous System

Neuropathies have remained common in HIV patients despite cART. Although recent epidemiological studies report varying prevalence rates due to differences in diagnostic tests (Ghosh et al., 2012), the general consensus is that at least a third of HIV patients suffer from peripheral neuropathies (Ellis et al., 2010; Evans et al., 2011; Anziska et al., 2012). Rare types of neuropathies caused by HIV include inflammatory demyelinating polyneuropathies, mononeuritis multiple and opportunistic infection-associated neuropathies (Pardo et al., 2001).

In the PNS, the two major neurological complications of HIV are distal sensory polyneuropathy (DSP) and acute toxic neuropathy (ATN). These both cause excruciating pain on the soles of the feet, as well as parasthesias, gait instability and autonomic dysfunction (Pardo et al., 2001). DSP and ATN primarily affect small unmyelinated sensory fibers in a "dying back" pattern (Pardo et al., 2001; Keswani and Hoke, 2003).

Although they have clinically identical pathologies, ATN and DSP have distinct etiologies. ATN is a dose-dependent consequence of treatment with the HIV antiviral nucleoside reverse transcriptase inhibitors (NRTIs) (Moyle, 2000). Discontinuation of NRTI treatment will gradually resolve the symptoms (Moyle, 2000). DSP, on the other hand, is attributed directly to HIV infection. Prior to cART, DSP was associated with immune suppression, and viral load was correlated with symptom severity (Simpson et al., 2002). However, since cART was introduced this association has become diminished (Kranick and Nath, 2012)

(Morgello et al., 2004). The prevalence of DSP is now primarily associated with age, as well as low CD4+ nadir, diabetes mellitus (DM), height, cART use and infections with hepatitis C (Ellis et al., 2010; Nakamoto et al., 2010; Evans et al., 2011; Anziska et al., 2012). Although the etiology of DSP may be complex, the impact of DSP on patients remains a major problem.

2.3. Distal Sensory Polyneuropathy Overview and Pathology

DSP is thought to be a slowly progressive complication, as evidence of subclinical damage is common among HIV patients (Keswani et al., 2002). For example, the recent CHARTER study found that out of the 57% of the HIV patients that had detectable clinical signs of sensory neuropathies, only 38% reported pain (Ellis et al., 2010). Virtually all AIDS patients show subclinical signs of nerve damage (Keswani et al., 2002).

DSP is marked by dying back neurodegeneration of DRG distal axons, with prominent involvement of small unmyelinated fibers (Keswani et al., 2002) that can eventually spread to larger sensory and motor fibers as the disease progresses (Dorsey and Morton, 2006). Patients have a decreased number of epidermal nerve fibers, especially in distal sites (Holland et al., 1997). DRG's are infiltrated by nodes of Nageotte, macrophages, lymphocytes, and inflammatory cytokines (Nagano et al., 1996).

Treatment options for DSP remain limited. A meta-analysis of randomly controlled trials revealed a lack of efficacy by traditional drugs used to treat neuropathic pain including gabapentin, amitriptyline, pregabalin, prosaptide, peptide-T, acetyl-L-carnitine, mexilitine, lamotrigine and topical capsaicin

(Phillips et al., 2010). The only treatments that were effective include high concentration capsaicin (8%), smoked cannabis and recombinant human nerve growth factor (rhNGF; Phillips et al., 2010). Since rhNGF is unavailable to patients and cannabis cannot be recommended for routine use, new treatments need to be developed (Phillips et al., 2010).

2.4 Theories of Mechanisms for HIV-Associated Neurocognitive Disorders and Distal Sensory Polyneuropathy

Given that HIV does not productively infect neurons, how might HIV infection lead to HAND or DSP? Theories must also take into account the fact that HAND and DSP persist despite cART, demonstrating that HAND and DSP can develop even in the presence of tight control of viral load. The two major theories posit that either HIV indirectly causes neurotoxicity through activation of inflammatory pathways, or that HIV might itself possess neurotoxic properties that cause HAND and DSP. Both are discussed in detail below.

2.4.1 Indirect mechanism of neurotoxicity

For the indirect mechanism of neurotoxicity, it thought that either glial cells infected by HIV or activated glial cells in response to HIV infection secrete neurotoxic and inflammatory factors, such as excitatory amino acids and cytokines (Kaul et al., 2005; Kamerman et al., 2012). For example, neurotoxic products produced by infected macrophages may cause neuronal death or inhibit neurite growth (Giulian et al., 1990; Pulliam et al., 1991; Hahn et al., 2008). Evidence for enhanced inflammation in HAD patients exists as well. Patients

with HAD have a higher amount of activated CD14+ circulating monocytes, soluble CD14 and lipopolysaccharide levels compared to HIV patients without HAD (Pulliam et al., 1997; Ryan et al., 2001; Ancuta et al., 2008). In a Simian Immunodeficiency Virus (SIV) model, animals with CNS functional impairment had over 5 times more activated CD8+ T cells in the CNS compared to animals without CNS impairment (Marcondes et al., 2001). In the PNS, inflammatory cytokines such as tumor necrosis factor-α (TNF-α), interferon-γ (IFN- γ), interleukin (IL)-1β, and IL-6 have been detected in dorsal root ganglia from AIDS patients (Nagano et al., 1996). However, proving that these inflammatory elements are causal for HAD has been problematic. For example, HIV viral proteins may trigger an inflammatory action for cells in the vicinity of affected neurons. In one such case, gp120 was linked to the innate immune system in a study that found that gp120 binding to DRG neurons activated the complement cascade leading to neuronal death (Apostolski et al., 1994).

Evidence has accumulated that the HIV glycoprotein gp120 induces the release of certain cytokines, such as TNF-α. In the PNS, epineural application of gp120 led to axonal swelling, increased TNF-α at the site of application in the nerve trunk, and allodynia and hyperalgesia, suggesting that activation of TNF-α might play in role in the production of symptoms of pain in DSP (Herzberg and Sagen, 2001). Additionally, it was found that gp120 application to the sciatic nerve caused an upregulation of TNF-α in glial cells of the spinal cord and mechanical allodynia; intrathecal administration of TNF-α inhibitors attenuated allodynia (Zheng et al., 2011). DRG neurons might also produce TNF-α

themselves to cause neurotoxicity through autocrine regulation. The mechanism that has been proposed for this is that gp120 binding to CXCR4 on Schwann cells leads to release of the chemokine CCL5, which activates CCR5 receptors on DRG neurons, inducing TNF-α activation in DRG neurons.

In the CNS, similar mechanisms have been proposed for indirect neurotoxicity by HIV. For example, cognitively impaired HIV patients have an increased amount of soluble TNF-α type II receptors in the plasma, suggesting that TNF-α activation may also play a role in HAND (Ryan et al., 2001). TNF-α activation and chemokines have been implicated in development of neurotoxicity, with an involvement of astrocytes and microglia. In one study, gp120 activated CXCR4 on astrocytes and microglia, leading to release of TNF-α and glutamate, which had an excitotoxic effect on neurons (Bezzi et al., 2001).

The HIV protein tat may also activate inflammatory pathways in the CNS. Tat can activate chemokines and matrix metalloproteinases in astrocytes, leading to recruitment of activated T cells, macrophages and monocytes into the brain (Kutsch et al., 2000; Johnston et al., 2001). In addition to gp120, tat can also activate TNF-α in macrophages (Chen et al., 1997).

An assumption of the indirect theory is that activated macrophages and microglia are responsible for neurotoxicity. However, the presence of activated microglia is not sufficient to explain the pattern of synaptic, axonal and dendritic loss seen in HAND patients (Masliah et al., 1997) and in rodent models of HIV (Toggas et al., 1994; Dash et al., 2011; Rao et al., 2011; Mocchetti et al., 2012). For example, an HIV transgenic rat model showed spatial memory deficits and

synaptic loss in the hippocampus without the presence of activated microglia or inflammatory cytokines (Rao et al., 2011; Mocchetti et al., 2012). Similarly, injection of gp120 into the brain caused neuronal apoptosis days before microglia infiltration (Ahmed et al., 2009). Additionally, activated microglia can be neuroprotective. Macrophages in contact with apoptotic neurons suppress inflammatory responses as they perform phagocytosis of some toxic species (Lucas et al., 2006; Mocchetti et al., 2012). Activated microglia can also play a supportive role in remyelination, and can internalize and degrade toxic oligomeric proteins (Yong and Rivest, 2009). These data suggest that the indirect mechanism for neurotoxicity may not completely explain neuropathology caused by HIV.

2.4.2 Direct mechanism of neurotoxicity

Although HIV does not productively infect neurons, certain HIV proteins have been shown to have direct neurotoxic effects. Even without productive infection, viral proteins can interact with neurons in multiple ways, due to exposure in the extracellular environment. Viral proteins can enter the extracellular environment through formation of viral proteins during restricted infection, formation of defective viral particles, viral protein loss from a cytopathic infection, active release of viral proteins, shedding of viral coat proteins and interactions by cell-to cell contact (Nath, 2002). The most evidence for direct neurotoxicity involves the two HIV viral proteins tat and gp120, so the focus will be on tat and gp120. However, other HIV viral proteins that have been implicated in neurotoxicity include gp41, Vpr, Nef and Rev (Nath, 2002).

2.4.2.1 Tat

Tat is an HIV protein with a primary function of activating transcription of HIV double stranded DNA. However, it is also actively secreted from HIV-infected cells, and is overexpressed by HIV-infected astrocytes (Nath, 2002). Tat binds to the lipoprotein related protein receptor (LRP) on neurons (Liu et al., 2000), and undergoes transport within neurons (Bruce-Keller et al., 2003). Uptake of tat into neurons has been linked to calcium dysregulation (Haughey et al., 1999; King et al., 2006) and ultimately leads to induction of apoptosis (Kruman et al., 1998). Tat also activates the NMDA receptor (NMDAR), and this activation has been linked to impairments in learning (Li et al., 2004) and neurotoxicity (King et al., 2006). The areas in the brain that are primarily affected by tat neurotoxicity include the hippocampus and the striatum (Nath, 2002). Little information exists on the effect of tat in the PNS, but a recent study found that tat caused hyperexcitability in DRG neurons, leading to apoptosis that appeared to involve activation of the cyclin-dependent kinase 5 (cdk-5; Chi et al., 2011).

3. Gp120

3.1 Gp120 Overview

Gp120 is a highly glycosylated envelope protein that is responsible for binding of the virus to the host cell. Gp120 exists on the virion surface as a heterotrimeric “spike” bound to the transmembrane envelope protein gp41. Typically, gp120 binds to the cell surface receptor CD4, triggering a

conformational change that allows gp120 to bind to its coreceptor (either CXCR4 or CCR5). This binding allows viral entry into the host cell.

Gp120 is composed of 5 conserved and 5 variable regions (V1-V5). Of the 5 variable regions, the conserved region surrounding V4 is responsible for CD4 binding, while V3 interacts with coreceptors (Arrildt et al., 2012). Along with heavy glycosylation, the highly variable nature of gp120 aids HIV in immune evasion, with the gp120 coding domain changing at a rate of 1-2% a year (Leitner et al., 1997; Arrildt et al., 2012). The high variability of gp120 allows for many different strains to be produced; in fact, multiple strains of gp120 can be detected in one patient at once. A major categorization of gp120 is co-receptor usage. Typically in infection, patients are infected by a single strain of gp120 that binds to the CCR5 co-receptor on CD4+ T cells (Keele et al., 2008; Isaacman-Beck et al., 2009; Alexander et al., 2010). Over time, gp120 evolves into strains that can productively infect macrophages, strains that utilize CXCR4, and dual-tropic CXCR4 and CCR5 binding strains (Arrildt et al., 2012). Although it was thought in the past that neurotropism was specific to CCR5-binding gp120 strains, a study examining isolates from HIV patients with dementia or encephalitis found that neurotropism is linked to the ability of gp120 strains to infect macrophages and microglia, not to co-receptor usage (Gorry et al., 2001).

HIV productive infection is limited to cells of the immune system, but gp120 can be shed during viral entry and overproduced and shed from infected cells (Schneider et al., 1986). Since infected microglia and macrophages reside in the CNS, and infected macrophages are present in dorsal root ganglia, infected cells are in close proximity to neurons of the CNS and DRG neurons in the PNS

respectively. This could lead to high local concentrations of gp120. While free gp120 in the plasma has been measured to be between 2 pM and 0.8 nM (Gilbert et al., 1991; Oh et al., 2001), measurements of gp120 in the plasma may be a poor model of local concentrations of gp120. Local concentrations may remain high due to binding to extracellular matrix components or to local glial swelling, which decreases the volume of the extracellular compartment (Nath, 2002; Krathwohl and Kaiser, 2004). Additionally, DSP is a slowly progressive complication that takes decades to develop. Low levels of gp120 might be enough to gradually cause neurotoxicity over a period of years or even decades.

3.2 Gp120 and HIV-Associated Neurocognitive Disorders

Gp120 has been highly implicated in neuropathogenesis of HAND. One notable example comes from a study in which transgenic mice were developed with gp120 expressed under a glial fibrillary acidic protein (GFAP) promoter (Toggas et al., 1994). This manipulation was sufficient to induce neuropathology similar to that in HAD, including loss of presynaptic terminals and dendrites, vacuolization of dendrites, and marked astrocytosis (Toggas et al., 1994). Another transgenic mouse model developed with gp160 (composed of both gp120 and gp41) under a neurofilament promoter to allow expression of gp160 in neurons also developed gliosis and dendritic degeneration in addition to axonal swellings and cytoskeletal abnormalities (Michaud et al., 2001). Application of gp120 has been linked to memory impairment and long term potentiation (LTP) impairment in several studies (Sanchez-Alavez et al., 2000; Dong and Xiong, 2006; Fernandes et al., 2007); demonstrating that gp120 may be sufficient for

the cognitive impairment seen in HAND.

3.3 Gp120 and Distal Sensory Polyneuropathy

An extensive amount of research provides support for the involvement of gp120 in DSP. A model of DSP in mice was created that gave oral treatments of didanosine (ddI), an anti-retroviral implicated in ATN, to mice transgenic for gp120 under a GFAP promoter. This model replicated both the neuropathology of distal degeneration of sensory axons and the symptom of pain. Because the model required both gp120 and ddI to have these effects at a young age, the authors proposed a "double hit" hypothesis, in which gp120 is needed to sensitize the DRG neurons before ddI treatment (Keswani et al., 2006). The double-hit hypothesis might be relevant for HIV patients – perhaps those that are prone to developing ATN already have a subclinical amount of damage by gp120. Additional evidence for gp120 involvement in DSP is that administration of gp120 to rodents causes pain hypersensitivity, mimicking the symptoms of DSP (Meucci et al., 1998; Milligan et al., 2000; Herzberg and Sagen, 2001).

3.4 Cellular Mechanisms of Gp120-Induced Neurotoxicity

The ability of gp120 to induce neuronal cell injury and death is well established (Brenneman et al., 1988; Toggas et al., 1994; Lannuzel et al., 1995; Meucci and Miller, 1996; Hesselgesser et al., 1998; Meucci et al., 1998; Singh et al., 2005; Kaul et al., 2007). This chapter will review cellular mechanisms that have been identified for gp120 to directly interact with and impair neurons.

3.4.1. Gp120 Binding to Cells

Gp120 typically binds to CD4 before it can bind to its co-receptor. However, there is ample evidence that gp120 binds to neurons, although they lack CD4. How might this happen? For one thing, gp120 strains isolated from the brain have a reduced dependence on CD4 for viral entry compared to strains isolated from lymphoid tissue (Thomas et al., 2007). Additionally, gp120 might use other methods for attachment to neurons. For example, gp120 has a strong affinity for heparan sulfate proteoglycans (HSPG; Ugolini et al., 1999) with four binding domains (Crublet et al., 2008), and HSPG's are expressed on the surface of neurons. In fact, gp120 attachment has been shown to be dependent on binding to HSPG rather than to CD4 in several cell lines (Mondor et al., 1998; Bobardt et al., 2004; Vidricaire et al., 2007), leading to the hypothesis that the dependence of gp120 on CD4 for binding may be cell line specific (Mondor et al., 1998). Regardless, gp120 binding to its co-receptors appears to be a critical first step for neurotoxicity (Apostolski et al., 1993; Oh et al., 2001).

3.4.2 Gp120 and Lipid Rafts

Lipid rafts are small, mobile and specific microdomains in the plasma membrane composed of clusters of sphingolipid and cholesterol that are detergent-insoluble (Simons and Ikonen, 1997). Lipid rafts are thought to function as platforms for cellular processes such as biosynthetic sorting, signaling, endocytosis, and pathogen binding (Simons and Ikonen, 1997; Chazal and Gerlier, 2003). Evidence has accumulated that gp120 associates with lipid rafts for HIV internalization. Both CD4 and the coreceptor CCR5 reside in lipid

rafts (Millan et al., 1999; Popik et al., 2002); removal of CD4 from lipid rafts results in impaired HIV entry (Del Real et al., 2002). Gp120 binding to CD4 induces clustering of CD4, gp120 and its coreceptors (Nguyen et al., 2005). Although the coreceptor CXCR4 is only partially located in lipid rafts (Manes et al., 2000), gp120 promotes CXCR4 trafficking into lipid rafts, facilitating this clustering of these receptors and coreceptors (Kamiyama et al., 2009). Cholesterol depletion inhibits both this clustering and viral entry (Manes et al., 2000; Liao et al., 2001; Popik et al., 2002; Viard et al., 2002), demonstrating that gp120 association with lipid rafts is important for HIV infection. Notably, gp120 treatment of hippocampal neurons led to stabilized raft domains that NMDAR clustered in, allowing enhanced NMDAR activity (Xu et al., 2011). These results suggest that gp120 associates with and stabilizes lipid rafts, leading to altered host cell signaling. However, the extent of gp120 association with lipid rafts in neurons has not been elucidated.

3.4.3. Gp120 Activation of CXCR4 and Signaling Cascades

A number of studies have examined the binding of gp120 to CXCR4 as a cause of neurotoxicity. Gp120 binding can activate CXCR4 and CCR5, both G protein-coupled receptors (GPCR; (Davis et al., 1997). The activation of CXCR4 has been associated with neuronal injury to a greater extent than CCR5 (Zheng et al., 1999); in fact, there is some evidence that CCR5 activation might be neuroprotective (Kaul et al., 2007). Various mechanisms have been proposed for neuronal injury associated with gp120 activation of CXCR4.

Gp120 activation of CXCR4 has been linked to the disruption of calcium

homeostasis, leading to acute calcium increase within neurons (Pandey and Bolsover, 2000) through mobilization of intracellular calcium stores (Medina et al., 1999). CXCR4 activation by gp120 has also been linked to several signaling cascades. First of all, gp120-induced disruption of intracellular calcium homeostasis (Lannuzel et al., 1995) led to activation of RNA-activated protein kinase (PKR), a kinase linked to an antiviral response, stress response and activation of apoptosis through caspase-3 (Alirezaei et al., 2007). Gp120 activated the caspase-3 apoptotic cascade in several other studies as well (Bachis et al., 2003; Singh et al., 2004) (Melli et al., 2006). Intriguingly, gp120 binding to chemokine receptors and gp120 activation of a caspase pathway was localized along DRG axons in compartmentalized chambers (Melli et al., 2006).

Stress-activated protein kinases (SAPK), including c-Jun N-terminal kinase (JNK) and p38 mitogen activated protein kinase (p38 MAPK), were implicated in activation of CXCR4 by gp120 across different cell types, in addition to neurons (Kan et al., 2000; Misse et al., 2001; Kapasi et al., 2002; Trushin et al., 2007; Liu et al., 2012).

In the CNS, gp120 treatment caused an increase in phosphorylation of JNK in primary rat hippocampal neurons that was mediated by CXCR4 (Khan et al., 2004). Also, inhibiting an upstream activator of JNK and p38 MAPK, mixed lineage kinase-3 (MLK-3), prevented gp120-triggered apoptosis in hippocampal neurons (Bodner et al., 2002). Activation of JNK or p38 MAPK may be cell-type specific. For example, p38 MAPK but not JNK was activated by gp120 in mouse striatal neurons, leading to neurite loss and neuronal death (Singh et al., 2005). An increase in p38 MAPK in response to gp120 treatment has also been

demonstrated in primary cerebrocortical neurons in addition to primary fetal human neurons (Hu et al., 2005; Medders et al., 2010). In adult neural progenitor cells, gp120 arrested cell cycle progression through a signaling pathway involving p38 MAPK (Okamoto et al., 2007).

In the PNS, gp120 activation of CXCR4 was linked to hypernociception in DSP (Bhangoo et al., 2009). Chronic treatment with gp120 led to DRG apoptosis, which could be reversed using a MLK-3 inhibitor, pointing to a role for JNK and/or p38 MAPK activation by gp120 (Bodner et al., 2004). In an *in vivo* study, spinal application of gp120 led to an increase in phosphorylation of p38 in adjacent DRG sections along with pain hypersensitivity (Wilkerson et al., 2012) that was reversed using the cannabilactone AM1710. Systemic treatment with the p38 MAPK inhibitor CNI-1493 prevented thermal hyperalgesia and mechanical allodynia caused by intrethecal administration of gp120 (Milligan et al., 2001).

3.4.4 Internalization of Gp120 by Neurons

Evidence has emerged that in addition to binding chemokine receptors and activating signaling pathways, gp120 can also be internalized by neurons. For example, gp120 was internalized by cerebellar granule cells *in vitro* (Bachis et al., 2003). Injections of gp120 into the rat striatum and hippocampus also demonstrated internalization of gp120 by neurons (Bachis et al., 2006). Internalized gp120 has been linked to transport within neurons and activation of caspase-3, although the mechanisms remain undefined (Bachis et al., 2003; Bachis et al., 2006; Ahmed et al., 2009). Although both anterograde and

retrograde transport of gp120 were observed in the CNS, injections of gp120 in the sciatic nerve did not reveal any transport of gp120 in the PNS (Ahmed et al., 2009). However, it is possible that the gp120 could have dispersed before reaching the unmyelinated fibers from DRG neurons that are typically affected in DSP.

4. Fast Axonal Transport

4.1 Fast Axonal Transport Background

The process of translocation of membrane proteins and lipid components along axons of neuronal cells is collectively known as fast axonal transport (FAT; (Morfini, 2006). This process is dependent on the integrity of axonal microtubules (Kreutzberg, 1969), and the mechanochemical forces generated from adenosine triphosphate (ATP) hydrolysis by microtubule-based molecular motor proteins (Hirokawa and Noda, 2008). In axons, microtubules are organized in such way that their plus ends point towards the periphery, whereas the minus ends points towards the cell body (Baas and Ahmad, 1993). This unique spatial organization allows for the bidirectional transport of molecular components along axons.

Depending on the direction of movement, FAT can be divided into anterograde and retrograde FAT (Grafstein and Forman, 1980; Lasek, 1982). Anterograde FAT involves the transport of materials from their sites of synthesis in the neuronal cell body towards the cell periphery, at rates of 200-400 mm/day (Brady et al., 1985). On the other hand, retrograde FAT constitutes the movement of materials from the cell periphery towards the neuronal cell body, proceeding at

an average pace of 100-250 mm/day (Susalka et al., 2000). Anterograde FAT provides newly synthesized components required for neuronal membrane function and maintenance, and is mainly carried out by microtubule-dependent molecular motors of the kinesin superfamily (Hirokawa and Noda, 2008). Electron microscopic and biochemical studies indicate that the material moving in anterograde FAT includes various membrane-bounded organelles (MBOs), including synaptic vesicle and axolemma precursors, tubulovesicular structures, mitochondria and dense core vesicles (Hirokawa et al., 1991). MBOs moving in anterograde FAT are needed for supply and turnover of intracellular membrane compartments, as well as the maintenance of axonal metabolism. Using video-enhanced contrast-differential interference contrast (VEC-DIC) microscopy in isolated squid axoplasm, conventional kinesin was first discovered (Brady, 1985) and found to represent the most abundant microtubule-dependent molecular motor protein in mature neurons (Wagner et al., 1989). Accumulative evidence indicates that conventional kinesin is involved in the anterograde FAT of mitochondria, synaptic vesicles and coated vesicles (Leopold et al., 1992). Conventional kinesin is a heterotetrameric protein complex composed of a long, coiled-coil rod that incorporates two kinesin heavy chains (kinesin-1s, KHCs) on one end, and two kinesin light chains (KLCs), which form a fan-like structure (Bloom et al., 1988). Recent studies indicate that conventional kinesin holoenzymes are formed of KHC and KLC homodimers (DeBoer et al., 2008). KHCs contain both microtubule-binding and ATPase domains at their amino terminus, and are responsible for processivity along microtubules along with energy generation for this process (Bloom et al., 1988). KLCs on the other hand, bind (Stenoien and Brady, 1997)

and target (Wozniak and Allan, 2006) conventional kinesin to selected MBOs, through interactions involving their tandem repeat domain (Stenoien and Brady, 1997) and their alternatively spliced carboxy terminus (Cyr et al., 1991), respectively. Appropriate neuronal survival and maintenance also requires signaling complexes and MBOs containing degradation products to be transported in the retrograde direction from synaptic terminals and axons to the neuronal cell body (Ginty and Segal, 2002). The execution of retrograde FAT is carried out by the minus end-directed microtubule-based molecular motor cytoplasmic dynein (CDyn; (Paschal et al., 1987; Paschal and Vallee, 1987; Vallee et al., 1988). *In vivo,* CDyn exists as a large (1.2 MD), multisubunit protein complex formed by at least two heavy chains of 500 kDa (DHCs), two 74 kDa intermediate chains (DICs), four 53-59 kDa light intermediate chains (LICs), and several light chains (LCs; (Susalka and Pfister, 2000). A protein complex termed dynactin also appears associated with a small fraction of total CDyn in cells (Schroer, 2004). DHCs contain a motor protein domain and are responsible for the ATPase and microtubule-binding activities of CDyn (Vallee et al., 1988). Biochemically heterogeneous CDyn variants containing different DIC isoforms are bound to specific MBO cargos (Susalka and Pfister, 2000; Ha et al., 2008).

Basic neuronal functions including synaptic transmission and survival all depend upon the localized delivery of selected MBOs at specific neuronal and axonal subdomains. For example, neurotransmitter-bearing synaptic vesicles must be delivered in a regulated fashion to presynaptic terminals, whereas

vesicles carrying selected types of sodium channels need to be delivered to nodes of Ranvier (Morfini et al., 2001). These observations imply the existence of molecular mechanisms that allow for the regulation of MBO delivery to specific axonal domains (Morfini et al., 2001).

4.2 Regulation of Fast Axonal Transport

What is the molecular basis of FAT regulation *in vivo?* In recent years, it has become apparent that molecular motors are highly regulated by phosphtransferase activity (Hollenbeck, 1993; Morfini et al., 2002). The use of the squid axoplasm, a unique experimental model for the study of intra-axonal events, was instrumental for these findings (Brady, 1990). Multiple kinases and phosphatases that differentially affect conventional kinesin have been identified (Morfini et al., 2001; Donelan et al., 2002; Morfini et al., 2002; Morfini et al., 2004; Morfini et al., 2006; Morfini et al., 2007a) or CDyn (Dillman and Pfister, 1994, 1995; Brill and Pfister, 2000; Morfini et al., 2007b) function. These kinases can directly or indirectly modify specific subunits of molecular motors, and regulate certain aspects of their functionality (Morfini et al., 2001; Donelan et al., 2002; Morfini et al., 2002; Morfini et al., 2006), thus providing a molecular basis for the regulation of FAT *in vivo*.

Discrete functional activities of conventional kinesin include enzymatic (i.e. binding to microtubules and ATPase activity) and non-enzymatic activities (i.e. attachment to the transported cargos). It was found that the interaction of conventional kinesin with both cargos and microtubules is subject to regulation

by specific protein kinases. Conventional kinesin detachment from MBOs was found to be a process that involved the activities of chaperones and several protein kinases (Tsai et al., 2000; Morfini et al., 2001; Morfini et al., 2002). Because different cargos need to be targeted to specific axonal compartments, it is thought that multiple pathways mediate delivery of certain MBO subsets (Morfini et al., 2001). An example of such a pathway for removing conventional kinesin from MBOs involves the activity of the protein kinase glycogen synthase kinase 3 (GSK-3; Morfini et al., 2002). GSK-3 selectively phosphorylates KLC subunits and promotes detachment of conventional kinesin from the transported cargo (Morfini et al., 2002; Pigino et al., 2003). Both KHCs and KLCs can be phosphorylated by casein kinase 2 (CK2; (Morfini et al., 2001; Donelan et al., 2002), and this kinase inhibits both anterograde and retrograde FAT when introduced into isolated squid axoplasm (Morfini et al., 2001).

Kinesin heavy chains (KHC) are also targeted by regulatory protein kinases. For example, dephosphorylation of KHCs by the protein phosphatase calcineurin is required for mobilization of secretory granules (Donelan et al., 2002). On the other hand, phosphorylation of KHCs interferes with their binding to microtubules, and thus with the overall processivity of conventional kinesin (Morfini et al., 2006). Additional work has also helped delineating novel signaling pathways that lead to localized activation of these kinases above (Beffert et al., 2002; Morfini et al., 2004). For example, it was found that activation of axonal GSK-3 is subject to regulation by a pathway involving the activity of cyclin-dependent kinase 5 (CDK-5) and phosphatase 1 (PP1; Morfini et

al., 2004). Based on these findings above, it was suggested that the local activation of specific kinase pathways in axons allows for the delivery of specific cargos to selected axonal subcompartments (Morfini et al., 2004; DeBoer et al., 2008). Conventional kinesin-mediated cargo delivery thus depends upon precise tuning of kinase activities in specific axonal subdomains.

Following the discovery of CDyn, it was found that differentially phosphorylated pools of this molecular motor complex travel along axons. All CDyn subunits appear to be phosphorylated *in vivo* (Brill and Pfister, 2000). Metabolic labeling experiments *in vivo* showed that DHCs moving in the anterograde direction are less phosphorylated than DHCs in cytoplasmic pools (Dillman and Pfister, 1994), leading to the hypothesis that phosphorylation of DHCs might play a role in the regulation of CDyn activity (Dillman and Pfister, 1994). Supporting this idea, neurotrophin-induced stimulation of tropomyosin receptor kinase (Trk) receptors in cultured neurons induces phosphorylation of DICs (Salata et al., 2001) and activation of CDyn-dependent retrograde transport (Ha et al., 2008). Moreover, kinase-deficient forms of Trk fail to be retrogradely transported, again suggesting that Trk-induced kinase activity regulates CDyn function (Heerssen et al., 2004). Although the identity of kinases regulating CDyn *in vivo* is uncertain, experiments in both isolated squid axoplasm and the squid giant synapse indicate that Protein Kinase C (PKC) activation increases CDyn-dependent retrograde FAT (Morfini et al., 2007b; Serulle et al., 2007).

4.3 The Role of Fast Axonal Transport in Dying Back Neuropathies

Basic neuronal functions including growth, information processing and survival all depend upon exquisite compartmentalization and transport of membrane proteins, which is achieved by FAT. Supporting this idea, several loss-of-function mutations in conventional kinesin (Reid et al., 2002) and CDyn subunits (Hafezparast et al., 2003; Puls et al., 2005) have been found to cause inherited human neuropathologies, such as Hereditary Spastic Paraplegia (HSP) and various forms of sensory or motor neuron diseases. Interestingly, these diseases proceed following a dying back pattern of neurodegeneration (Griffin, 1995; Deluca et al., 2004; Fischer et al., 2004). Thus, genetic evidence demonstrates that even modest decrements in FAT can suffice to produce degeneration of specific neuronal populations (Roy et al., 2005). Additionally, alterations in regulatory mechanisms of FAT have also been implicated in neurodegeneration. Highlighting the importance of FAT regulation for neuronal function, recent experimental evidence indicates that alterations in kinase-dependent regulatory pathways for FAT can lead to neuronal degeneration (Mandelkow and Mandelkow, 2002; Pigino et al., 2003; Morfini et al., 2005; Morfini et al., 2006; Lazarov et al., 2007; Morfini et al., 2009). Abnormal patterns of protein phosphorylation have long been recognized in most human neurodegenerative diseases, and specific alterations in kinase and phosphatase activities have been reported in several animal models of these diseases. However, the targets of kinases and their relation to disease pathogenesis remain unknown.

A common link between certain neurodegenerative diseases that progress by dying-back axonal degeneration is abnormalities in the activity of kinases

regulating FAT, leading to the coinage of the term “dysferopathies” to describe these neurodegenerative diseases exhibiting dysfunction of vesicle transport and associated loss of synaptic function (Morfini et al., 2007b; Serulle et al., 2007; Morfini et al., 2009). Various human neurodegenerative conditions fall in this category. For example, abnormal activation of JNK by pathogenic, polyglutamine-expanded forms of huntingtin and androgen receptor polypeptides results in increased phosphorylation of kinesin-1, and inhibition of anterograde FAT (Szebenyi et al., 2003; Morfini et al., 2006). Similarly, neurons expressing familial Alzheimer’s Disease (AD)-linked mutations in presenilin-1 (PS1) showed increased activation of GSK-3, and a concomitant reduction in conventional kinesin-based motility (Pigino et al., 2003). Supporting these later findings, nerve ligation studies showed reductions in anterograde FAT in mice expressing FAD-linked PS1 mutations, and this reduction correlated with motor neuron deficits (Lazarov et al., 2007).

Alterations in FAT have also been found in association with Parkinson’s Disease (PD). For example, analysis of postmortem brains from sporadic PD in addition to analysis of a genetic rat model of PD found a marked decrease in kinesin at early stages of disease, with reductions of CDyn occurring later in the disease (Chu et al., 2012). In a MPP+ model of PD, increased CDyn-mediated motility that depended upon abnormal activation of axonal and synaptic PKC was observed (Morfini et al., 2007b). The above observations might be explained by an activation of retrograde transport in response to axonal damage co-existing with a reduction of anterograde transport due to loss of kinesin, leading to defective axonal transport (Chu et al., 2012). Additionally, multiple familial

amyotrophic lateral sclerosis (ALS) superoxide dismutase 1 (SOD1) mutations inhibited anterograde FAT through a p38 MAPK pathway (Morfini et al. submitted). This inhibition was replicated in oxidized SOD1 samples from patients that had suffered sporadic ALS, indicating a common mechanism (Bosco et al., 2010). In fact, *in vivo* studies revealed that p38 MAPK can phosphorylate kinesin to inhibit kinesin's motility (Morfini, 2013 (submitted)). These findings above provide a mechanistic explanation for the early degeneration of axons and synaptic dysfunction observed in these neurodegenerative diseases.

4.4 Gp120 and Fast Axonal Transport

DSP shares a similar phenotype to the dysferopathies outlined above, with axonal degeneration progressing in a dying-back manner. Additionally, distal axons of peripheral nerves of simian immunodeficiency virus (SIV) infected macaques showed an accumulation of damaged mitochondria (Lehmann et al., 2011), indicating FAT impairments. The activation of p38 MAPK and JNK by gp120, both kinases that regulate fast axonal transport, also signals a possible mechanism for DSP that involves FAT inhibition. However, it is unknown whether a link exists between gp120 and reduction of FAT.

Here we report a novel mechanism for DSP pathogenesis through the dysregulation of FAT. The studies described in this dissertation were designed to determine the effect that gp120 might have on regulation of FAT. Accordingly, internalization of gp120 and localization within the axon were assessed in F11 cells and primary DRG neurons. The mechanisms for endocytic internalization of gp120 were determined to involve fluid phase pinocytosis and internalization

through lipid rafts with partial dependence on CXCR4 binding, and transport of gp120 along DRG axons was revealed. Further, intra-axoplasmic gp120 profoundly impaired anterograde and retrograde FAT, through a signaling cascade causing activation of TAK-1, leading to activation of JNK, p38 MAPK and PP1.

CHAPTER III

MATERIALS AND METHODS

Berth, S., Morfini, G., Sarma T., Caicedo, H., Brady, S.T. (2015) Internalization and Axonal Transport of the HIV Glycoprotein gp120. ASN Neuro 7(1): pii: 1759091414568186

1. MATERIALS

1.1 Antibodies and Reagents

Antibodies and reagents were used according to protocols provided by manufacturers. Table I summarizes the fluorescent conjugates used, and Table II summarizes the antibodies used in this dissertation research.

Table I. Fluorescent conjugates used

Conjugate	Fluorescent tag	Concentration	Manufacturer
gp120	FITC	70 nM	Immunodiagnostics 1001-F
Dextran 10,000 MW, neutral	Rhodamine B	200 μg/mL	Invitrogen D1824
Cholera toxin B	Alexa Fluor 594	500 ng/mL	Invitrogen C34777
Transferrin	Alexa Fluor 594	50 μg/mL	Invitrogen T13343

1.2 Inhibitors Used in Axoplasm Studies

Table III outlines the following inhibitors used for studies in isolated squid axoplasm.

Table II. Antibodies Used

Name	Antigen	Species	Dilution	Manufacturer
H2	KHC	Mouse	1:1000K - ECL 1:1000 -Typhoon	Developed by Brady lab
p38	Total p38	Rabbit	1:2000	Cell Signaling 9212
p-p38	Phospho-p38	Rabbit	1:1000	Cell Signaling 9215
DIC 74-1	DIC	Mouse	1:500	Santa Cruz sc-13524
DM1A	α-tubulin	Mouse	1:100K-ECL 1:1000- Typhoon	Sigma Aldrich T9026
EEA1	EEA1	Rabbit	1:400	Cell Signaling 3288
LAMP2	LAMP2	Rabbit	1:1000	Thermo Scientific PA1-655
HRP-conjugated secondary	Mouse IgG	Goat	1:20K	Jackson Immuno 111-035-062
HRP-conjugated secondary	Rabbit IgG	Goat	1:20K	Jackson Immuno 111-035-144
Cy5-tagged secondary	Mouse IgG	Goat	1:2500	Amersham PA45010
Alexa Fluor 594-tagged secondary	Mouse IgG	Goat	1:400	Invitrogen A11032
Alexa Fluor 594-tagged secondary	Rabbit IgG	Goat	1:400	Invitrogen A11037

1.3 F11 Cells

F11 cells were obtained from Richard Miller (Northwestern University, Molecular Pharmacology and Biological Chemistry). F11 cells are rat DRG neurons hybridized with mouse neuroblastoma cells. These cells have similar properties to DRG neurons, with the advantange that they can be passaged like neuroblastoma cells.

1.4 Squid *Loligo peali*

The squid *Loligo peali* was used as a model organism for axoplasm studies. The Marine Biological Labs (MBL) in Woods Hole, MA provides fresh caught squid from the wild four days out of the week. Squids are typically used within a day of being caught.

Table III. Inhibitors Used in Isolated Squid Axoplasm

Name	Concentration	Source	Catalog Number
SB203580	10 µM	Calbiochem	559389
Okadaic acid	200 nM	Calbiochem	495620
MW01-2-069A-SRM	10 µM	Gift from Martin Watterson, Center for Molecular Innovation and Drug Discovery	N/A
SP600125	500 nM	Calbiochem	420119
I-2	50 nM	Calbiochem	14-162
DVD peptide	20 µM	Brady lab	N/A
ING-135	100 nM	Gift from Allen Kozikowski. UIC College of Pharmacy	N/A
(5Z)-7-Oxozeaenol	50 nM	Calbiochem	499610
IKK Inhibitor XII	500 nM	Calbiochem	401491
IKKb	50 nM	Signal Chem	I03-10BG-05
CEP-11004	200 nM	a gift from Cephalon	N/A

2. METHODS

2.1 F11 Cell Culture

F11 cells (a generous gift from Dr. Richard Miller) were grown in high glucose DMEM media (Invitrogen), supplemented with 10% fetal bovine serum, 10% glutamax, 10,000 U/ml penicillin-streptomycin. 6 channel μ-slides from Ibidi were coated with 0.1 μg/ml poly-L-lysine (Sigma) and then rinsed 4 times with autoclaved, deionized water for half an hour each. 300 cells were added to each channel. Cells were maintained at 37°C in 5% CO_2 and 95% O_2. To differentiate the F11 cells, 24 hours after plating the amount of fetal bovine serum was reduced to 5%, and then 24 hours after that the cells were treated with 0.5 mM dibutryl-cAMP (Sigma) in media with 0.5% fetal bovine serum for 4 days.

2.2 Analysis of Gp120 Internalization by Confocal Microscopy

Differentiated F11 cells were treated with fluorescein-conjugated gp120 IIIB (Immunodiagnostics) for varying time points. For heat-inactivation, gp120 IIIB was boiled for 1 hour prior to treating with F11 cells. For AMD3100 (NIH AIDS Reference & Reagent Program) pre-treatment experiments, F11 cells were incubated with 2 μM AMD3100 for 1 hour, then co-treated with 2 μM AMD3100 and 70 nM fluorescein-gp120 for a 2 hour time course. For methyl-β-cyclodextrin (CD) pre-treatment experiments, F11 cells were incubated with 5 mM CD (Sigma) for 20 minutes, washed three times with media, then incubated with 70 nM fluorescein-gp120 for a 2 hour time course. To examine the effect of CD pre-treatment on transferrin internalization, differentiated F11 cells were treated with

either 5 mM CD or washed with media for 20 min at 37°C, then incubated with 50 μg/mL transferrin on ice for 15 minutes, then washed and incubated at 37°C for 15 min. For co-treatments with dextran, the F11 cells were co-treated with 70 nM fluorescein-gp120 and 200 μg/mL dextran. For colocalization analysis with cholera toxin B, the F11 cells were treated with 500 ng/mL cholera toxin B on ice for 15 minutes, washed, then treated with 70 nM fluorescein-gp120 at 37°C for a time course.

After treatments, F11 cells were washed with PBS, fixed with 4% paraformaldeyde and 0.01% glutaraldehyde in PBS for 10 minutes, and quenched with 50 mM ammonium chloride in PBS. Mounting media with DAPI (Vectashield) was dropped into wells. The DM1A antibody was used to visualize the F11 cells and their neurites. For the DM1A antibody, F11 cells were quenched and fixed as described above, permeabilized with 0.1% triton-X-100 for 10 minutes, then blocked with 5% milk in phosphate-buffered saline for 1 hour. Cells were incubated with DM1A antibody at room temperature for 1 hour, and then incubated with Alexa Fluor 594 secondary antibody for 45 minutes. Mounting media with DAPI (Vectashield) was dropped into wells. For endocytosis experiments using the early endosome antigen-1 (EEA1) and lysosome-associated membrane protein 2 (LAMP2) antibodies, after quenching the F11 cells were permeabilized and blocked with 5% normal goat serum (Santa Cruz) and 0.25% triton-X-100 in phosphate buffered saline for 1 hour, incubated with primary antibody for 1 hour at room temperature, then incubated with Alexa Fluor 594 secondary antibody for 1 hour. Mounting media with DAPI (Vectashield) was dropped into wells. Cells were imaged using a Zeiss LSM 510

laser scanning confocal microscope with a 100X objective. 1 μm thick z-stacks of the cells were obtained, with at least 10 cells per condition analyzed for each time point.

2.3 Image Analysis

Images were deconvolved and analyzed using Volocity software (Perkin Elmer). To quantitate the amount of internalized gp120, Z-stacks of cells were cropped to remove the bottom and top slices of the cells. The inner boundary of each cell was traced, and the average fluorescence unit was determined within that ROI using Volocity. For colocalization analysis, ROI's were obtained as described as above. The Pearson's correlation coefficient, which calculates the correlation between intensities of different channels, was obtained for each cell. Additionally, the Colocalization Coefficient M1 (green channel) and Colocalization Coefficient M2 (red channel) were also calculated. These coefficients provide further insight into colocalization by calculating the fraction of each channel that overlaps with the other channel. The student's t-test was used for statistical analysis. Quantitative data was expressed as mean $\pm$ SEM and significance was determined at $p<0.05$. A one-way analysis of variance (ANOVA) followed by the post-hoc Tukey's honest significance test (HSD) for multiple comparisons was performed to determine the difference between the amount of gp120 internalized between the gp120 only group, the heat-inactivated gp120 group, and the AMD3100 pre-treated group. The p value was set at 0.05.

2.4 Compartmentalized Microfluidic Devices

Microfluidic devices can be used to compartmentalize axons through

nanofabricated microgrooves that are small enough (length of 900 μm and a width of 8 μm) that only axons can grow through from the somatodendritic compartment (SDC) to the axonal terminal compartment (ATC). Fluidic isolation of a compartment is maintained by volume differences of 200 μl, as well as through a perpendicular central channel 23 mm long and 50μm wide, so that the pressure gradient overcomes diffusion. The microfluidic chambers were fabricated using photolithography and replica molding techniques, as described in (Caicedo et al 2013, in preparation). Briefly, patterned layers of polydimethylsiloxane (PDMS) chips were exposed to plasma generated by a laboratory corona treater (BD-20AC, Electro-Technic Products, Inc., Chicago, IL), as were glass coverslips. The plasma-treated surfaces were then immediately placed in conformal contact and incubation of the whole setup at 80° C overnight resulted in irreversible bonding. The compartments were loaded with 70% ethanol for 30 minutes, rinsed with autoclaved water 4 times, and treated with 0.1% triton in PBS to remove bubbles from the microgrooves if needed. Afterwards compartments were washed with autoclaved water 3 times for 5 minutes each.

The devices were incubated overnight with 0.5 mg/mL poly-L-lysine (Sigma) in 0.1M Borate buffer pH 8.5, and then washed with autoclaved water 4 times for half an hour each. Then the devices were incubated overnight with 10 μg/mL laminin (Invitrogen) in Neurobasal media (Invitrogen) at 37°C prior to plating the DRG neurons.

2.5 Primary Dorsal Root Ganglion Neuron Cell Culture

All experiments involving animals were conducted according to the protocols approved by the Institutional Animal Care and Use Committee at University of Illinois-Chicago. E15 Dorsal root ganglion (DRG) neurons were dissected from pregnant Sprague-Dawley rats, as described in (Hall, 2006), and placed into ice-cold 1X Hank's balanced salt solution. Trypsin was added to 0.25%, and the cells were incubated at 37°C. To stop the reaction, fetal bovine serum was added to 10%. Cells were collected by centrifugation at 600*g* for 6 minutes. Next cells were resuspended in serum-free Neurobasal media (Invitrogen) with 2% B-27 (Invitrogen), 1% glutamax (Invitrogen), and 0.5% penicillin/streptomycin (10,000 U/mL each, Invitrogen) with 2.5S nerve growth factor (NGF; 20 ng/mL, Invitrogen). 90,000 cells were added to the SDC of the prepared microfluidic devices (30,000 cells per SDC compartment). The ATC compartment used the same media but with 50 ng/mL 2.5S NGF to maintain a gradient to attract DRG axons into the ATC. Half of the cell media was replaced with fresh media every other day. 10 μm of 5-Fluoro-2'-dexyuridine was added to the cell media every other time the media was replaced to kill non-neuronal cells.

2.6 Cell Lysates

F11 cells were differentiated in 100 mm petri dishes, following the protocol above. After 4 days of 0.5 mM dibutryl-cAMP (Sigma) treatment, cells were treated with 5 nM gp120 (Immunodiagnostics) for either 5, 15 or 30 minutes. For pre-treatment with AMD3100, cells were first treated with 2 μM AMD3100 for 1 hour at 37°C prior to treatment with 5 nM gp120 for 5, 15 or 30 minutes. Treatment with PBS, the diluent, was used as a negative control. After

the treatments, cells were scraped and collected in 700 μL lysis buffer (1% sodium dodecyl sulfate (SDS) in phosphate-buffered saline, pH 7.4) and sonicated for two short, 3 second bursts each. Cells were spun at 14,000 rpm at 4°C in a Beckman tabletop centrifuge. Protein concentration of the clarified supernatants was determined using a bicinchoninic acid assay kit (Pierce). Sample buffer was added to the clarified supernatants, and the samples were placed in the -80° C freezer prior to analysis via SDS-PAGE.

2.7 SDS-Polyacrylamide Gel Electrophoresis (PAGE) and Immunoblotting:

Protein samples loaded onto a 4-12% bis/tris gradient gel (Invitrogen) and separated using 35 mAmps/gel for 2 hours. Proteins from the gels were transferred (at 4°C) to Immobilon-P transfer membranes (PVDF, Millipore) at 0.4 Amps for 2 hours in 1X Tobin buffer. After transfer, the membranes were stained with Ponceau red to visualize proteins, then cut as needed. Membranes were blocked at room temperature for 60 minutes with 5% milk in PBS. Primary antibodies in 1% BSA were added overnight at 4°C with gentle rocking. Primary antibodies were washed 3 x 10 minutes with PBST (0.25% Tween), and secondary antibodies were added for 1 hour at 4°C with gentle rocking. Membranes were again washed 3 x 10 minutes and visualized with ECL (Amersham) and exposed on film (Kodak) for HRP secondary. Since ECL is semi-quantitative, band intensities in the linear range were quantitated and analyzed using Quantity One software. For more precise quantitation, we used fluorescent secondary antibodies. Membranes were washed 3 x 10 minutes with 0.1% triton-PBS after

incubation in the dark. After drying overnight, the membranes were visualized via a Variable Mode Imager Typhoon 8600 (Amersham Pharmacia Biotech. ImageQuant software (GE) was used to quantify the band intensity.

2.8 Vesicle Motility Assays in Isolated Axoplasm

"Axoplasms were extruded from giant axons of the squid *Loligo pealii* (Marine Biological Laboratory) as described previously" (Brady et al., 1993; Morfini et al., 2013). "Gp120 IIIB or gp120 BaL were diluted into X/2 buffer (175 mM potassium aspartate, 65 mM taurine, 35 mM betaine, 25 mM glycine, 10 mM HEPES, 6.5 mM $MgCl_2$, 5 mM EGTA, 1.5 mM $CaCl_2$, 0.5 mM glucose, pH 7.2) supplemented with 2-5 mM ATP and 20 μl added to perfusion chambers. Preparations were analyzed on a Zeiss Axiomat with a 100X, 1.3 n.a. objective, and DIC optics. Hamamatsu Argus 20 and Model 2400 CCD camera were used for image processing and analysis. Organelle velocities were measured with a Photonics Microscopy C2117 video manipulator (Hamamatsu)." (Morfini et al. 2009) All experiments were repeated at least 3 times. The data from 30-50 min time points were pooled and statistically analyzed by one way ANOVA followed by the post-hoc Tukey's HSD for multiple comparisons. Quantitative data was expressed as mean ± SEM and significance was determined at $p<0.05$.

2.9 Primary Mouse Cortical Neuron Cultures

Cortices were dissected from C57BL6 mouse embryos at gestation day 17. Tissues were dissociated in 0.25% Trypsin in 1x Hank's Balanced Salt Solution (Invitrogen) for 10 minutes in a 37°C water bath. Cells were counted and plated at

80~100,000 cells/cm2 on Poly-L-Lysine (0.1mg/ml) coated plates. Cells were initially plated in MEM media containing 0.6% D-Glucose, 100U/ml Pen-Strep, and 5% fetal bovine serum. After 2-4 hours, culture media was changed to MEM media containing 0.6% D-Glucose, 100U/ml Pen-Strep, N2 and B27 supplements (Invitrogen), and culture was maintained under humidified atmosphere containing 5% CO2 at 37℃. One-third of the culture media was replaced every 3-4 days.

2.10 Microtubule Binding Assays

Microtubule binding assays were performed as described before (Morfini et al., 2006) with slight modifications. Primary mouse cortical neurons were scraped in HEPES80 (80mM HEPES, pH6.8, 1mM EGTA, 1μM Staurosporine, 50nM Okadaic Acid, 200nM Microcystin, and 1/100 protease inhibitor cocktail for mammalian tissue), and homogenized by passing the lysate through a 27G needle attached to a syringe three times and through a 30G needle twice. The lysate was centrifuged first at 14,000 RPM in a tabletop centrifuge for 1 minute at 4˚C and then at 55,000RPM in Optima TL centrifuge (Beckman for 5 minutes at 4˚C. The clarified lysate was incubated with 0.5mM adenylyl imidodiphosphate (AMP-PNP; Sigma), polymerized porcine tubulin, 20μM Taxol, and the appropriate effector for 30 minutes at 37˚C. The mixture was then loaded onto a 20% sucrose cushion and centrifuged at 50,000RPM for 20 minutes at 37˚C. The resulting supernatant and microtubule enriched pellet were analyzed with immunoblotting for kinesin and dynein.

CHAPTER IV

RESULTS

Berth, S., Morfini, G., Sarma T., Caicedo, H., Brady, S.T. (2015) Internalization and Axonal Transport of the HIV Glycoprotein gp120. ASN Neuro 7(1): pii: 1759091414568186

1. Determination of the Mechanisms of Internalization and Intracellular Location of Gp120.

1.1 Gp120 is Internalized by F11 Cells Over a Distinct Time Course.

Although it is commonly thought that gp120's neurotoxicity is due to binding to its coreceptor CXCR4 (Kaul et al., 2005), internalization of gp120 by certain neurons of the central nervous system was recently discovered (Bachis et al., 2003; Bachis et al., 2006). However, gp120 uptake by PNS neurons has not been established. As a result, this novel interaction of gp120 with neurons has not yet been examined in the context of DSP. Examining the mechanism of gp120 internalization by sensory neurons could lead to a new understanding of sensory neuron responses to gp120 in HIV infection, and provide insight to the development of DSP. To address this, F11 cells, which are rat DRG neurons hybridized with mouse neuroblastoma cells, were differentiated with dibutryl-cAMP (Ghil et al., 2000) and then treated with 70 nM fluorescein-conjugated gp120 IIIB. F11 cells were chosen due to their similar properties to DRG neurons, their ability to proliferate and differentiate, and to avoid heterogeneity of cell types observed in primary cultures. Z-stack images demonstrated that gp120 accumulated within the cell (Fig. 1*a-c*). A time-course study (Fig. 2*a-e*) indicated

Figure 1

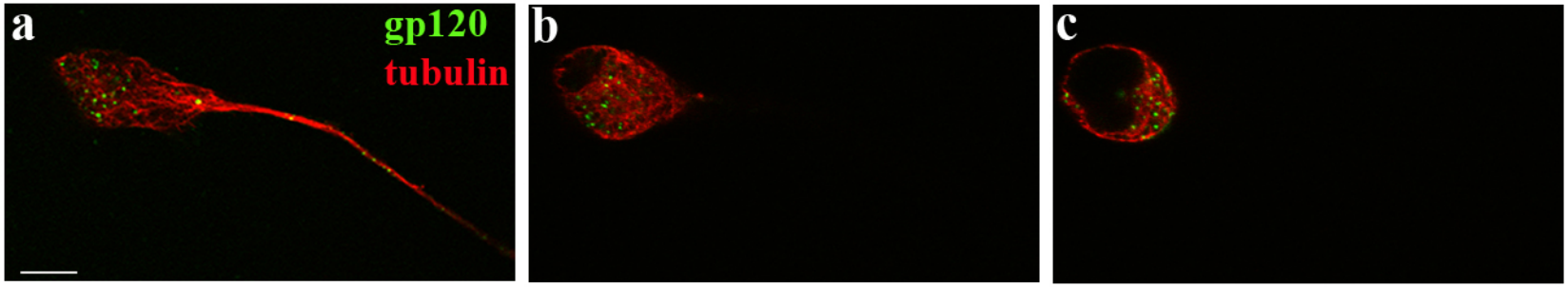

Figure 1. Gp120 is internalized by F11 cells.
Representative z-stack from a confocal microscopic analysis of F11 cells treated with fluorescein-gp120 for two hours, showing the bottom of the cell **(a)**, middle of the cell **(b),** and top of the cell **(c)**. Fluorescein-gp120 (green) accumulated in the perinuclear region of the middle slices of the cell, demonstrating that gp120 was internalized. Cells were also stained for tubulin (red). The scale bar denotes 10 μm.

Figure 2

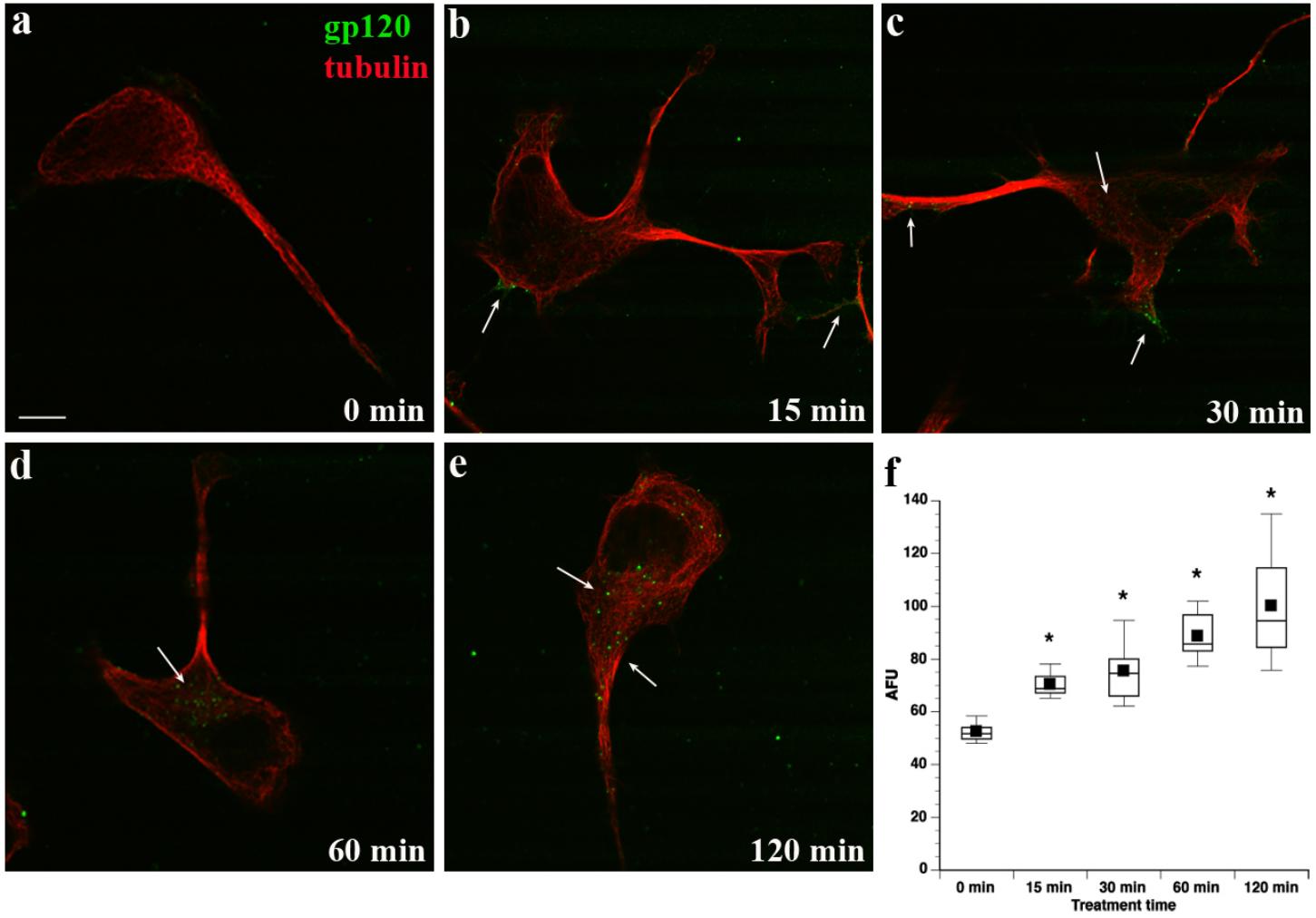
a
gp120
tubulin
0 min
b
15 min
c
30 min
d
60 min
e
120 min
f
AFU
140
120
100
80
60
40
20
0
0 min
15 min
30 min
60 min
120 min
Treatment time
*
*
*
*
*

Figure 2. F11 cells internalize gp120 with a distinct time course. F11 cells were treated with fluorescein-gp120 (green) for 0 minutes **(a),** 15 minutes **(b)**, 30 minutes **(c)**, 60 minutes **(d)** and 120 minutes **(e).** Arrows in **(b)** and **(c)** point to fluorescein-gp120 that has accumulated at the cell membrane and processes. By 30 minutes, gp120 begins to accumulate in perinuclear areas of the cell **(c)**, with the amount of perinuclear gp120 increasing at later time points **(d)** and **(e)**. Cells were stained for tubulin (red). The scale bar denotes 10 μm. Z-stacks were taken of at least 10 cells per time point on a laser scanning confocal microscope, and images were deconvolved and analyzed in Volocity for average fluorescence within each cell. Box plots were generated for each time point **(f)**. The amount of fluorescence significantly increased by 15 minutes of treatment (*$p<0.0001$), and continued to increase for the duration of the treatment **(f)**. that F11 cells began to internalize gp120 after 30 minutes (Fig. 2*c*) and internalized most gp120 by two hours (Fig. 2e). Gp120 was first localized within neuritic processes, and at later time points accumulated in the perinuclear region of the cell bodies. Gp120 internalization was quantitated from 0 minutes to 2 hours (Fig. 2*f*). A student's two-tailed t-test revealed that the amount of average fluorescence in each cell significantly increased after 15 minutes of treatment ($p<0.0001$), and continued to increase for the duration of the treatment, for up to two hours.

that F11 cells began to internalize gp120 after 30 minutes (Fig. 2*c*) and internalized most gp120 by two hours (Fig. 2e). Gp120 was first localized within neuritic processes, and at later time points accumulated in the perinuclear region of the cell bodies. Gp120 internalization was quantitated from 0 minutes to 2 hours (Fig. 2*f*). A student's two-tailed t-test revealed that the amount of average fluorescence in each cell significantly increased after 15 minutes of treatment ($p<0.0001$), and continued to increase for the duration of the treatment, for up to two hours.

1.2 Gp120 Internalization is Specific and Partially Dependent on Binding to CXCR4

To evaluate whether gp120 internalization was specific, fluorescein-gp120 was heat-inactivated by boiling for 1 hour, then used to treat F11 cells. Significantly, internalization was abrogated by heat-inactivation of gp120 (Fig. 3*b,d,e*), demonstrating that internalization of gp120 is activity-dependent. Since T-tropic gp120 binds to its coreceptor CXCR4 on DRG neurons (Apostolski et al., 1993; Oh et al., 2001), the necessity of this binding for internalization was evaluated. Immunocytochemistry experiments confirmed the presence of CXCR4 on the surface of F11 cells (data not shown). F11 cells were pre-treated with 2 μM AMD3100, a small molecule inhibitor of gp120 binding to CXCR4 (De Clercq et al., 1994; Donzella et al., 1998); then a time course experiment was performed using fluorescein-gp120. Pre-treatment of F11 cells with AMD3100 markedly reduced the amount of internalized gp120 (Fig. 3*c,d,e*) compared to no pre-treatment (Fig. 3*a*), although not to the extent that heat inactivation did (Fig.

3*d,e*). A one-way ANOVA was performed to determine the difference between the amount of gp120 internalized between the gp120 only group, the heat-inactivated gp120 group, and the AMD3100 pre-treated group. The p value was set at 0.05. The groups were found to be significantly different ($p<0.0001$), so a Tukey HSD test was performed to compare each group to each other. Each group was found to be statistically significantly different from each other ($p<0.0001$ for each comparison), confirming that AMD3100 pre-treatment partially reduces gp120 internalization, as opposed to heat-inactivation of gp120, which abrogates gp120 internalization. This indicates that a fraction of gp120 is internalized into F11 cells independently of binding to its co-receptor CXCR4.

1.3 Mechanisms of Gp120 Internalization

The highly punctate staining of fluorescein-conjugated gp120 (Fig. 1) suggested gp120 internalization through an endocytic mechanism. To evaluate this possibility, F11 cells were treated with fluorescein-conjugated gp120 for a time course over 4 hours, and then stained with antibodies recognizing markers of the early (EEA1) and late (LAMP2) endosomal/lysosomal compartment. However, Gp120 did not colocalize with either EEA1 (Fig. 4) or LAMP2 (Fig. 5) throughout the entire time course, ruling out the common endolysosomal pathway for internalization. To analyze colocalization, the Pearson's correlation coefficient was used to quantify the intensity of correlation between red and green channels (Table IV). Colocalization Coefficient M1 and Colocalization Coefficient M2 were calculated to determine the fraction of green that overlapped

Figure 3

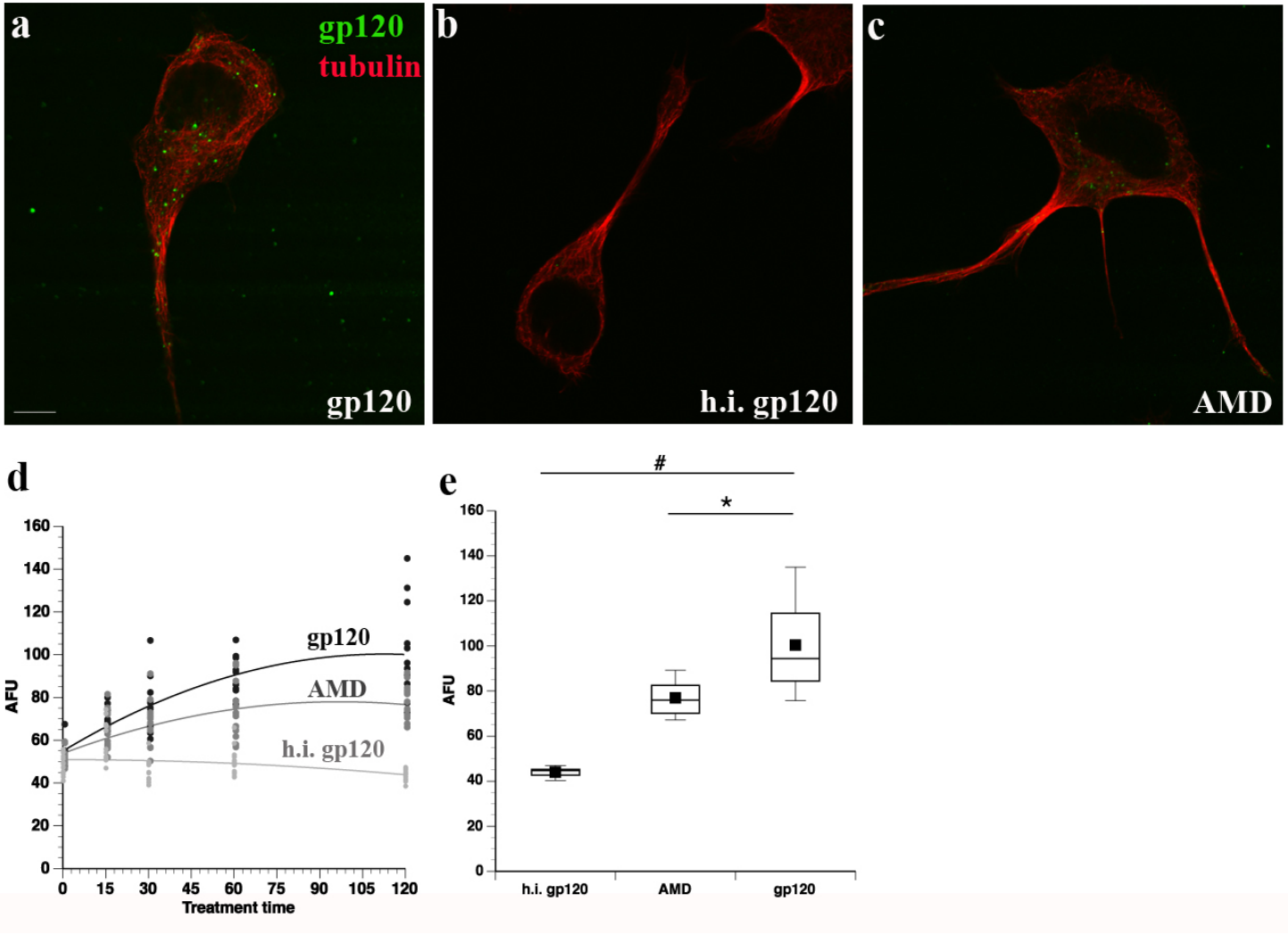
a
gp120
tubulin
gp120
b
h.i. gp120
c
AMD
d
AFU
Treatment time
gp120
AMD
h.i. gp120
e
#
*
AFU
h.i. gp120
AMD
gp120

Figure 3. Gp120 internalization is abolished by heat inactivation and reduced by AMD3100 treatment. Time courses were performed on F11 cells that had been treated with heat-inactivated (h.i.) gp120 or pre-treated with 2 μm AMD3100 for 1 hour. A representative image of a cell treated with heat-inactivated fluorescein-gp120 for 2 hours is shown in **(b).** Heat inactivation prevented internalization of fluorescein-gp120 by F11 cells, demonstrating that internalization is specific to gp120's activity. To determine if gp120 internalization was dependent on gp120 binding to its coreceptor CXCR4, F11 cells were pre-treated with 2 μm AMD3100 for one hour to block gp120 binding to its co-receptor CXCR4 before the time course of treatment with fluorescein-gp120 was performed. A representative image of a F11 cell pre-treated with AMD3100, then co-treated with fluorescein-gp120 and AMD3100 for 2 hours is shown in **(c)**. AMD3100 treatment reduced gp120 internalization, demonstrating that internalization of gp120 is dependent on binding to CXCR4. However, the partial reduction of internalization indicates that gp120 is internalized through a mechanism independent of CXCR4. A representative image of a F11 cell that was not pre-treated or heat-inactivated and treated with fluorescein-gp120 for 2 hours is shown in **(a)** for comparison. Cells were stained for tubulin (red). The scale bar denotes 10 μm. Z-stacks were taken of at least 10 cells per time point on a laser scanning confocal microscope, and images were deconvolved and analyzed in Volocity for average fluorescence within each cell **(d)**. Each circle denotes an individual measurement. The time course of heat-inactivated gp120 (light gray) is compared to the time course of gp120 pre-treated with AM3100 (dark gray) and fluorescein-gp120 treatment (black) in **(d)**. The box plots show quantitation of gp120 internalization after two hours of treatment. Both AMD3100 pre-treatment and heat inactivation of gp120 significantly reduced the amount of gp120 internalization to varying extents **(e)**. *$p<0.005$, #$p<0.0001$.

with red (Colocalization Coefficient M1; Table V), and the fraction of red that overlapped with green (Colocalization Coefficient M2; Table VI; Manders, 1993). These three colocalization variables were obtained for all colocalization experiments.

Next, fluid phase pinocytosis was assessed as a mechanism for gp120 internalization. To this end, differentiated F11 cells were treated with fluorescein-gp120 and rhodamine-dextran (MW 10,000), a marker of fluid phase pinocytosis. Significantly, partial colocalization between gp120 and dextran was observed (Fig. 6, Tables IV-VI), indicating that at least a small fraction of extracellular gp120 is internalized into F11 cells through fluid phase pinocytosis.

Since gp120 did not internalize through the common endolysosomal pathway and fluid phase pinocytosis only accounted for a fraction of total gp120 internalized, we hypothesized that gp120 is also internalized through lipid raft-mediated endocytosis, another non-clathrin-mediated process (Lajoie and Nabi, 2010). Gp120 and its receptors cluster in lipid rafts (Popik et al., 2002), and this clustering is important for HIV infection (Kamiyama et al., 2009). Consistent with this possibility, internalized fluorescein-gp120 was found to colocalize with cholera toxin B (Fig. 7, Tables IV-VI).

To further evaluate this possibility, cholesterol was depleted with 5 mM methyl-β–cyclodextrin (CD) for 20 minutes to disrupt lipid rafts in differentiated F11 cells, and a 2 hour time course of fluorescein-gp120 internalization was performed. CD significantly decreased the amount of gp120 internalization after

Figure 4

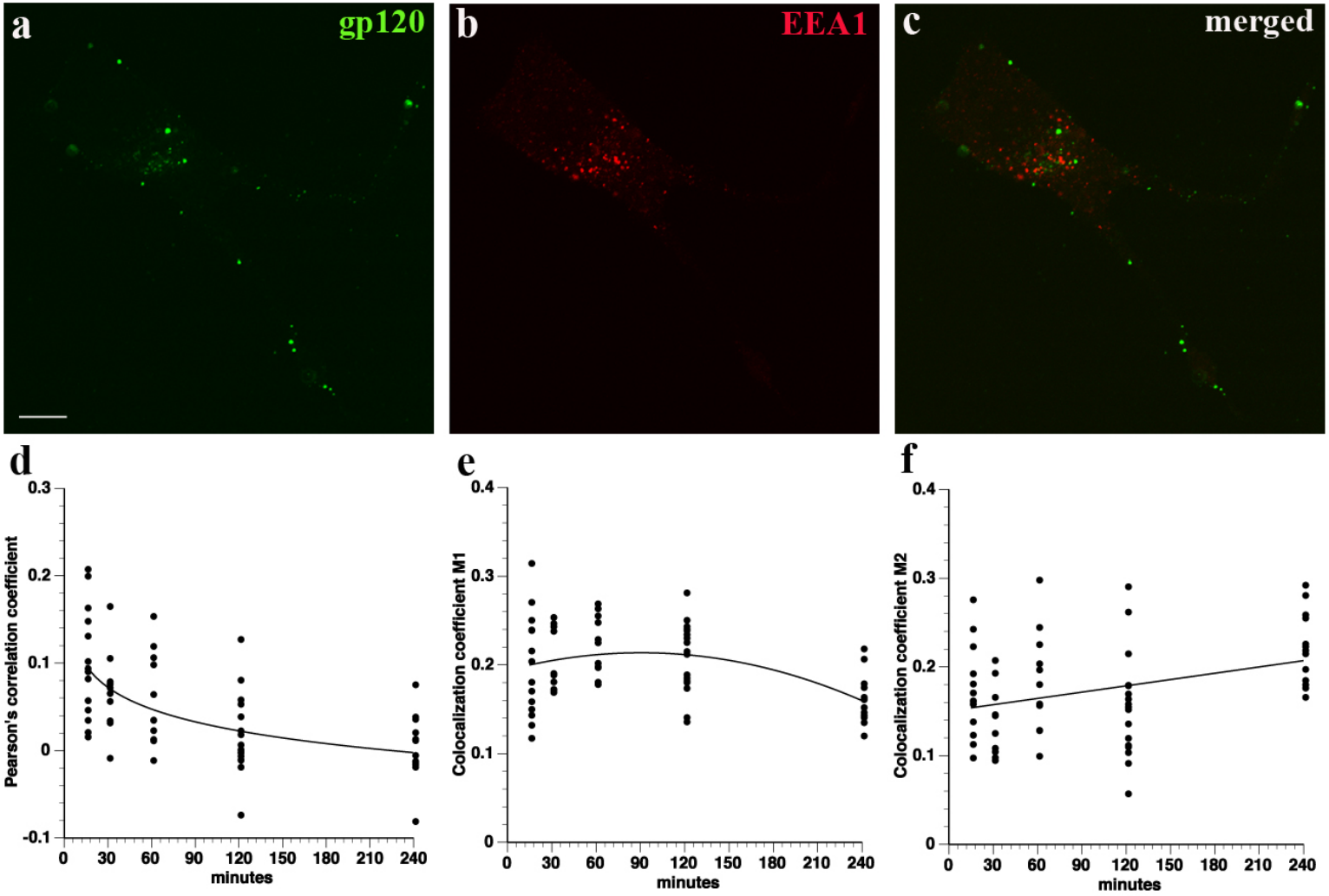
a
gp120
b
EEA1
c
merged
d
Pearson's correlation coefficient
0.3
0.2
0.1
0
-0.1
0 30 60 90 120 150 180 210 240
minutes
e
Colocalization coefficient M1
0.4
0.3
0.2
0.1
0
0 30 60 90 120 150 180 210 240
minutes
f
Colocalization coefficient M2
0.4
0.3
0.2
0.1
0
0 30 60 90 120 150 180 210 240
minutes

Figure 4. Gp120 does not colocalize with EEA1. A time course of fluorescein-gp120 internalization by F11 cells was performed, and cells were stained with an antibody for EEA1. The scale bar denotes 10 μm. A representative image of a F11 cell treated for two hours is shown in **(a-c)**. Note noncolocalization in **(c)** between green and red channels. Z-stacks were taken of at least 10 cells per time point on a laser scanning confocal microscope, and images were deconvolved and analyzed for colocalization in Volocity. The Pearson's correlation coefficient **(d)**, Colocalization coefficient M1 (green channel; **(e)**) and Colocalization coefficient M2 (red channel; **(f)**) all show very low values, demonstrating that fluorescein-gp120 does not colocalize with EEA1. Since EEA1 is a marker of early endosomes in the common endosomal pathway, this demonstrates that gp120 is not internalized through the common endosomal pathway.

Figure 5

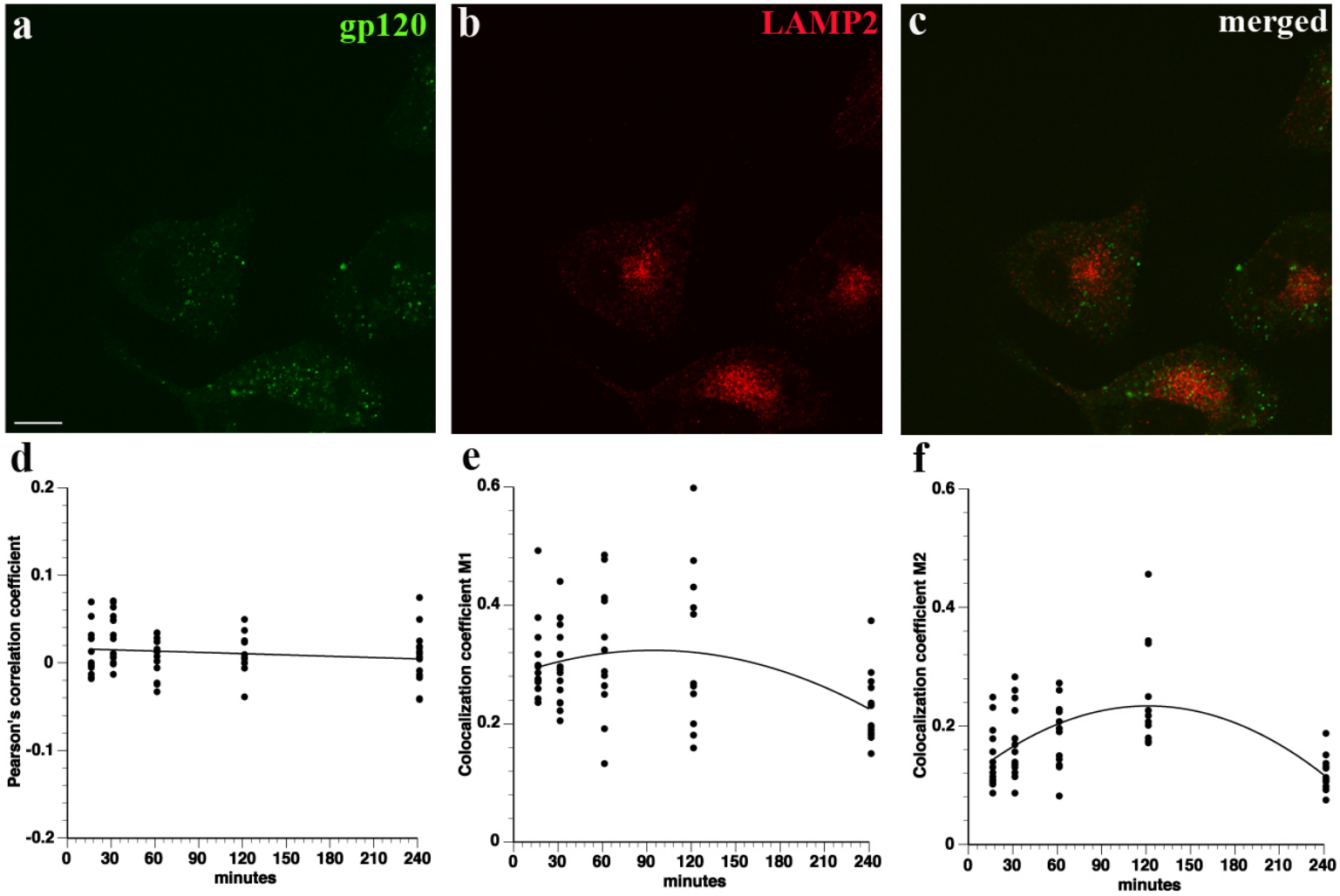
a
gp120
b
LAMP2
c
merged
d
Pearson's correlation coefficient
0.2
0.1
0
-0.1
-0.2
0 30 60 90 120 150 180 210 240
minutes
e
Colocalization coefficient M1
0.6
0.4
0.2
0
0 30 60 90 120 150 180 210 240
minutes
f
Colocalization coefficient M2
0.6
0.4
0.2
0
0 30 60 90 120 150 180 210 240
minutes

Figure 5. Gp120 does not colocalize with LAMP2. A time course of fluorescein-gp120 (green) internalization by F11 cells was performed, and cells were stained with an antibody for LAMP2 (red). The scale bar denotes 10 μm. A representative image of a F11 cell treated for two hours is shown in **(a-c)**. Note the lack of colocalization in **(c)** between green and red channels. Z-stacks were taken of at least 10 cells per time point on a laser scanning confocal microscope, and images were deconvolved and analyzed for colocalization in Volocity. The Pearson's correlation coefficient **(d)**, Colocalization coefficient M1 (green channel; **(e)**) and Colocalization coefficient M2 (red channel; **(f)**) all show very low values, demonstrating that fluorescein-gp120 does not colocalize with LAMP2. Since LAMP2 is a marker of lysosomes in the common endosomal pathway, this indicates that gp120 is not internalized through the common endosomal pathway.

Figure 6

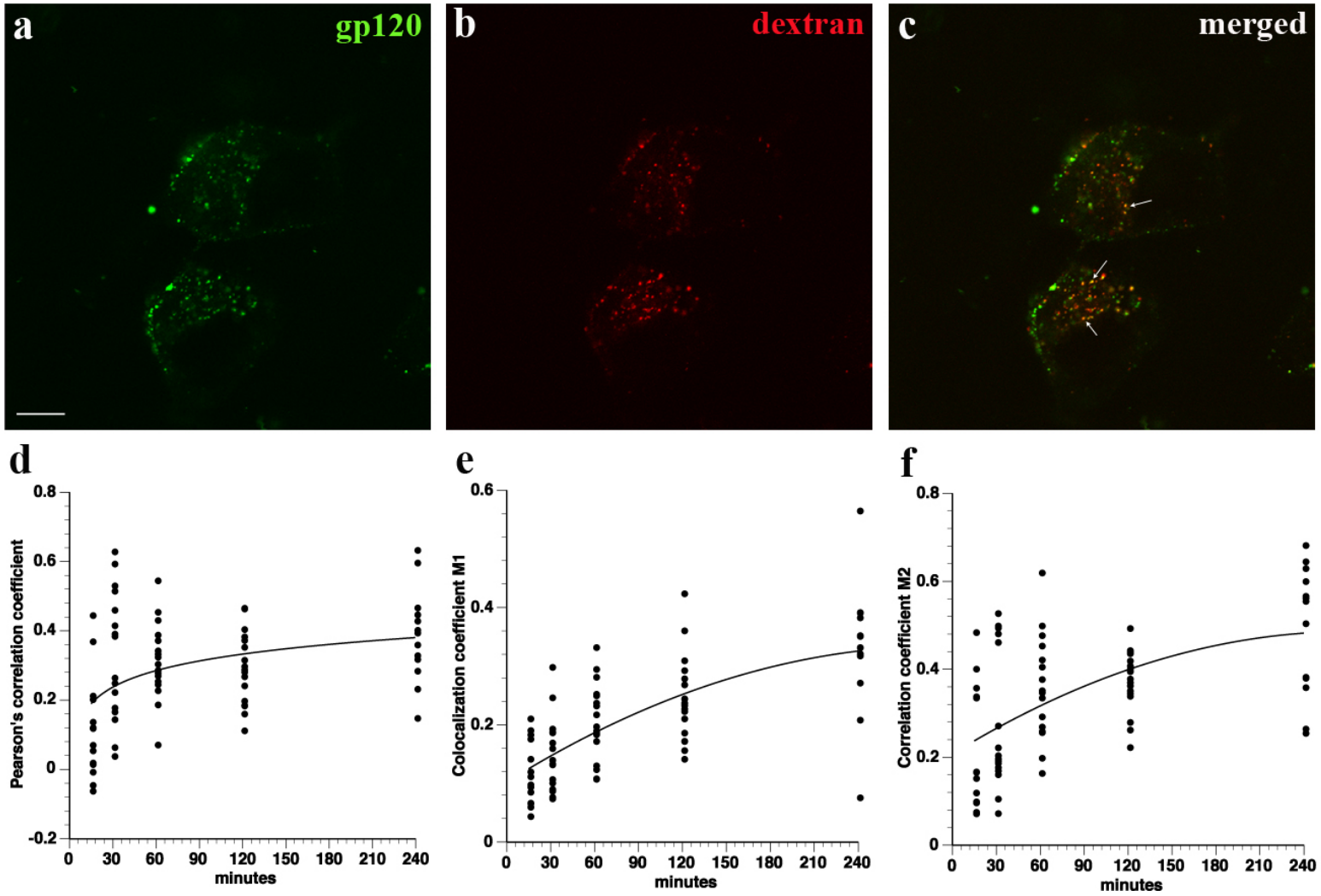
a
gp120
b
dextran
c
merged
d
Pearson's correlation coefficient
minutes
e
Colocalization coefficient M1
minutes
f
Correlation coefficient M2
minutes

Figure 6. Gp120 partially colocalizes with dextran. F11 cells were co-treated with fluorescein-gp120 (green) and rhodamine-dextran (red), and a time course of internalization was performed. The scale bar denotes 10 μm. A representative image of a F11 cell treated for two hours is shown in **(a-c)**. Note the partial colocalization in **(c)** between green and red channels. Arrows in **(c)** point to colocalized puncta. Z-stacks were taken of at least 10 cells per time point on a laser scanning confocal microscope, and images were deconvolved and analyzed for colocalization in Volocity. The Pearson's correlation coefficient **(d)**, Colocalization coefficient M1 (green channel; **(e)**) and Colocalization coefficient M2 (red channel; **(f)**) all show values indicative of partial colocalization between gp120 and dextran. Since dextran is a marker of fluid phase pinocytosis, this demonstrates that a component of gp120 is internalized through fluid phase pinocytosis.

Figure 7

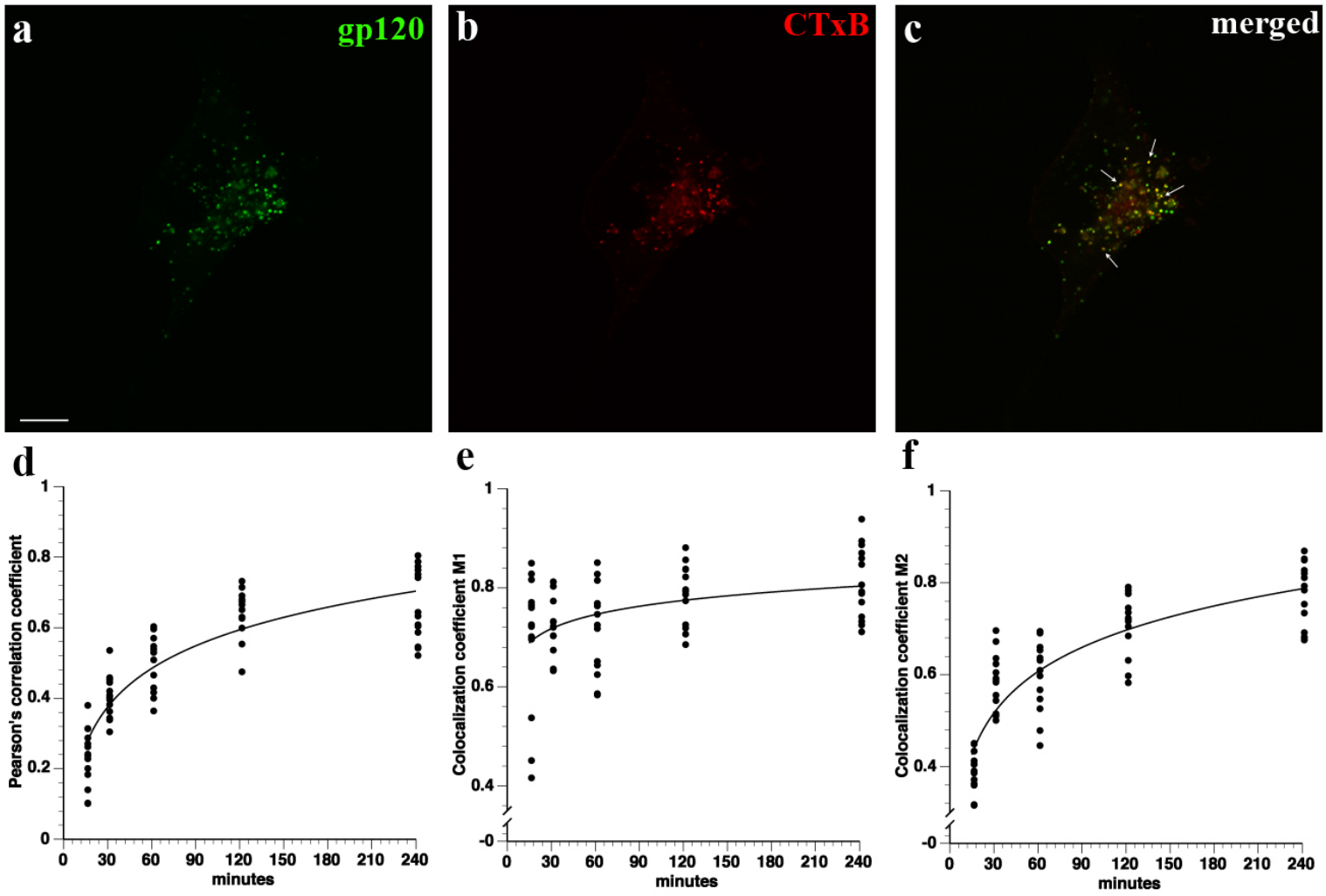
a
gp120
b
CTxB
c
merged
d
Pearson's correlation coefficient
minutes
e
Colocalization coefficient M1
minutes
f
Colocalization coefficient M2
minutes

Figure 7. Gp120 partially colocalizes with cholera toxin B. F11 cells were co-treated with fluorescein-gp120 (green) and Alexa Fluor 594-cholera toxin B (red), and a time course of internalization was performed. The scale bar denotes 10 μm. A representative image of a F11 cell treated for two hours is shown in **(a-c)**. Note the colocalization in **(c)** between green and red channels. Arrows in **(c)** point to colocalized puncta. Z-stacks were taken of at least 10 cells per time point on a laser scanning confocal microscope, and images were deconvolved and analyzed for colocalization in Volocity. The Pearson's correlation coefficient **(d)**, Colocalization coefficient M1 (green channel; **(e)**) and Colocalization coefficient M2 (red channel; **(f)**) all show values indicative of colocalization between gp120 and cholera toxin B, especially by 2 hours treatment. Since cholera toxin B is a marker of internalization through lipid rafts, this indicates that gp120 is also internalized through lipid rafts.

Table IV. Comparison of Average Pearson's Correlation Coefficient for Gp120 and Various Endocytic Markers

Treatment time	EEA1	LAMP2	Dextran	CTxB
0 min	0.004	-0.010	0.030	0.111
15 min	0.098	0.012	0.114	0.230
30 min	0.067	0.026	0.325	0.404
60 min	0.058	0.002	0.309	0.488
120 min	0.015	0.009	0.288	0.641
240 min	0.001	0.006	0.384	0.662

Table V. Comparison of Average Colocalization Coefficient M1 for Gp120 and Various Endocytic Markers

Treatment time	EEA1	LAMP2	Dextran	CTxB
0 min	0.126	0.295	0.046	0.500
15 min	0.198	0.304	0.115	0.695
30 min	0.203	0.295	0.146	0.725
60 min	0.058	0.294	0.203	0.713
120 min	0.015	0.326	0.241	0.784
240 min	0.001	0.224	0.328	0.810

Table VI. Comparison of Average Colocalization Coefficient M2 for Gp120 and Various Endocytic Markers

Treatment time	EEA1	LAMP2	Dextran	CTxB
0 min	0.074	0.058	0.035	0.178
15 min	0.172	0.146	0.207	0.380
30 min	0.138	0.171	0.273	0.584
60 min	0.182	0.238	0.359	0.593
120 min	0.155	0.250	0.372	0.705
240 min	0.220	0.115	0.489	0.771

30 minutes (Fig. 8*b-d*) compared to untreated cells (Fig. 8*a,c,d*). In a concurrent experiment, CD treatment did not decrease the amount of transferrin that was internalized (Fig. 8*e*), demonstrating that this effect was specific to lipid rafts and did not impair clathrin-mediated internalization. Taken together, these experiments indicated that the major mechanism for gp120 internalization is through lipid raft-mediated endocytosis.

1.4 Gp120 is Transported Retrogradely, but not Anterogradely, Along Dorsal Root Ganglion Neuron Axons

A number of viral proteins have the capability to highjack the host axonal transport machinery to travel and access different compartments within the cell (Berth et al., 2009). Having established internalization of gp120 by DRG neurons, and considering the extreme degree of polarization that is characteristic of these cells, we examined axonal transport of gp120 using compartmentalized microfluidic devices as described in (Caicedo et al, in preparation). These devices connect chambers using nanofabricated microgrooves small enough such that only axons can grow through. Primary neurons are plated in the somatodendritic compartments (SDC), and then their axons grow through the microgrooves into the axonal terminal compartment (ATC). These devices exhibit fluidic isolation, due to the central channel and 2 rows of microgrooves. Also, volume differences to create a pressure gradient to allow fluidic isolation are easily maintained, since one chamber is larger than the other. This leads to a volume difference of 200 μL between each compartment.

Figure 8

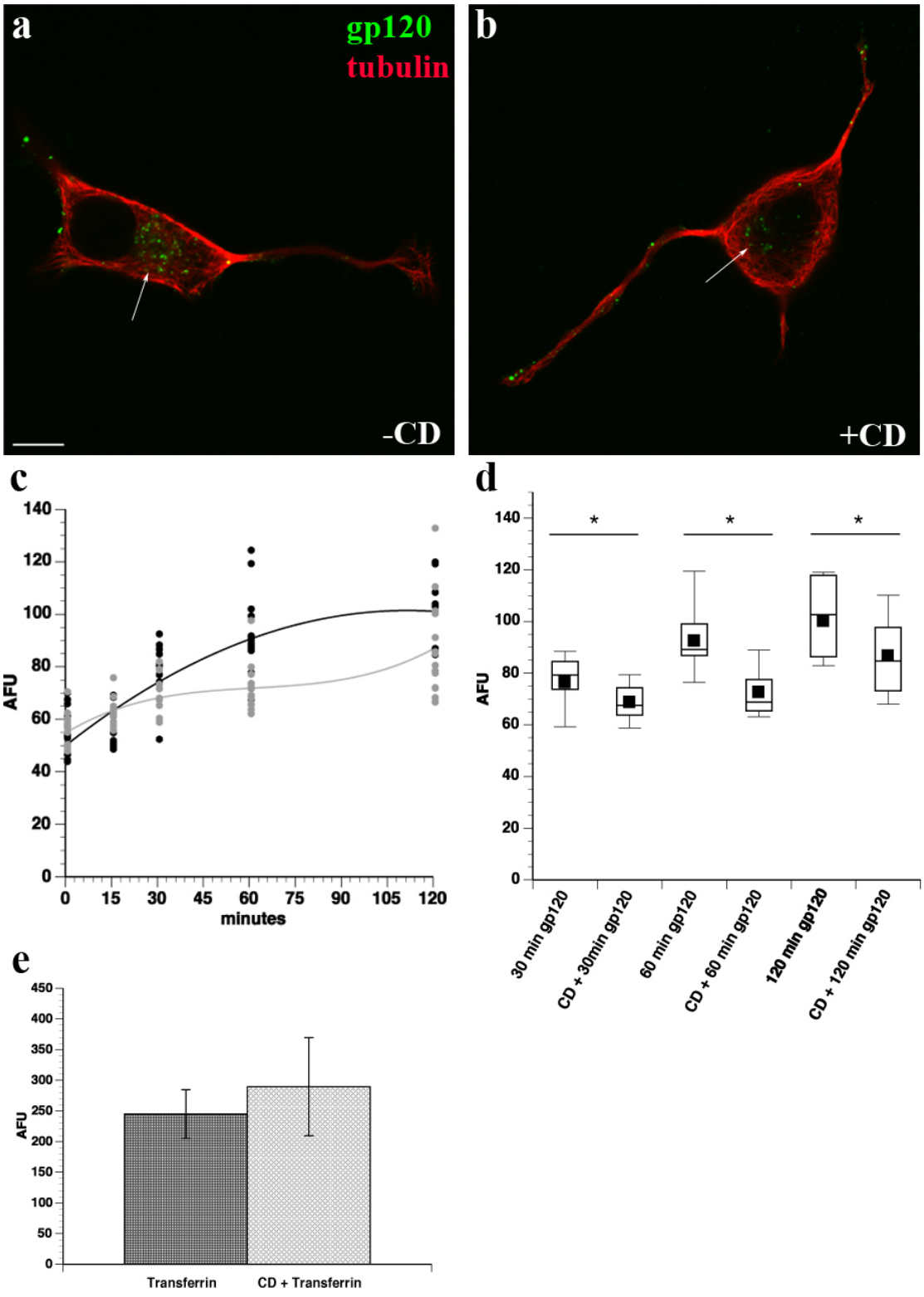
a
gp120
tubulin
-CD
b
+CD
c
AFU
minutes
0
15
30
45
60
75
90
105
120
d
AFU
*
*
*
30 min gp120
CD + 30min gp120
60 min gp120
CD + 60 min gp120
120 min gp120
CD + 120 min gp120
e
AFU
Transferrin
CD + Transferrin

Figure 8. Cyclodextrin treatment reduces internalization of gp120. F11 cells were pre-treated with 5 mM methyl-β-cyclodextrin (CD) for 20 minutes to disrupt lipid rafts, and then a time course of internalization of fluorescein-gp120 was performed. The scale bar denotes 10 μm. Representative images of cells treated with fluorescein-gp120 for two hours with or without CD pre-treatment are shown **(a-b**), with DM1A staining for tubulin to show the outline of the cell. Compared to F11 cells that were not pre-treated **(a)**, F11 cells pre-treated with cyclodextrin had a reduced amount of gp120 internalization **(b)**. Z-stacks were taken of at least 10 cells per time point on a laser scanning confocal microscope, and images were deconvolved and analyzed in Volocity for average fluorescence in each cell. Pre-treatment of 5 mM CD for 20 minutes was sufficient to disrupt internalization through lipid rafts, as evidenced by the decreased amount of cholera toxin B internalization after two hours **(c)**. *$p<0.05$. Each measurement of individual cells is plotted in **(c)**, with gray denoting pre-treatment with CD and black denoting no pre-treatment. Box plots demonstrate that internalization of gp120 was significantly reduced at the 30, 60 and 120 minute timepoints, further confirming that gp120 is internalized through lipid rafts **(d)**. Pre-treatment of 5 mM CD for 20 minutes was insufficient to disrupt internalization through the clathrin-mediated pathway, as evidenced by the lack of inhibition of transferrin internalization after pre-treatment with CD **(e)**.

Primary DRG neurons were seeded in SDC compartment to fluidically isolate the cell bodies and dendrites from the axonal compartment. After this, 70 nM fluorescein-gp120 was added to the ATC compartment of mature DRG neurons for 4 hours. Neurons were then fixed, stained with the DM1A antibody, and the microfluidic grooves and SDC were examined for fluorescein-gp120. As shown in Fig. 9*a*, fluorescein-gp120 was found along axons in the microfluidic grooves and within cell bodies in the SDC, demonstrating that gp120 had been internalized and retrogradely transported along axons into neuronal cell bodies. Further, the time course of the experiment indicate that gp120 was transported by fast, and not slow axonal transport, a microtubule motor-dependent process (Morfini, 2006). Anterograde transport was examined by adding 70 nM fluorescein-gp120 for 4 hours to the SDC compartment. As shown in Fig. 9*b*, the microfluidic grooves and ATC compartment lacked fluorescein-gp120, revealing that gp120 does not undergo anterograde transport in DRG neurons.

Figure 9

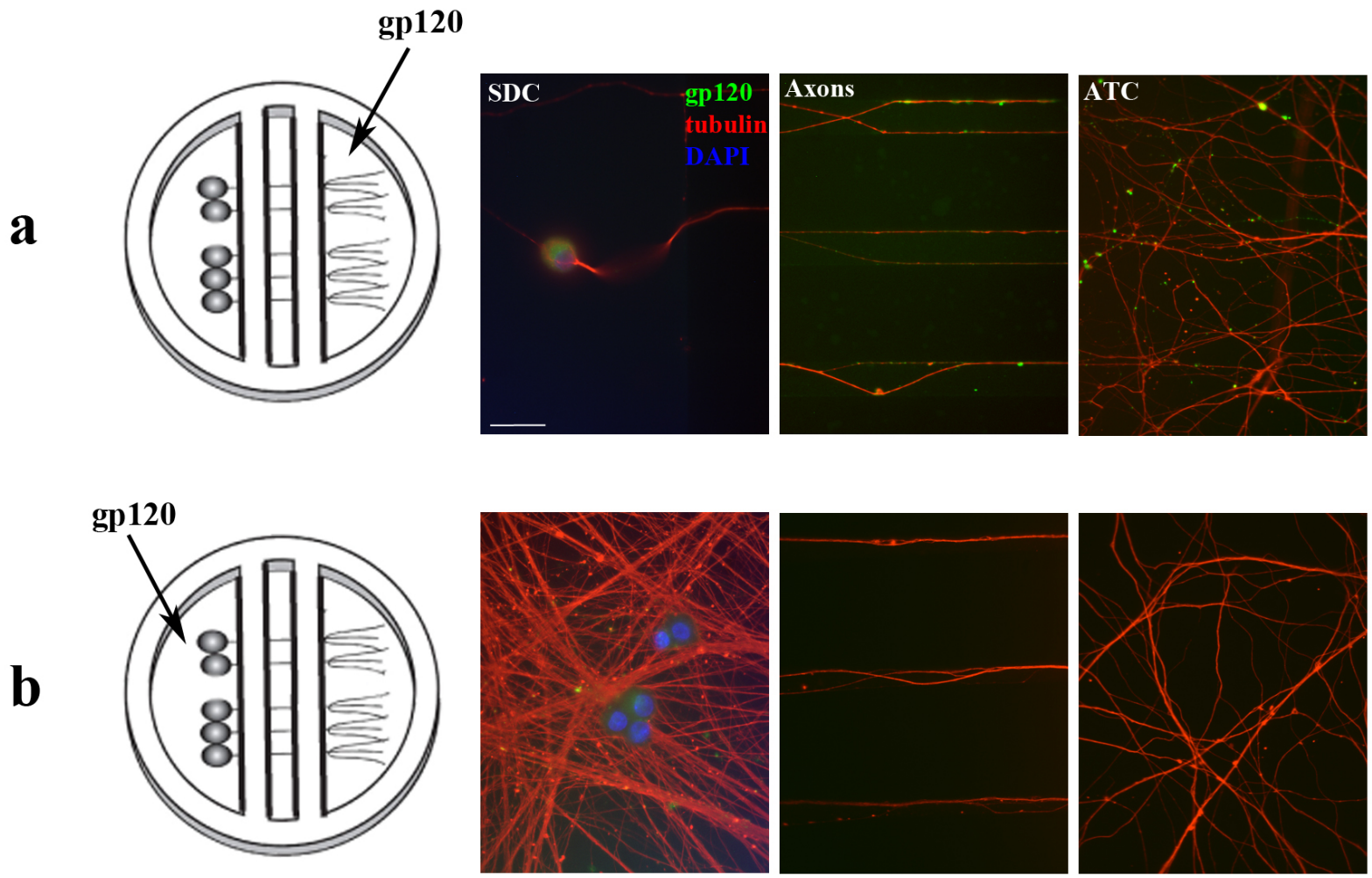

Figure 9. Internalized gp120 utilizes retrograde but not anterograde transport along DRG axons. Primary DRG neurons were grown in compartmentalized microfluidic devices. To examine retrograde transport, DRG neurons were seeded in the larger compartment to fluidically isolate cell bodies. The ATC compartment was treated with 70 nM gp120 for 4 hours, and then the cells were fixed and stained with DM1A for tubulin **(a)**. The left panel of **(a)** is a schematic of the devices, and the images to the right are representative images of DRG neurons. The scale bar denotes 15 μM. Note that after 4 hours of treatment, gp120 is apparent within the microfluidic grooves as well as cell bodies in the SDC, demonstrating that gp120 has been transported from the ATC to the SDC. Next, DRG neurons were seeded in the smaller compartment to fluidically isolate their axons. The SDC was treated with 70 nM gp120 for 4 hours, and then the cells were fixed and stained with DM1A for tubulin **(b)**. The left panel of **(b)** is a schematic of the devices, and the images to the right are representative images of DRG neurons. Fluorescein-gp120 was not detected in the microfluidic grooves or in the ATC, revealing that gp120 was not transported in the anterograde direction from the SDC to the ATC.

2. Identification of Intra-axonal Signaling Pathways Underlying Gp120-induced Alterations in Fast Axonal Transport.

2.1 CXCR4 Involvement in the Activation of p38 MAPK by Gp120

Previous studies of DSP have indicated that gp120 binding to CXCR4 activates signaling cascades, including ones that lead to activation of JNK and p38 MAPK (Bodner et al., 2004) (Wilkerson et al., 2012). The interpretation has been that gp120 binding leads to activation of CXCR4, a GPCR, thus leading to activation of signaling cascades (Oh et al., 2001). We chose to further explore the mechanism of activation of p38 MAPK. To do so, a time course was performed in which differentiated F11 cells were treated with 5 nM gp120. It was found that gp120 activated p38 MAPK in differentiated F11 cells after 5 minutes of treatment, which was subsequently deactivated at the later time points of 15 minutes and 30 minutes (Fig. 10). Next, to examine the role of CXCR4 activation, differentiated F11 cells were pre-treated with 2 μM AMD3100, a small molecule bicyclam that inhibits binding of gp120 to CXCR4 (De Clercq et al., 1994; Donzella et al., 1998), for 1 hour at 37°C prior to performing the same time course with 5 nM gp120 and 2 μM AMD3100. The AMD3100 pre-treatment abolished activation of p38 MAPK after treatment of differentiated F11 cells with gp120 for 5 minutes, demonstrating that activation of p38 MAPK after 5 minutes of treatment is due to CXCR4 activation (Fig. 10). Intriguingly, in F11 cells that had been pre-treated with AMD3100, activation of p38 MAPK was increased after 30 minutes of treatment (Fig. 10), demonstrating a CXCR4-independent activation of p38 MAPK by gp120 treatment.

Figure 10

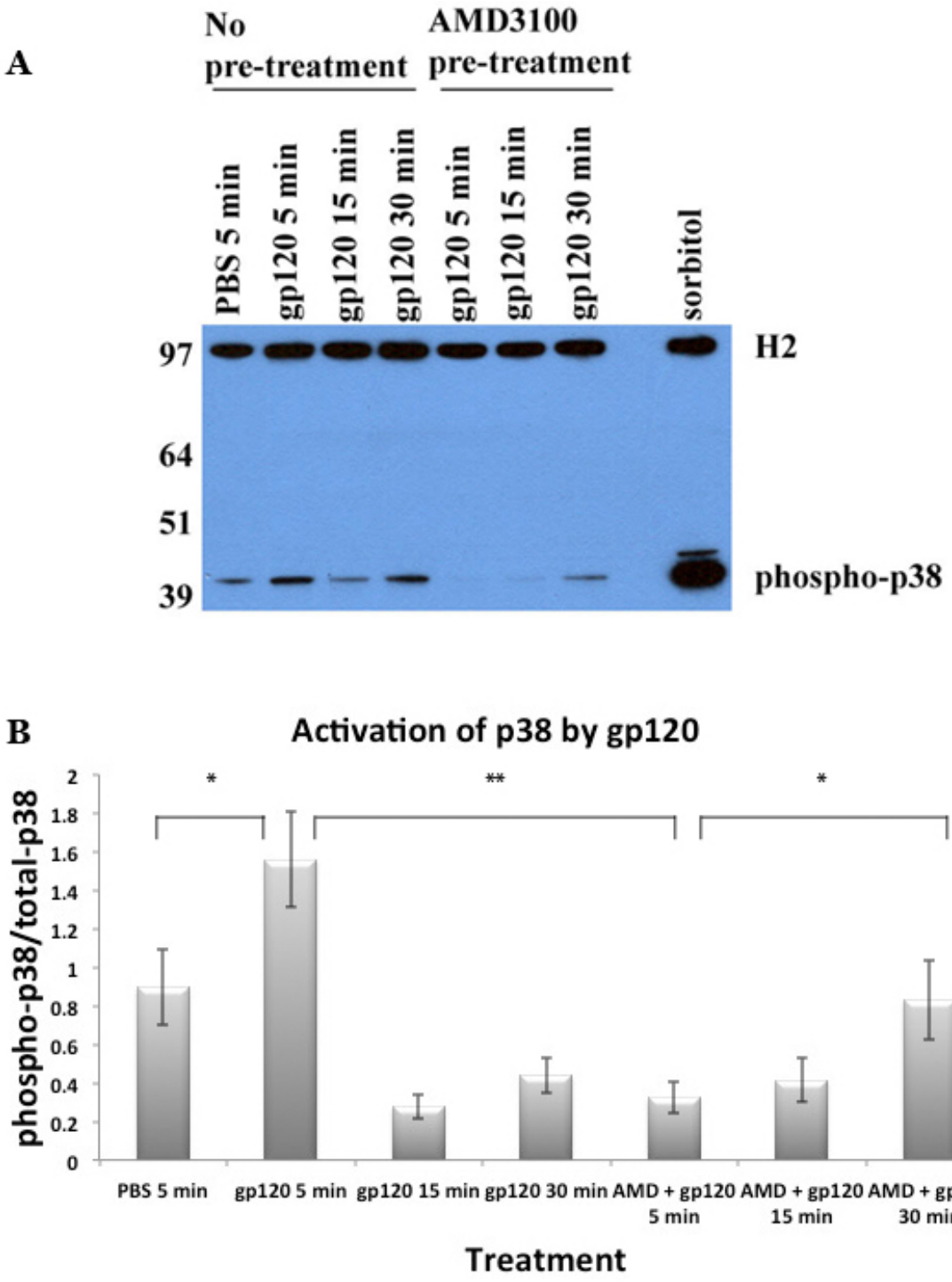
A
No pre-treatment
AMD3100 pre-treatment
PBS 5 min
gp120 5 min
gp120 15 min
gp120 30 min
gp120 5 min
gp120 15 min
gp120 30 min
sorbitol
97
64
51
39
H2
phospho-p38
B
Activation of p38 by gp120
phospho-p38/total-p38
2
1.8
1.6
1.4
1.2
1
0.8
0.6
0.4
0.2
0
*
**
*
PBS 5 min
gp120 5 min
gp120 15 min
gp120 30 min
AMD + gp120 5 min
AMD + gp120 15 min
AMD + gp120 30 min
Treatment

Figure 10. Activation of p38 MAPK by gp120 treatment.
(**a)** Representative Western blot of F11 of cell lysates of differentiated F11 cells treated with 5 nM gp120. A phospho-specific antibody for p38 (Cell Signaling #9215) demonstrated an increased phosphorylation of p38 at 5 minutes, which subsequently decreased in future time points. AMD3100 pre-treatment blocked the phosphorylation of p38 at 5 minutes, demonstrating that this quick activation of p38 was due to CXCR4 activation. However, in the AMD3100 pre-treatment condition, the amount of phosphorylation of p38 significantly increased after 30 minutes of treatment, unmasking an activation of p38 at a later time point. H2 (a KHC antibody) was used as a loading control. The negative control was treatment with the same volume of diluent, and 0.5M treatment of F11 cells with sorbitol was used as a positive control. The chart **(b)** shows the result of quantification of phospho-p38 levels, which were expressed as a ratio to total p38 levels. Values are the mean $\pm$ SEM; n = 16 independent experiments. The student's t-test was used to determine significance. * denotes $p<0.05$; ** denotes $p<0.0001$

2.2 Gp120 Impairs Fast Axonal Transport in Isolated Squid Axoplasm

Since AMD3100 treatment unmasked the activation of p38 MAPK in F11 cells, we hypothesized that intracellular gp120 that had been internalized in a pathway independent of CXCR4 might be responsible for the kinase activation. Because DSP has the same phenotype of dying-back neuropathy as seen in dysferopathies, we chose to test whether intracellular gp120 might also cause dysregulation of FAT.

The use of axoplasm from the squid *Loligo peali* is instrumental in defining the signaling pathways that regulate fast axonal transport rates (Brady et al., 1985; Brady et al., 1993). Axoplasms can be extruded from individual axons onto a coverslips with glass spacers, creating a perfusion chamber for addition of various proteins and inhibitors. Then video enhanced contrast-differential interference contrast (VEC-DIC) microscopy is performed, and fast axonal transport is tracked using a calibrated cursor.

Perfusion of 10 nM gp120 profoundly impaired FAT, both in anterograde and retrograde directions (Fig. 11*b*). To examine whether this effect was specific to gp120's activity, gp120 was heat-inactivated by boiling at 100 degrees Celsius for one hour, and then 10 nM of heat-inactivated gp120 was perfused into squid axoplasm. The heat-inactivated gp120 had no inhibitory effect on transport (Fig. 11*a*). Statistical comparison between 10 nM gp120 and 10 nM heat-inactivated gp120 revealed a significant difference between both anterograde and retrograde FAT velocities (Fig. 11*e*).

Next, 100 pM of gp120 was perfused to see if a lower, more physiologically relevant concentration of gp120 might still have an effect on FAT (Figure 11*c*). In fact, 100 pM gp120 also impaired FAT in both directions compared to heat inactivated gp120 (Figure 11*c,e*)**.**

There have been some studies that suggest that neurotoxicity differs between gp120 strains that prefer the co-receptor CXCR4 and those that prefer the co-receptor CCR5 (Bachis et al., 2009; Bachis et al., 2010), so we chose to compare the inhibition of FAT between gp120 IIIB, which binds to CXCR4, and gp120 BaL, a CCR5-preferring strain**.** 10 nM gp120 BaL showed similar impairments of FAT to 10 nM gp120 IIIB (Figure 11*d,e*) compared to heat inactivated gp120, demonstrating that the ability to inhibit of FAT is conserved across gp120 strains**.**

2.3 Gp120 Activates p38 MAPK and JNK to Impair Fast Axonal Transport

Previous work has established that FAT is regulated by phosphotransferases (Morfini et al., 2002; Morfini et al., 2006; Morfini et al., 2009), so it was hypothesized that gp120 might impair FAT through altering regulatory enzymatic activity. To define which signaling pathways that gp120 activated to impair fast axonal transport,

Figure 11

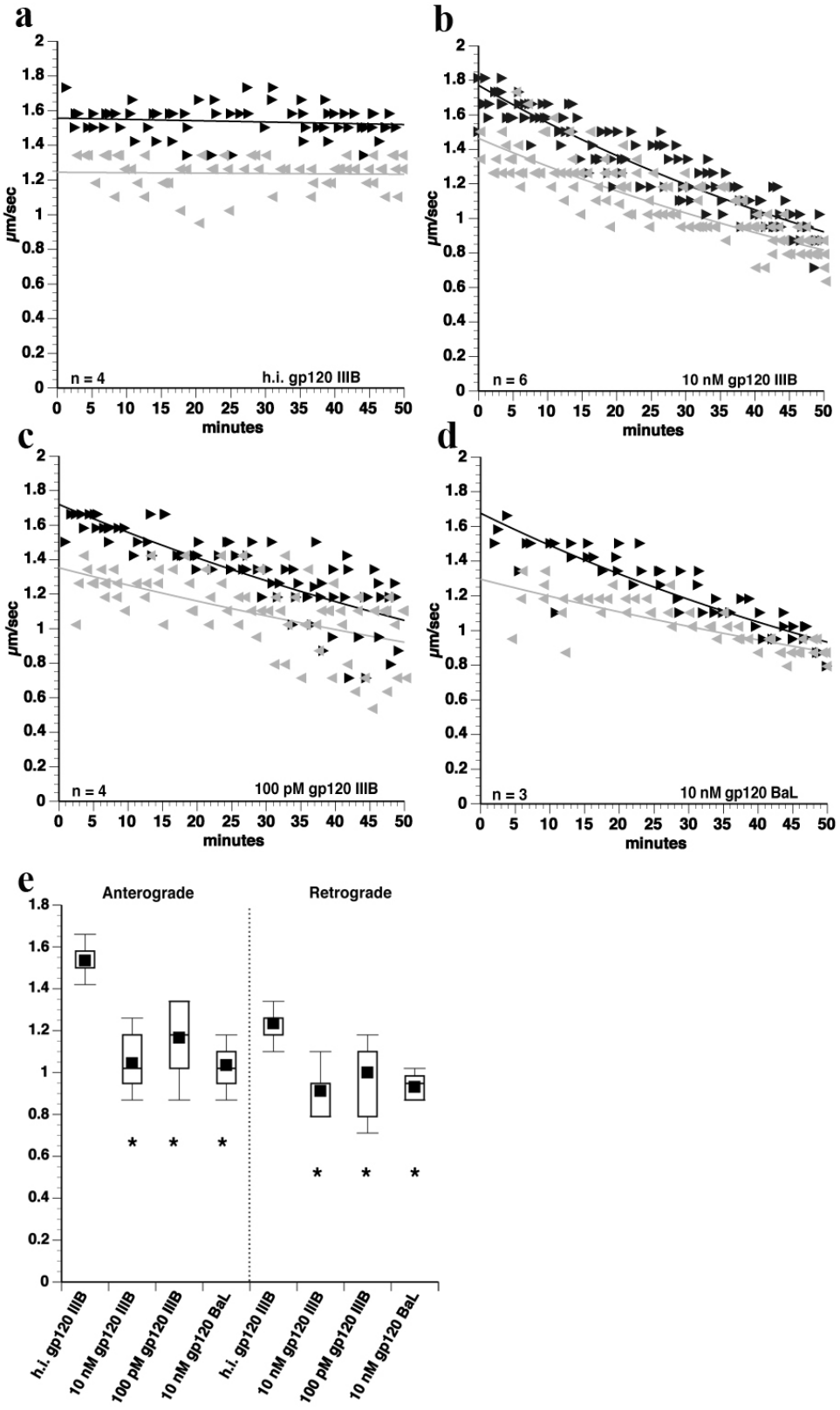
a
b
c
d
e
µm/sec
minutes
n = 4
h.i. gp120 IIIB
n = 6
10 nM gp120 IIIB
n = 4
100 pM gp120 IIIB
n = 3
10 nM gp120 BaL
Anterograde
Retrograde
h.i. gp120 IIIB
10 nM gp120 IIIB
100 pM gp120 IIIB
10 nM gp120 BaL
h.i. gp120 IIIB
10 nM gp120 IIIB
100 pM gp120 IIIB
10 nM gp120 BaL

Figure 11. Gp120 impairs fast axonal transport. (a-d) "Vesicle motility assays in isolated squid axoplasm. Individual velocity (μm/sec) rate measurements (arrowheads) are plotted as a function of time (minutes). Dark arrowheads and lines represent anterograde, conventional kinesin-dependent rates. Grey arrows and lines represent retrograde, CDyn-dependent FAT rates." (Morfini et al. 2013) While heat-inactivated gp120 IIIB **(a)** had no effect on FAT velocities, 10 nM gp120 IIIB **(b)** profoundly impaired FAT in both anterograde and retrograde directions. Perfusion of 100 pM gp120 IIIB **(c)**, a more physiologically relevant concentration of gp120, also severely reduced FAT**.** BaL, another strain of gp120 that uses a different coreceptor CCR5, also profoundly impaired FAT with the same curve as gp120 IIIB **(d).** Statistical analysis of the impairment by 100 pM gp120 IIIB, 10 nM gp120 IIIB, and 10 nM gp120 BaL 10 nM gp120 IIIB revealed that these impaiments all similarly impaired FAT in both directions compared to heat-inactivated gp120 IIIB **(e)**, *$p<0.0001$. These data indicate that gp120 specifically and severely impairs FAT in both anterograde and retrograde directions.

gp120 IIIB was co-perfused with various inhibitors of FAT regulatory kinases and phosphatases to search for an inhibitor that would prevent the reduction of FAT velocity caused by 10 nM gp120 IIIB. The first to be targeted were kinases that inhibit both anterograde and retrograde transport, which are p38β MAPK, JNK3, CK1 and CK2. Inhibition of CK1 and CK2 had no effect (data not shown). However, 5 μM of the p38 MAPK and JNK inhibitor SB203580 (Calbiochem; IC50 p38: 5-500 nM; IC50 JNK: 3-40 μM) partially prevented the impairment of FAT (Fig. 12*a*). Quantitative analysis revealed that this rescue was statistically significant compared to 10 nM gp120 alone. However, the rescue did not completely inhibit gp120's impairment of FAT; although retrograde velocities were restored to buffer control levels, anterograde FAT velocities were still significantly lower than buffer control values. To narrow down whether p38 MAPK or JNK specifically were activated to impair FAT, 10 μM of the specific p38 inhibitor MW01-2-069A-SRM (069A; Munoz et al., 2007) was co-perfused with 10 nM gp120 (Fig. 12*b)*. Additionally, 500 nM of the specific JNK inhibitor SP600125 (Calbiochem) was co-perfused with 10 nM gp120 to test the involvement of the JNK pathway (Fig. 12*c)*. Quantitative analysis revealed that coperfusion of each of these inhibitors with gp120 significantly protected FAT to the same extent compared to 10 nM gp120 alone. However, the velocities remained significantly lower than buffer control to varying extents. These data demonstrate that gp120 activates signaling pathways involving both p38 and JNK to impair FAT.

Figure 12

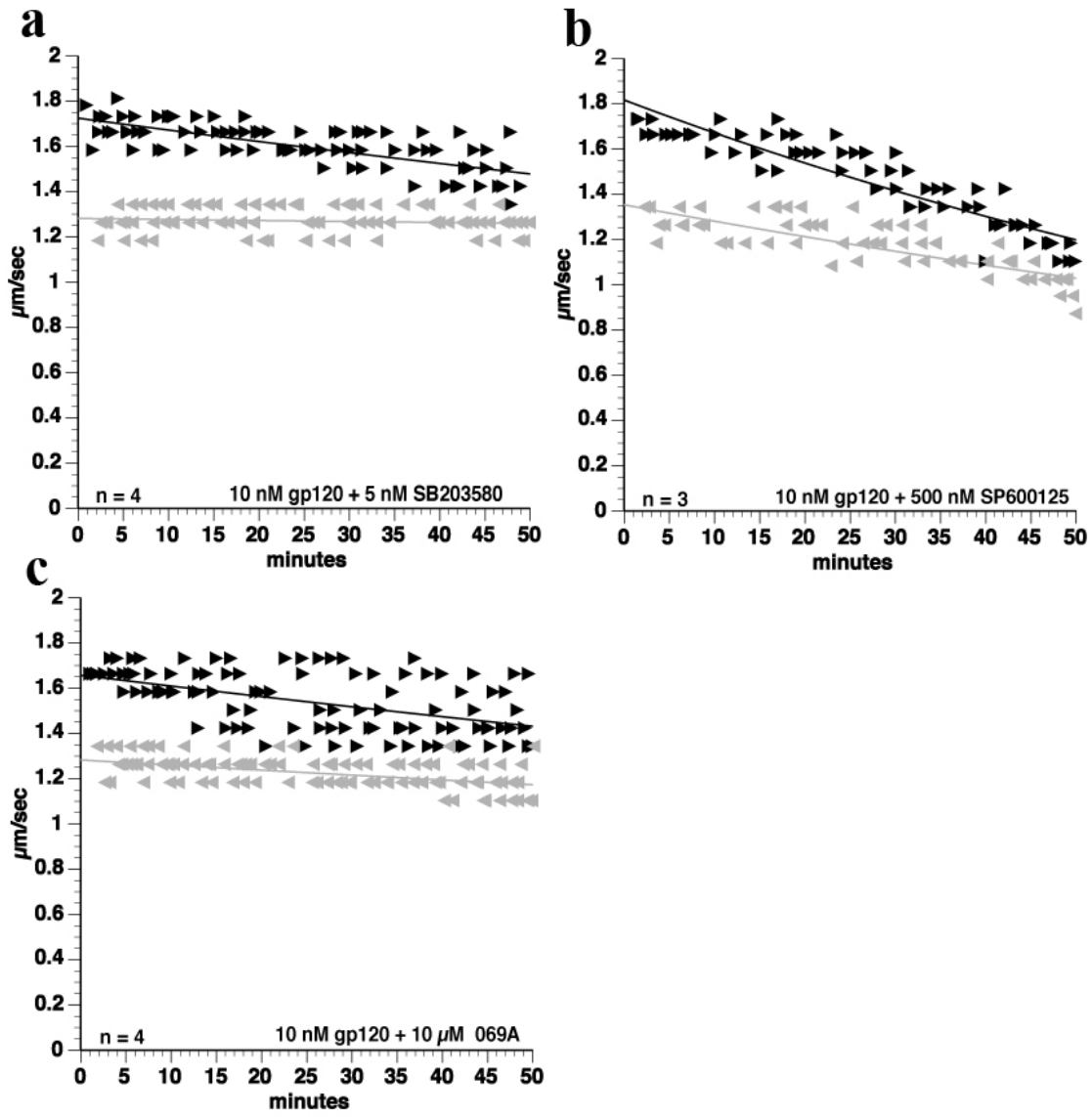

Figure 12. Gp120 activates p38 MAPK and JNK to impair fast axonal transport.

(a-c) "Vesicle motility assays in isolated squid axoplasm. Individual velocity (µm/sec) rate measurements (arrowheads) are plotted as a function of time (minutes). Dark arrowheads and lines represent anterograde, conventional kinesin-dependent rates. Grey arrows and lines represent retrograde, CDyn-dependent FAT rates." (Morfini et al. 2013) Co-perfusion of 10 nM gp120 with SB203580, an inhibitor of both p38 MAPK and JNK, partially protected FAT **(a).** To narrow down the kinase involvement further, gp120 was co-perfused with the JNK-specific inhibitor SP600125 **(b)** or the p38 MAPK specific inhibitor 069A **(c)**. Both of these inhibitors showed partial protection, demonstrating that both p38 MAPK and JNK are activated by gp120 to impair FAT.

2.4 Gp120 Activates PP1 to Impair Fast Axonal Transport

The partial rescue of FAT by inhibiting p38 and JNK led us to postulate that gp120 activates multiple regulatory pathways for FAT, so other inhibitors were tested. 200 nM okadaic acid (OA), a serine/threonine phosphatase 1, 2A and 2B inhibitor (IC50: 10 nM), also reduced the decrement of FAT caused by gp120 IIIB (Fig. 13*a*). This rescue was statistically significant compared to 10 nM gp120 alone; however, this rescue was not complete either, as the anterograde FAT velocities remained significantly lower than buffer control.

To narrow down which phosphatase was activated by gp120 to inhibit FAT, 50 nM of the specific PP1 inhibitor I-2 was co-perfused with 10 nM gp120 IIIB (Fig. 13*c)*. Co-perfusion of squid axoplasm with gp120 and I-2 also partially protected FAT, with velocities remaining significantly lower than buffer control (Fig. 13*c*).

Since it has previously been shown that PP1 can impair FAT through activation of GSK3β (Morfini et al., 2004), we co-perfused axoplasm with gp120 and 100 nM of the specific GSK3β inhibitor ING-135 to test the role of GSK3β in gp120-induced FAT impairment. In fact, ING-135 did not protect FAT from the effects of gp120 (Fig. 13*d*), disproving our hypothesis that the downstream target of PP1 activated by gp120 perfusion was GSK3β.

To test whether the activation of PP1 in addition to p38 and JNK activation was sufficient to cause the FAT impairment by gp120, squid axoplasms were perfused with SB203580 and okadaic acid in addition to 10 nM gp120 IIIB (Fig. 14*b*). This treatment completely rescued the impairment of FAT caused by gp120 IIIB. This rescue was statistically significant compared to 10 nM gp120 alone, but not significantly different

Figure 13

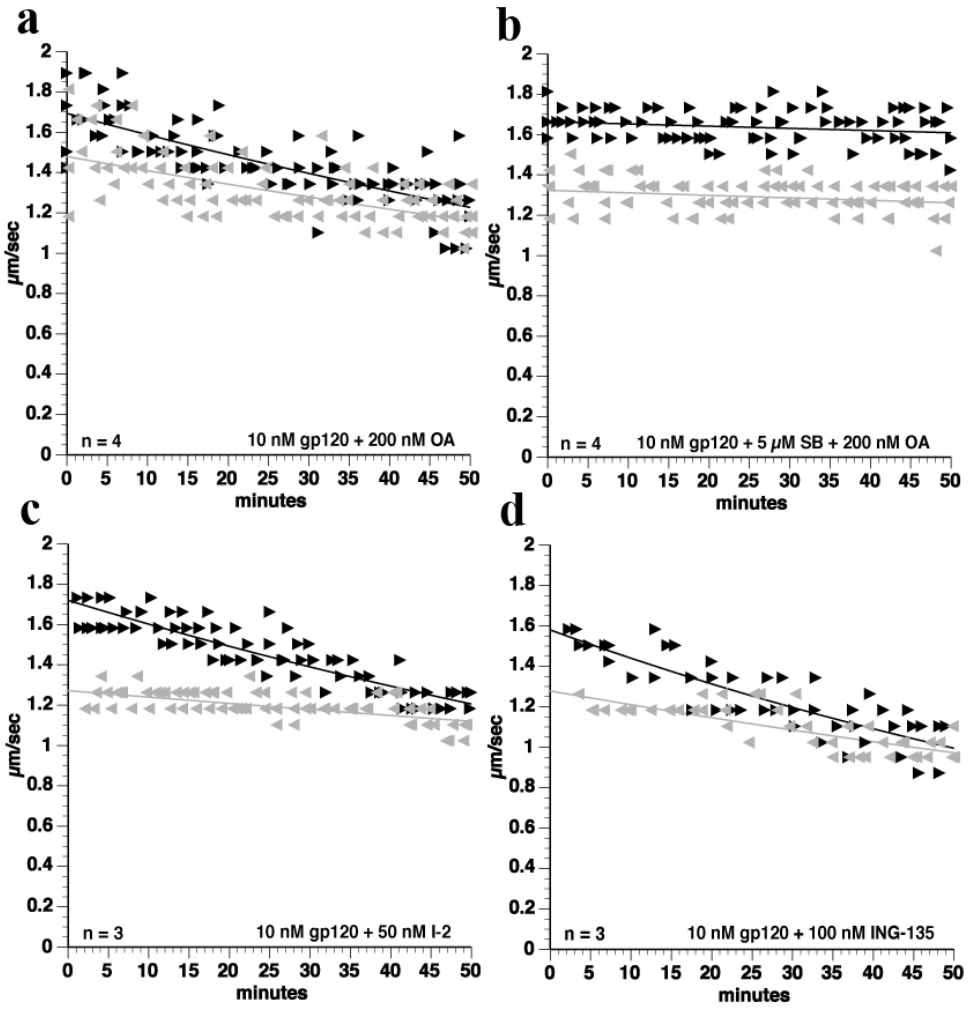

Figure 13. Gp120 activates a novel PP1 regulatory pathway to impair fast axonal transport. (a-d) "Vesicle motility assays in isolated squid axoplasm. Individual velocity (µm/sec) rate measurements (arrowheads) are plotted as a function of time (minutes). Dark arrowheads and lines represent anterograde, conventional kinesin-dependent rates. Grey arrows and lines represent retrograde, CDyn-dependent FAT rates." (Morfini et al., 2013) Co-perfusion of gp120 with okadaic acid, a serine/threonine phosphatase 1, 2A and 2B inhibitor, also partially protected FAT **(a)**; adding both okadaic acid and SB203580 to 10 nM gp120 had an additive effect to completely protect FAT **(b)**, demonstrating that the activation of a phosphatase is through a separate pathway from p38 and JNK. Coperfusing the PP1-specific inhibitor PP1 with gp120 replicated the partial inhibition of okadaic acid **(c)**, demonstrating that PP1 is the phosphatase that is activated by gp120 to impair FAT. However, this PP1 activation did not cause the activation of GSK3-β to impair FAT, since coperfusion with gp120 and ING-135, a GSK3-β inhibitor did not protect FAT **(d)**. This led to the hypothesis that PP1 activates a novel regulatory pathway to impair FAT.

from buffer control. These data indicate that gp120 activates a signaling pathway that activates p38, JNK and PP1 to impair FAT. Further, the activation of PP1 is likely to be in a parallel pathway to p38 and JNK since coperfusion of the two different inhibitors completely rescued FAT.

2.5. Gp120 Activates a Tak1 Pathway to Impair Fast Axonal Transport

Next the upstream activator of p38 and JNK by gp120 IIIB was investigated. First the mixed lineage kinase (MLK) pathway upstream of both JNK and p38 MAPK was tested using the pharmacological inhibitor CEP-11004. MLK's are a family of serine-threonine MAPK kinase kinases (MAP3K). MLK's are one of several potential upstream activators of JNK, with some evidence for activation of p38 MAPK as well (Gallo and Johnson, 2002; Kim et al., 2004). Co-perfusing 10 nM gp120 with 200 nM CEP-11004 did not prevent the reduction of FAT by gp120 (Fig. 14*a*), demonstrating that the pathway activated by gp120 to impair FAT does not include activation of MLK's.

Some MAP3K's other than MLK's, including Tak-1 and Ask-1, can also activate both p38 and JNK (Gallo and Johnson, 2002), so we next targeted these. First gp120 was co-perfused with the DVD peptide, a peptide that blocks the conserved docking domain for certain MAP3K's (Takekawa et al., 2005), and found partial protection (Fig. 14*b*). This led us to narrow down which MAP3K was activated by gp120 to impair FAT. Next 50 nM of the selective Tak-1 inhibitor (5Z)-7-Oxozeaenol was co-perfused with gp120 (Fig. 14*c*), leading to complete protection of FAT velocities, indicating that Tak1 is the upstream kinase responsible for gp120 induced-impairment of FAT. Notably, since the Tak-1 inhibitor (5Z)-7-Oxozeaenol completely protected FAT, activation of PP1 must occur in a pathway downstream of Tak-1.

We searched for known downstream pathways activated by Tak-1, and found that PP1 has been demonstrated to mediate activation of the Inhibitor of Kappa B kinase (IKK) complex by Tak1, which leads to IKK-2 induced activation of nuclear factor kappa-light-chain-enhancer of activated B cells (NF-kB; Mitsuhashi et al., 2008). To test this pathway, first recombinant IKK-2 (Signal Chem) was perfused into the axoplasm to determine if IKK-2 had an effect on transport. In fact, IKK-2 inhibited both anterograde and retrograde FAT (Fig. 14*d*), demonstrating that IKK-2 can have a role in regulation of FAT.

Co-perfusing gp120 with the IKK-2 inhibitor XII (Calbiochem) resulted in a partial protection of FAT (14*e*), demonstrating that IKK-2 is a downstream target of PP1 to impair FAT. These axoplasm results map out a novel pathway through which intra-axonal gp120 can cause dysregulation of FAT. Gp120 activates a pathway leading to Tak1 activation. Tak1 then activates p38 and JNK through MAP2Ks and activates IKK-2 through PP1, ultimately impairing FAT.

Figure 14

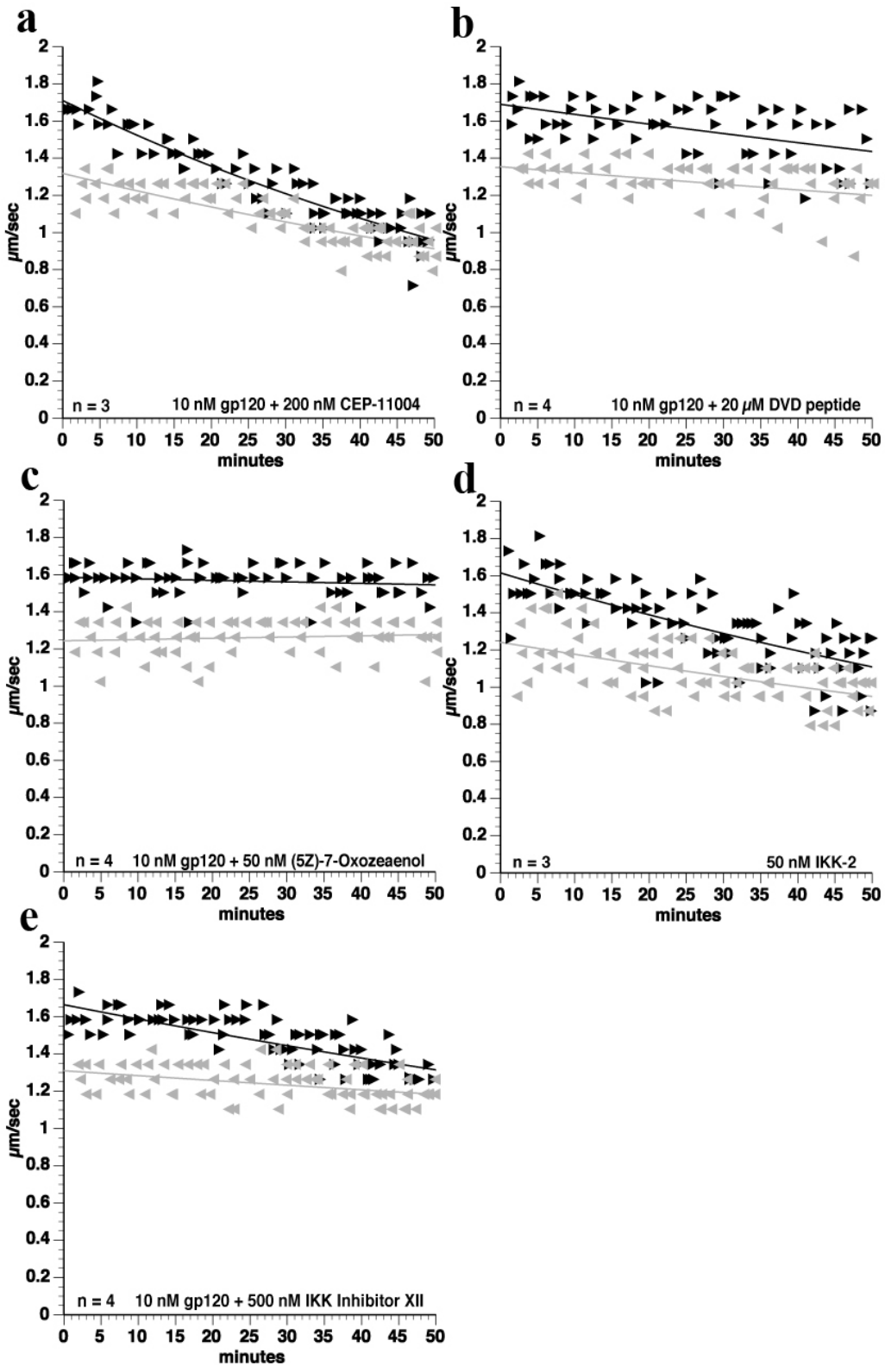
a
b
c
d
e
μm/sec
minutes
n = 3
10 nM gp120 + 200 nM CEP-11004
n = 4
10 nM gp120 + 20 μM DVD peptide
n = 4
10 nM gp120 + 50 nM (5Z)-7-Oxozeaenol
n = 3
50 nM IKK-2
n = 4
10 nM gp120 + 500 nM IKK Inhibitor XII

Figure 14. Gp120 activates a NFκB pathway downstream of Tak1 to impair fast axonal transport. (a-d) "Vesicle motility assays in isolated squid axoplasm. Individual velocity (μm/sec) rate measurements (arrowheads) are plotted as a function of time (minutes). Dark arrowheads and lines represent anterograde, conventional kinesin-dependent rates. Grey arrows and lines represent retrograde, CDyn-dependent FAT rates." (Morfini et al. 2013) Squid axoplasms were tested for upstream activators of p38 MAPK, JNK and PP1. First, upstream activators of p38 MAPK and JNK were targeted. The mixed lineage kinase inhibitor CEP-11004 did not protect FAT velocities when co-perfused with gp120 **(a)**, demonstrating that mixed lineage kinases are not activated by gp120. Next, squid axoplasms were co-perfused with gp120 and the DVD peptide, a peptide that blocks the conserved docking domain of several MAP3K's. FAT measurements showed partial protection **(b)**, indicating that a MAP3K is activated by gp120 upstream of p38 MAPK and JNK. To narrow down which MAP3K, next a specific inhibitor (5Z)-7-Oxozeaenol of the MAP3K Tak1 was co-perfused with gp120. This co-perfusion led to complete protection of FAT **(c)**, indicating that Tak1 is upstream of PP1 in addition to p38 MAPK and JNK. To test whether the activation of PP1 occurred through a NfκB pathway downstream of Tak1, recombinant IKK-2 was perfused in axoplams, leading to inhibition of FAT **(d)**. Next, the co-perfusion of the IKK-2 inhibitor XII with gp120 partially rescued FAT impairment **(e)**, demonstrating that the activation of PP1 downstream of Tak1 is linked to IKK-2 activation.

2.6 The Effect of Gp120 on Kinesin and Cytoplasmic Dynein Microtubule Binding

One method for regulation of kinesin and CDyn is through phosphorylation, which causes them to detach from microtubules (Morfini et al., 2009). To examine whether gp120 utilizes this method to impair FAT, microtubule binding assays were performed. Differentiated F11 cells were treated for 2 hours with gp120 or with the diluent as a control, and then processed for microtubule binding assays. An immunoblot analysis was performed to examine the effect of gp120 treatment on the amount of kinesin and CDyn in the microtubule enriched pellets. To examine kinesin, an antibody for kinesin heavy chain (KHC) was used, and to examine CDyn an antibody for dynein intermediate chain (DIC) was used. DM1A, an antibody for tubulin, was also used to demonstrate that tubulin had successfully polymerized into microtubules and was thus concentrated in the microtubule-enriched pellet. ATP treatments released the majority of kinesin and CDyn into the supernatant, verifying the ATPase activity of kinesin and CDyn. AMP-PNP, a non-hydrolyzable analogue of ATP, causes kinesin to remain attached to microtubules. If gp120 had caused phosphorylation of kinesin and dynein to release them from microtubules, then it would be expected that less kinesin and dynein would be in the microtubule-enriched pellet in the AMP-PNP condition.

Figure 15*a* shows a representative immunoblot from the microtubule binding assay. Analysis of the immunoblots revealed that gp120 caused a significant decrease in the amount of DIC in the microtubule-enriched pellet in AMP-PMP conditions (Figure 15*c*; $p<0.05$), demonstrating that DIC had been released from dynein heavy chain (DHC), which binds to microtubules. Although there may be a slight trend for gp120 to cause the reduction of kinesin in the pellet, (Figure 15*c*) this was not

Figure 15

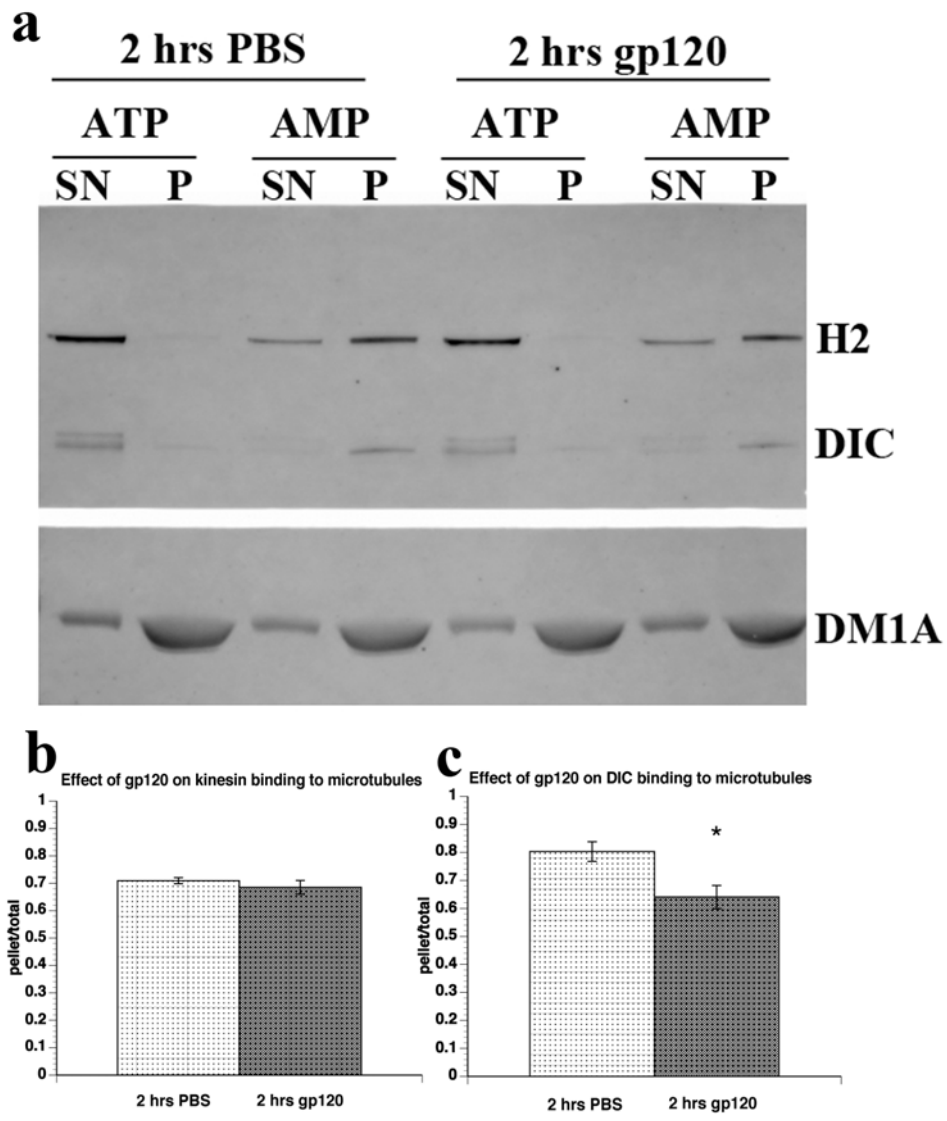
a
2 hrs PBS
2 hrs gp120
ATP
AMP
ATP
AMP
SN
P
SN
P
SN
P
SN
P
H2
DIC
DM1A
b
Effect of gp120 on kinesin binding to microtubules
pellet/total
2 hrs PBS
2 hrs gp120
c
Effect of gp120 on DIC binding to microtubules
*
pellet/total
2 hrs PBS
2 hrs gp120

Figure 15. Microtubule binding assays indicate that gp120 induces detachment of cytoplasmic dynein, but not kinesin, from microtubules. Representative Western blot of microtubule binding in mouse primary cortical neurons **(a)**. H2 is used as an antibody for kinesin, DIC for CDyn, and DM1A is used as an antibody for tubulin. In conditions with ATP added, kinesin and CDyn were released into the supernatant (SN), serving as a control for their ATPase activity. DMIA staining revealed that tubulin remained in the microtubule pellet. When AMP-PNP (AMP), a non-hydrolyzable analogue of ATP was present, then kinesin and CDyn remained within the microtubule pellet. Quantitative analysis with a student's t-test revealed that although gp120 does not significantly decrease the amount of kinesin associated with microtubules in the AMP-PNP condition **(b)**, it does significantly decrease the amount of CDyn attached to microtubules **(c);** these results indicate that gp120 treatment releases CDyn from microtubules. *$p<0.05$.

statistically significant. It is possible that the microtubule binding assay was not sensitive enough to detect kinesin release from microtubules in this model.

CHAPTER V

DISCUSSION

Berth, S., Morfini, G., Sarma T., Caicedo, H., Brady, S.T. (2015) Internalization and Axonal Transport of the HIV Glycoprotein gp120. ASN Neuro 7(1): pii: 1759091414568186

1. Dying back neuropathies

Dying back neuropathies are a class of neurodegenerative disorders characterized by development of synaptic dysfunction and axonal transport abnormalities, leading to progressive distal-to-proximal dying-back axonal degeneration (Figure 16; Coleman, 2005). Dying back neuropathies are characteristic of a variety of CNS and PNS diseases, including Alzheimer's disease, amyotrophic lateral sclerosis (ALS), polyglutamine expansion diseases, prion disease, diabetes mellitus, and HIV to name a few (Coleman, 2005). Neuronal cell death occurs as an end stage response to synaptic and axonal dysfunction. Although neuronal cell death has been the focus of much research in these disorders, the end stage nature of apoptosis as a programmed response to axonal degeneration is not disease specific and occurs late in the disease process. As a result, targeting cell death has not been found to be effective at ameliorating disease in dying-back neuropathies. For example, attempts to rescue neurodegeneration in a *pmn* model of axonal degeneration by crossing *pmn* mice with anti-apoptotic Bcl-2 expressing mice did not rescue axonal degeneration or improve survival, although motor neuron cell body death was prevented (Sagot et al., 1997). Other studies using Bax knockouts to prevent apoptosis in both a prion protein (PrP) disease model and a ALS disease model in transgenic mice had similar results, with a rescue of the neuronal cell bodies affected in these diseases, but with little to no improvement in axonal

Figure 16

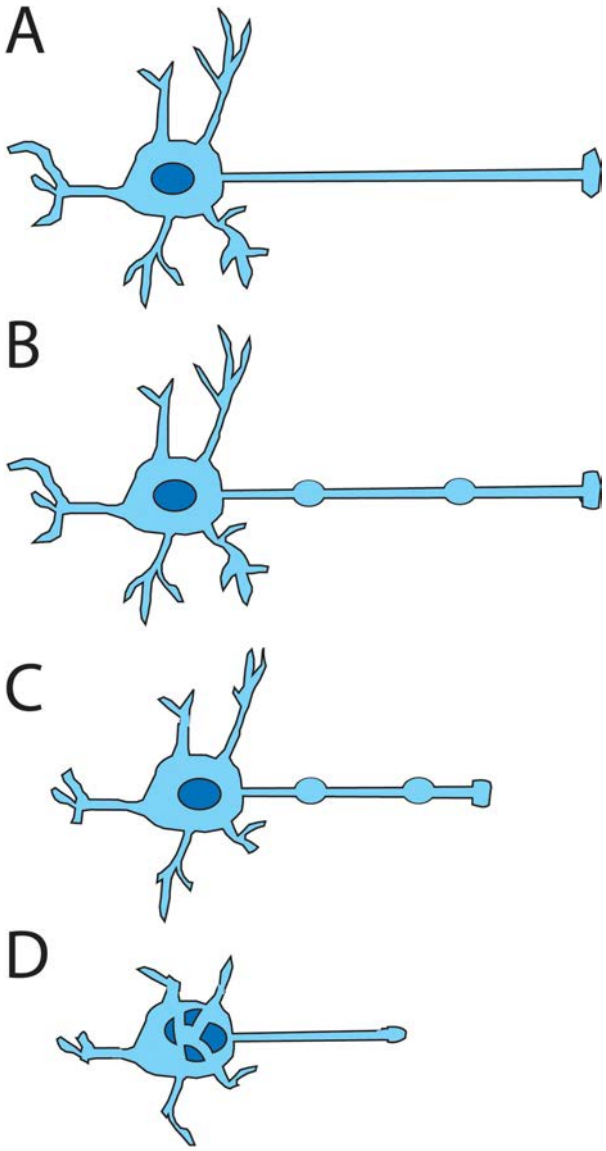

Figure 16. gp120-induced dying back neuropathy. In the initial stages of HIV infection, DRG neurons remain healthy (A). As the disease progresses, DRG neurons begin to exhibit signs of synaptic and axonal dysfunction (B), which underlie the neurodegeneration observed within the PNS. A prominent degeneration of unmyelinated nociceptive C fibers is seen, which progresses as a "dying-back neuropathy". This pattern of neuronal degeneration is marked by early synaptic loss (or nerve end degeneration in the case of DRGs) and distal axon degeneration that gradually progresses in the retrograde direction (towards the cell body) (C). Neurons fail to sustain proper synaptic connections with their target cell, gradually losing their trophic support. The sequence of events above (B to C) ultimately results in neuronal cell death, typically by activation of apoptotic pathways (D).

degeneration and disease phenotype (Chiesa et al., 2005; Gould et al., 2006). These studies highlight the importance of examining events upstream to apoptosis to define the mechanism of dying back neuropathies.

1.1 Evidence that Distal Sensory Polyneuropathy is a Dying-Back Neuropathy

DSP is characterized by dying-back axonal degeneration of primarily small, unmyelinated sensory neuron axons (Keswani et al., 2002). This axonal degeneration progresses distally to proximally in a "stocking and glove" fashion (Keswani et al., 2002). Reduced epidermal nerve fiber density is more prominent in the distal then proximal leg, demonstrating the dying-back nature of DSP (Holland et al., 1997). Centrally directed axons in the gracile tracts also exhibit dying-back neurodegeneration (Rance et al., 1988). DSP is prominently marked by axonal degeneration, with minimal apoptosis in DRG neurons in AIDS patients (Bradley et al., 1998).

However, the induction of apoptosis in neurons by gp120 has been the parameter most commonly studied. For example, several studies examined the activation of caspase-3 leading to apoptosis in neurons in response to gp120 treatment (Bachis et al., 2003; Singh et al., 2004; Singh et al., 2005). Additionally, perineural treatment of gp120 led to activation of caspase-3 in 25% of DRG neurons (Wallace et al., 2007). Further, certain inhibitors have been used to block apoptosis induced by HIV. For example, in one study human neurons and rat cerebellar neurons were treated with HIV virions or with gp120

itself, and then apoptosis was measured using the terminal deoxynucleotidyl transferase-mediated dUTP nick-end labeling (TUNEL) assay. Treatment with HA1004, a nonselective kinase inhibitor of several pathways, prevented apoptosis (Zheng et al., 1999). In another study, the inhibitor CEP-1347, which primarily inhibits a MLK pathway that activates JNK, was found to rescue rat DRG neurons from apoptosis caused by gp120 (Bodner et al., 2004). However, examining the mechanism for gp120 induction of apoptosis may have limited meaning for DSP, because apoptosis is not a major feature of the disease. Additionally, this approach fails to address pathogenic mechanisms for DSP, since prevention of cell death has not been demonstrated to improve symptoms or axonal degeneration in dying-back neuropathies.

1.2 Gp120 Causes Axonal Degeneration in Distal Sensory Polyneuropathy

Several studies have linked gp120 to events upstream of apoptosis in dying-back neuropathies. For example, a transgenic mouse model that expressed gp120 in astrocytes exhibited synaptic loss and reduced synaptodendritic complexity (Toggas et al., 1994). In another study using these mice to examine signs of DSP, aged mice that were 12-15 months old had decreased intra-epidermal nerve fiber density in the plantar footpad (Keswani et al., 2006). This late onset replicates what is seen in humans, with DSP taking decades to develop and age being a primary risk factor. Another transgenic model that expressed gp160 (which is composed of gp120 and gp41) in neurons exhibited degeneration of synapses, dendrites and axons along with axonal swellings (Michaud et al.,

2001). Humanized mice infected with HIV demonstrated reduction in synaptic architectures, as evidenced by decreased microtubule-associated protein 2 (MAP2), synaptophysin and neurofilaments (Dash et al., 2011).

Other DSP studies utilizing gp120 treatment of rodents also found axonal pathology. For example, perineural application of gp120 to the rat sciatic nerve led to a painful neuropathy in addition to axonal swellings (Herzberg and Sagen, 2001). Another study used Campenot chambers to compartmentalize rat DRG neurons from their axons, and found that treating only axons with gp120 caused axonal degeneration, as evidenced by decreased axonal length (Melli et al., 2006). Blocking gp120 binding to axons with antibodies for CXCR4 and CCR5 was able to prevent this degeneration, pointing to a role for the chemokine receptors in axonal degeneration (Melli et al., 2006). An additional study that used human fetal DRG neurons primarily composed of nociceptive fibers found that gp120 treatment caused a decrease in neurite length without neuronal cell death (Robinson et al., 2007), further demonstrating that gp120 is sufficient to induce axonal degeneration that models the dying-back neuropathy phenotype seen in DSP. These studies provide evidence that links gp120 to events upstream of apoptosis in DSP, indicating that gp120 might activate a disease-specific mechanism leading to dying back neuropathy.

2. Dying Back Neuropathies and Fast Axonal Transport

Evidence has accumulated that impaired FAT is an early step in dying back neuropathies; in fact, impairments of FAT can directly cause dying-back neuropathies. Loss of function mutations in the motor proteins kinesin and

CDyn lead to dying-back neurodegeneration, as does misregulation of signaling pathways that affect these motors and FAT.

2.1 Loss of Function of Kinesin Causes Dying Back Neuropathies

One such case of loss of function of kinesin leading to dying-back neurodegeneration is Hereditary Spastic Paraplegia (HSP), a collection of inherited neurodegenerative diseases marked by a profound dying-back degeneration of distal corticospinal tracts (Roy et al., 2005). A missense mutation of KHC (Kif5A) in the genetic locus SPG10 was discovered in a family that suffered from HSP; only family members that had HSP or were presymptomatic exhibited this mutation (Reid et al., 2002). In fact, a homologous mutation in yeast demonstrated impaired ATPase activity by kinesin, providing a mechanism of direct impairment of FAT by kinesin that leads to HSP (Song and Endow, 1998). Since that discovery, several other point mutations of Kif5a have been found to be responsible for HSP (Fichera et al., 2004; Blair et al., 2006; Lo Giudice et al., 2006), confirming that loss of function mutations of kinesin cause some forms of HSP. All four of these Kif5a mutations demonstrated impaired motility through either reduced gliding velocity or impaired microtubule binding, or both (Ebbing et al., 2008).

Recently, whole exome sequencing coupled to disease network-analysis linked a mutation in another kinesin family member, Kif1A, to HSP in a family as well (Erlich et al., 2011). A truncating mutation of Kif1A has also been linked to hereditary sensory and autonomic neuropathy type 2, another familial group of sensory neuropathies marked by peripheral nerve degeneration and profound

distal sensory loss (Riviere et al., 2011). Evidence also exists for mutated kinesin in Charcot-Marie-Tooth (CMT) disease, a familial group of neuropathies with both sensory and motor components (Roy et al., 2005). Mutations in Kif1Bβ have been reported to be causative for CMT type 2a, a type of CMT marked by axonal degeneration (Ben Othmane et al., 1993; Zhao et al., 2001). In fact, heterozygous knockouts of Kif1Bβ in mice reproduced the phenotype of CMT type 2a (Zhao et al., 2001), demonstrating that the loss of function of one allele of a kinesin isoform is sufficient to cause peripheral neuropathy. However, this study has not been replicated, so further examination is needed.

2.2 Loss of Function of Cytoplasmic Dynein Causes Dying Back Neuropathies

Evidence has accumulated that the retrograde motor for FAT, CDyn, also needs to properly function to prevent dying-back neuropathies. For example, missense mutations of CDyn heavy chain 1 led to progressive sensory neuropathies in mice (Dupuis et al., 2009). A mutation in CDyn heavy chain 1 has also recently been reported in a family suffering from CMT type 2a (Weedon et al., 2011). The presence of both kinesin and CDyn mutations that are causative of CMT type 2a provides converging evidence that impaired FAT is responsible for the development of CMT type 2a.

A missense mutation in p150^{glued}, a subunit of dynactin responsible for binding to CDyn, was linked to a family suffering from hereditary progressive motor neuron disease (Puls et al., 2003). Upon autopsy of several of these affected family members, inclusions of dynactin and CDyn were found in motor

neuron cell bodies and their dendrites, which is suggestive of impairments of FAT in the motor neurons (Puls et al., 2005). Several mutations in p150^{glued} have also been linked to ALS (Munch et al., 2005), demonstrating that impairment of dynactin-CDyn coupling may progress to multiple types of dying-back neuropathies.

The role that loss of function mutations of kinesin and CDyn play in the development of progressive neuropathies with slow onset is indicative that impaired FAT causes dying-back neurodegeneration of axons. However, many dying-back neuropathies are sporadic, and mutations in kinesin and CDyn are rare. A common feature of many of these dying-back neuropathies is the accumulation of axonally transported proteins such as amyloid precursor protein (APP) in axonal swellings and spheroids, due to faulty FAT (Coleman, 2005). Because of this evidence, the regulation of kinesin and CDyn has been focused on to determine how impairments of FAT lead to dying-back degeneration of axons. It is now understood that phosphorylation of kinesin and CDyn changes the rate of FAT, through causing dissociation of cargo from the motors or dissociation of the motor from the microtubules (Morfini et al., 2009b). Accordingly, abnormal activation of certain signaling pathways that regulate FAT exists in a multitude of dying-back neuropathies, including Alzheimer's disease (Pigino et al., 2009; Kanaan et al., 2012), Parkinson's disease (Morfini et al., 2007; Chu et al., 2012), ALS (Bosco et al., 2010), and Huntington's disease (Morfini et al., 2009a). In fact, these dying-back neuropathies are linked by a common mechanism for neuropathogenesis, causing the coinage of the term "dysferopathies" for dying-back neuropathies in which impaired FAT has a prominent role (Morfini et al.,

2007). The studies in this dissertation were undertaken to elucidate if HIV-associated DSP is a dysferopathy as well, by examining whether the neurotoxic HIV glycoprotein gp120 impairs FAT.

3. Internalization of Gp120 and Distal Sensory Polyneuropathy

Combination anti-retroviral treatment has dramatically improved HIV patient mortality and decreased a number of HIV complications (Greene, 2007; Clifford, 2008). However, the prevalence of DSP continues unabated (Ghosh et al., 2012), making this an important disease complication that requires treatment. Since HIV does not productively infect neurons, the mechanism for HIV-induced peripheral nerve damage is believed to involve indirect mechanisms. These include neurotoxicity by secretion of inflammatory factors, cytokines, and viral proteins such as gp120 (Kaul et al., 2005). Gp120 binds to its coreceptor CXCR4 on DRG neurons (Apostolski et al., 1993), and it has been thought that this binding causes the activation of signaling cascades leading to pain hypersensitivity (Oh et al., 2001; Bhangoo et al., 2009), axonal degeneration, and apoptosis (Melli et al., 2006). However, a new possibility for gp120 neurotoxicity was discovered in experiments that demonstrated that gp120 is internalized by neurons of the CNS (Bachis et al., 2003; Bachis et al., 2006). It has remained unclear whether neuronal uptake of gp120 might occur in sensory neurons affected by DSP, and whether this might be a pathogenic mechanism for DSP.

Results from these experiments indicate that F11 cells, a neuroblastoma cell line hybridized with DRG neurons, and primary DRG rat neurons both

internalized gp120 in a time-dependent manner. Imaging analysis showed that the majority of gp120 was located within the cells after 2 hours of incubation with recombinant gp120. The highly punctate nature of the intracellular gp120 staining is consistent with that reported for other cell types (Cefai et al., 1992), including CNS neurons (Bachis et al., 2003). Additionally, the heat-inactivation and AMD3100 pre-treatment experiments demonstrate that this internalization is specific to gp120.

Pharamacological experiments with the inhibitor AMD3100 indicated that this internalization was partially dependent on gp120 binding to its coreceptor CXCR4. This observation provides a basis for an alternative mechanism of gp120 toxicity to DRG neurons. Although previously this binding was proposed to cause neurotoxicity through CXCR4 activation of signaling cascades (Oh et al., 2001; Trushin et al., 2007), it is also possible that this binding is an initial step for gp120 internalization, and intra-neuronal gp120 directly causes toxicity.

Colocalization studies with markers of different endosomal pathways defined the pathways through which gp120 is internalized. The lack of gp120 colocalization with the EEA1 and LAMP2, markers of early endosomal compartment and late endosomal/lysosomal compartment, respectively, demonstrated that gp120 is not internalized through the common endolysosomal pathway. Rather, colocalization analysis of gp120 with cholera toxin B and dextran indicated the bulk of gp120 was internalized through lipid rafts, with a minor fraction being internalized through fluid phase pinocytosis. Accordingly, disrupting lipid rafts through CD treatment decreased the amount of internalized gp120. These observations were consistent with previous research showing that

gp120 clustering with its co-receptors in lipid rafts is important for HIV infection (Manes et al., 2000; Liao et al., 2001; Popik et al., 2002). Moreover, gp120 was shown to induce CXCR4 clustering into lipid rafts for HIV entry (Kamiyama et al., 2009). Based on these results, it is plausible that gp120 binds to CXCR4 in association with lipid rafts for internalization. Although gp120 has been shown to co-internalize with CXCR4 in T-cells (Misse et al., 1999), this is unlikely to happen in sensory neurons since it has been demonstrated that internalized CXCR4 localizes to EEA1 and recycling endosomes in hematopoetic progenitor cells (Zhang et al., 2004). However, this possibility cannot be ruled out since neuronal cells might utilize a different pathway to internalize CXCR4 than hematopoietic cells.

What is the fate of internalized gp120 in DRG neurons? If internalization occurs within axons, then gp120 would not be immediately degraded, since degradation of endocytosed protein by lysosomes occurs in the perinuclear region of the neuron (Parton et al., 1992; Tai and Schuman, 2008). In fact, gp120 was transported in the retrograde direction from isolated DRG axons to their fluidically isolated cell bodies. Retrograde transport of gp120 is consistent with time course studies in F11 cells, since gp120 appeared in the neurites during early time points, and as time progressed began accumulating in perinuclear regions. Further, colocalization studies rule out a lysosomal destination for gp120, since there was no colocalization between gp120 and LAMP2, a lysosomal marker. Intriguingly, gp120 was not transported in the anterograde direction from the cell body to the periphery. This is consistent with selective retrograde transport of

viruses and viral proteins that has been previously reported (Leopold and Pfister, 2006; Berth et al., 2009).

It is unclear why the main bulk of gp120 was internalized through lipid rafts, with a small fraction internalized through fluid phase pinocytosis. However, the fraction of gp120 that taken up by fluid phase pinocytosis may be due to the non-selectivity of the process (Lim and Gleeson, 2011). Additionally, these two mechanisms have been found concurrently in the internalization of HIV in brain microvascular endothelial cells (Liu et al., 2002), demonstrating that both lipid raft internalization and fluid phase pinocytosis might mediate gp120 and/or HIV virion internalization in multiple types of cells. These data suggest that targeting lipid raft internalization and fluid phase pinocytosis through cholesterol lowering drugs such as statins along with inhibitors of fluid phase pinocytosis such as sodium proton exchange inhibitors like dimethyl amiloride, respectively, might have beneficial effects by preventing gp120 internalization. Further studies are needed to evaluate these possibilities.

Understanding the mechanism of internalization and intracellular actions of gp120 may be crucial for defining mechanisms underlying the toxic effect of gp120 to DRG neurons. The majority of research examining direct gp120 neurotoxicity in DSP has focused on its binding to CXCR4 and subsequent activation of signaling cascades (Kamerman et al., 2012). However, the transient nature of activation of p38 MAPK in cell lysates by CXCR4 illustrates that other mechanisms, such as intracellular actions of gp120, may also play a role in the development of dying-back neurodegeneration. For example, the location of gp120 within axons may affect regulatory pathways for fast axonal transport that

are critical for maintaining neuronal health (Berth et al 2009, Morfini et al 2009). Defining mechanisms for gp120 internalization and identifying intracellular effects of this protein within axons may provide important information that leads to the development of novel therapeutic treatments for HIV-related DSP. Determining the intracellular targets of gp120 could provide more selective treatment targets than inhibitors of fluid phase pinocytosis and lipid raft internalization, allowing fewer side effects.

4. Gp120 Activates Phosphotransferases to Impair Fast Axonal Transport

Since we had found that F11 cells and DRG neurons internalized gp120, our next step was to assess the possibility of intracellular toxicity caused by gp120. Since DSP is a dying-back neuropathy, we chose to determine whether intracellular gp120 might interfere with kinase regulation of FAT.

4.1 Gp120 Activates p38 MAPK Independently of CXCR4

First, we examined abnormal activation of regulatory kinases for FAT by gp120 in F11 cells. Previously, gp120 treatment had been found to activate JNK (Bodner et al., 2004; Khan et al., 2004) and/or p38 MAPK in neurons (Hu et al., 2005; Singh et al., 2005; Medders et al., 2010), both of which regulate FAT (Morfini et al., 2006; Bosco et al., 2010). The interpretation of these experiments had been that gp120 binding to its coreceptor CXCR4 was responsible for activating CXCR4, leading to activation of kinase signaling cascades. However, we questioned whether intracellular gp120 might have the capability of activating

signaling cascades directly. To test this, differentiated F11 cells were treated with 5 nM gp120, and a quick activation of p38 MAPK was observed after 5 minutes, which subsequently decreased by 15 minutes. It is not known why phosphorylation of p38 MAPK decreased after the five minutes of treatment, but this pattern has been seen in other studies (Singh et al., 2005) and may be caused by a feedback mechanism that provides a protective response for the cells to abnormal activation. Blocking gp120 binding to CXCR4 using the small molecule inhibitor AMD3100 abolished the early increase of phosphorylation of p38 MAPK after 5 minutes, confirming that this early activation of p38 MAPK was likely due to CXCR4 activation. However, elimination of the CXCR4 response with AMD3100 pretreatment unmasked a slower activation of p38 MAPK after 30 minutes of gp120 exposure. How might this phosphorylation of p38 MAPK occur with no CXCR4 activation? Previously we had found that a portion of gp120 internalization is in fact independent of CXCR4 binding. We hypothesized that this later activation of p38 MAPK, which corresponds to the time point that gp120 begins to get internalized, could be due to the activation of signaling cascades by intracellular gp120. This activation would be masked by CXCR4 activation, since it causes such a strong and quick response of p38 MAPK phosphorylation, which is then quickly quenched by the neuron.

4.2 Gp120 Impairs Fast Axonal Transport in the Squid Axoplasm

Perfusing proteins of interest into extruded squid axoplasm and then measuring FAT velocity is a useful way to determine how proteins might modulate FAT. With the previous results in mind, we chose to test the effect that

intra-axoplasmic gp120 might have on FAT. Gp120 profoundly impaired both anterograde and retrograde transport, in a manner specific to gp120's activity since heat-inactivation of gp120 abolished this effect. The divergent strains T-tropic gp120 IIIB and the M-tropic gp120 BaL inhibited FAT in a similar manner to each other, demonstrating that this effect on FAT is likely to be conserved across strains. The effects of gp120 on FAT remained even after decreasing the concentration of perfused gp120 to 100 pM.

The conservation of neurotoxicity of gp120 across strains is in contrast to some past studies that found that T-tropic gp120 was more neurotoxic than M-tropic gp120 (Zheng et al., 1999; Frost et al., 2009; Bachis et al., 2010). However, other studies found that T-tropic and M-tropic gp120 strains have similar neurotoxic profiles (Yi et al., 2004; Kaul et al., 2007). An intriguing explanation for seeing similar neurotoxic effects between the two strains is that the squid axoplasm is a membrane-free preparation, so any effects are independent of co-receptor activation. Consistent with this, some studies reported that CCR5 has a neuroprotective effect (Kaul et al., 2007), so reduced gp120 neurotoxicity in CCR5-binding strains might be due to activation of CCR5 that compensates for the neurotoxicity induced by internalized gp120.

Since the amount of free gp120 in plasma has been determined to be in the low picomolar to low nanomolar range (Gilbert et al., 1991; Oh et al., 1992), 100 pM gp120 was perfused to determine if a lower, more physiological relevant concentration might still have an effect on transport. In fact, 100 pM gp120 impaired FAT to a similar extent as 10 nM gp120. Local concentrations of gp120 around DRG neurons are likely to be higher than plasma concentrations due to

the close proximity of infected cells, binding to extracellular matrix components or local glial swelling (Nath, 2002; Krathwohl and Kaiser, 2004). However, the local concentration of gp120 around DRG neurons has not been directly measured. One important point to take into account is that DSP takes decades to develop, although subclinical signs are commonly manifested in HIV patients. It is quite possible that the effect of even the much smaller amounts of gp120 internalized by DRG neurons could gradually compromise neuronal function over decades to cause FAT impairments in DRG neurons.

It is highly unlikely that gp120 produced inhibition of FAT through direct interactions with motor proteins or microtubules. Since the concentration of kinesin is 0.5 μM and tubulin is 25 μM in squid axoplasm (Morris and Lasek, 1984; Brady et al., 1990), the concentration of perfused gp120 was not enough to cause sequestration of kinesin or impair FAT through binding to microtubules (Brady et al., 1990). Further, gp120 perfusion did not alter microtubule structure in the squid axoplasm (data not shown). Therefore, it is much more plausible that the severe effect on FAT by gp120 at the low concentrations perfused is due to amplification through enzymatic signaling cascades that regulate FAT.

4.3 Gp120 Impairs Fast Axonal Transport Through Phosphotransferase Activation

To determine which regulatory signaling pathways were activated by gp120 to impair FAT, gp120 was co-perfused with inhibitors of enzymes known to regulate FAT in an attempt to rescue FAT. Since gp120 impaired FAT in both anterograde and retrograde directions, kinases that are known to inhibit both

directions of FAT (p38β MAPK, JNK3, CK1 and CK2) were targeted initially. While CK1 and CK2 inhibition did not prevent FAT inhibition (data not shown), the p38 and JNK2/3 inhibitor SB203580 exhibited partial protection of FAT velocities. Next, the specific p38 MAPK inhibitor MW01-2-069A-SRM and the specific JNK inhibitor SP600125 also partially protected FAT. These results suggest that both p38 MAPK and JNK are activated by gp120 to impair FAT.

The activation of p38 MAPK confirms results from treating F11 cells. However, in F11 cell treatments, activation of JNK by gp120 treatment was not detected (data not shown). As the p38 MAPK inhibitor showed stronger protection than the JNK inhibitor, it is possible that JNK is activated to a lesser extent, and that this activation was not detected in the F11 cells. Another potential reason is that 10 isoforms of JNK exist (Waetzig and Herdegen, 2005); the JNK isoform that was activated in axoplasm may not be expressed in F11 cells.

Because SB20350 only partially protected FAT, it was postulated that gp120 might activate additional signaling pathways that also impair FAT. More inhibitors were co-perfused with gp120 to identify other signaling pathways activated by gp120. Okadaic acid, an inhibitor of serine-threonine phosphatases, also displayed partial protection of FAT when co-perfused with gp120. In fact, co-perfusion of axoplasm with gp120, SB203580 and okadaic acid completely protected FAT. Since the protective effects of SB203580 and okadaic acid were additive, this suggests that the activation of phosphatases is in a parallel pathway not related to the activation of JNK and p38.

To narrow down which phosphatase had been activated, I-2, an inhibitor of PP1, was co-perfused with gp120 and found to partially protect FAT as well. A regulatory FAT pathway has been established in which PP1 activates GSK3-β to phosphorylate KLCs and decrease FAT velocity (Morfini et al., 2002; Morfini et al., 2004). To test this pathway, a specific inhibitor of GSK3-β, ING-135, was coperfused with gp120 but did not change the effect of gp120 on transport. These results ruled out activation of GSK3-β by PP1 as a component in inhibition of FAT, meaning that the activation of PP1 by gp120 to impair FAT involves a novel regulatory pathway for FAT.

Next, upstream activators of JNK and p38 MAPK were tested for their involvement in gp120-induced inhibition of FAT. First, mixed lineage kinases, a family of MAP3K's that activate both JNK and p38 MAPK (Gallo and Johnson, 2002), were targeted. However, the MLK inhibitor CEP-11004 failed to decrease the inhibition of transport caused by gp120, ruling out MLK's as the upstream activators of p38 MAPK and JNK. To examine other MAP3K's the DVD peptide, which blocks the conserved docking domains of certain MAP3K's (Takekawa et al., 2005), was coperfused with gp120 and found to partially protect FAT. This narrowed down the MAP3K activated by gp120 to those targeted by the DVD peptide, including MTK1 (MEKK4), Ask-1, Tak-1, TAO2, MEKK1, and Raf-1 (Takekawa et al., 2005). Of these, both Ask-1 and Tak-1 can activate both JNK and p38 MAPK, narrowing down the list of candidate MAP3Ks. Co-perfusion of axoplasms with gp120 and the Tak-1 inhibitor (5Z)-7-Oxozeaenol completely protected FAT. This result not only identified the MAP3K activator to be Tak-1, but also demonstrated that Tak-1 is upstream of both PP1 activation and p38

MAPK/JNK activation, since the Tak-1 inhibitor was able to abolish FAT inhibition by gp120. It is unclear why (5Z)-7-Oxozeaenol showed complete FAT protection, while the DVD peptide only partially protected FAT. Since they both targeted Tak-1, they would be expected to both protect FAT to the same extent. It may be that the DVD peptide was less effective at Tak-1 inhibition than the specific Tak-1 inhibitor (5Z)-7-Oxozeaenol. Alternatively, the action of Tak-1 on the phosphatase pathway may be independent of MAPKK.

Since Tak-1 is likely to be upstream of PP1 based on the ability of (5Z)-7-Oxozeaenol to completely protect FAT, downstream signaling cascades of Tak-1 were examined for PP1 involvement. Tak-1 is well defined as a regulator of inflammatory and immune signaling pathways through activation of the NF-κB pathway (Sakurai, 2012). To do so, Tak-1 activates the IKK complex, which is composed of IKK-1, IKK-2 and NF-κB essential modulator (NEMO; Sakurai, 2012). Activation of the IKK complex through phosphorylation then triggers phosphorylation of Inhibitor of Kappa B (IκB) by IKK-2 (Karin, 1999). IκB normally exists bound to NF-κB to inhibit its translocation into the nucleus; phosphorylation of IκB by IKK-2 targets it for proteasomal degradation (Hacker and Karin, 2006). This releases NF-κB, allowing it to traffic to the nucleus and stimulate transcription of target genes (Hacker and Karin, 2006).

Recently it was found that PP1 interacts with the IKK complex to positively regulate IKK-2 activation (Mitsuhashi et al., 2008). Based on this evidence, we chose to examine whether this pathway might be activated by gp120 treatment. Perfusing axoplasm with IKK-2 inhibited FAT in both anterograde and

retrograde directions, demonstrating that IKK-2 may also regulate FAT. Next, co-perfusion of axoplasm with gp120 and the IKK-2 inhibitor XII exhibited partial protection, indicating that gp120 activates IKK-2 to inhibit FAT.

These results define a novel role for IKK-2 in regulation of FAT, which is outside of its role in activating NF-κB. In fact, accumulations of both IKK-2 and phosphorylated IκBα have been detected in axons, primarily in initial segments and nodes of Ranvier extending into paranodes (Schultz et al., 2006; Politi et al., 2008). Phosphorylated IκBα was associated with microtubules (Politi et al., 2008), placing it in an appropriate location to regulate FAT. IκBα has also been associated with dynein light chain (DLC) through a yeast two-hybrid screen, coimmunoprecipitation in cell lines, and colocalization in immunofluorescence (Crepieux et al., 1997). However, the mechanism for IKK-2 or IκBα regulation of motor proteins remains to be defined. Future experiments will need to be completed to determine whether IKK-2 or IκBα might directly phosphorylate kinesin or dynein, or if they activate a downstream kinase that phosphorylates either of the motor proteins to regulate FAT.

The gp120 in the axoplasm experiments was intra-cytoplasmic, and it is unknown whether gp120 gets released into the cytoplasm. Although an iodixanol flotation assay was performed to address this question, the assay did not separate the cytoplasm sufficiently well from vesicle markers to be useful. Subcellular fractionation is another experiment that should be done in the future to examine whether internalized gp120 has access to the cytoplasm. However, evidence has accumulated that proteins in the surrounding environment may have greater

access to the cytoplasm of neurons than had previously been thought. For example, in epilepsy cases Immunoglobulin G (IgG) has been found to cross the blood brain barrier and accumulate in the cytoplasm of certain neurons (Rigau et al., 2007; Michalak et al., 2012). Albumin also enters the cytoplasm of neurons in response to cryogenic brain lesions (Loberg et al., 1992). In fact, a study examining brains sections of rabbits, mice and rats detected IgG in within the cytoplasm of certain neurons, demonstrating that IgG can accumulate in the cytoplasm even in healthy neurons (Yoshimi et al., 2002).

Other non-plasma, extracellular proteins might also accumulate in the cytoplasm of neurons, despite the fact that they were long believed to remain within endolysosomal compartments until degradation by lysosomes (Ren et al., 2009). For example, it was discovered that fetal neurons transplanted into two individuals with Parkinson's disease developed Lewy bodies in the cytoplasm, indicating that α-synuclein from the recipient had access to the cytoplasm of the transplanted neurons (Li et al., 2008). In addition, treating cultured cells with polyglutamine aggregates led to an accumulation of the aggregates in the cytoplasm of the cells, as demonstrated by deep-etch transmission electron microscopy and colocalization of the aggregates with cytoplasmic quality control proteins (Ren et al., 2009). In another study, homogenized brains from transgenic mice for a human tau mutant that forms aggregates were injected into transgenic mice expressing tau that does not form aggregates, leading to tau aggregation and spreading to other brain regions (Clavaguera et al., 2009). In order for this to occur, it was postulated that tau aggregates can be internalized into neurons and seed new tau aggregates (Clavaguera et al., 2009). In fact, this

was shown to be the case in cultured cells that were treated with extracellular tau aggregates, leading to internalization of tau into intracellular cytoplasmic compartments and development of tau aggregates (Frost et al., 2009). Similarly, oligomeric amyloid β (Aβ), an extracellular neurotoxic peptide in Alzheimer's disease, has been found to have an intracellular effect on FAT through dysregulation of certain regulatory kinases (Pigino et al., 2009) and there is considerable evidence for the presence of cytoplasmic Aβ oligomers in neurons of Alzheimer's patients. Taken together, these studies demonstrate that extracellular proteins may enter cytoplasm of neurons to a much greater extent than had previously been thought. It is not implausible that extracellular gp120 might have access to the cytoplasm as well.

Here we defined the enzymatic pathway that gp120 can activate to inhibit FAT (Figure 17). Intra-axoplasmic gp120 activates Tak-1. This activation may be direct or through an upstream activator of Tak-1. Tak-1 activation leads to activation of two separate signaling pathways that regulate FAT: one that activates p38 MAPK and JNK, and another that activates PP1 and IKK-2. Both p38 MAPK and JNK directly phosphorylate kinesin (Morfini et al., 2006; Morfini, 2013 (submitted)) to inhibit FAT. The role of IKK-2 in regulation of FAT has not been examined before and remains a promising area of research to define new mechanisms of FAT regulation. Future studies that can improve our understanding of gp120's effects on FAT include the determination of which domain of gp120 is responsible for activating the Tak-1 signaling cascade, whether upstream activator(s) of Tak-1 exist, and elucidation of downstream targets of IKK-2 to impair FAT.

Figure 17

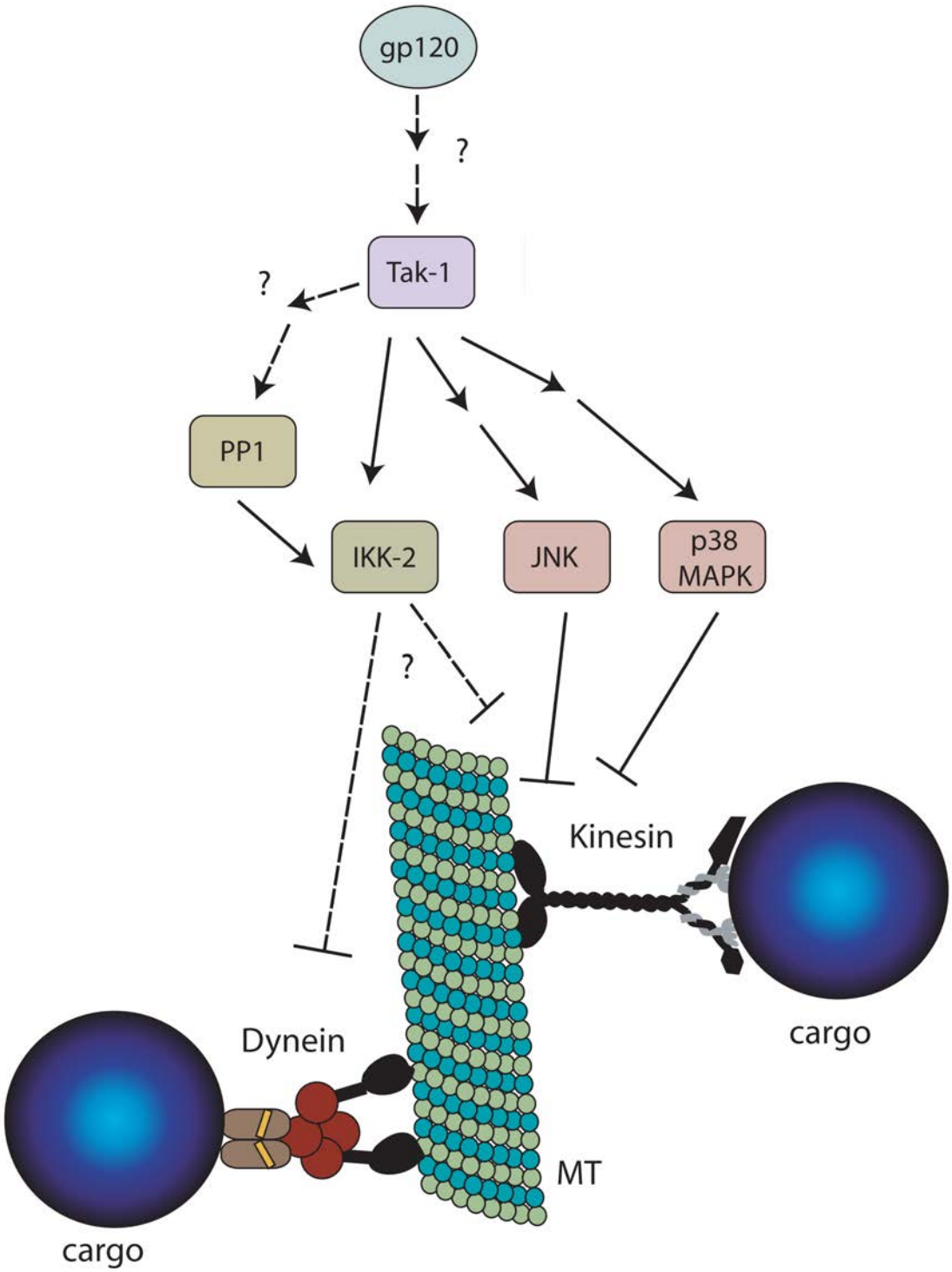
gp120
?
Tak-1
?
PP1
IKK-2
JNK
p38
MAPK
?
Kinesin
cargo
Dynein
MT
cargo

Figure 17. Schematic for the regulatory kinase signaling pathways activated by gp120 to impair FAT. Gp120 activates a signaling cascade leading to Tak-1 activation. This upstream activation remains to be defined. Tak-1 then activates PP1, IKK-2, JNK and p38 MAPK to impair FAT. While both JNK and p38 MAPK are known to directly interact with KHC to inhibit binding to microtubules, the role for IKK-2 in impairment of FAT remains to be determined. PP1 exists in a complex with IKK-2 and activates IKK-2 downstream of Tak-1 to enhance IKK-2 activity.

4.4 Gp120 Treatment Reduces Dynein Intermediate Chain Association with Microtubules

To examine whether gp120 treatment decreases the amount of kinesin and CDyn that are bound to microtubules, a microtubule binding assay was performed. Although gp120 treatment caused a slight decrease in kinesin binding to microtubules, this decrease was not statistically significant. However, gp120 treatment did reduce the amount of DIC in the microtubule pellet. This indicates that gp120 treatment either released the CDyn complex from microtubules or uncoupled DIC from DHC, which remained bound to microtubules. Further studies are needed to determine the precise mechanism for changes in DIC association with microtubules in response to gp120 treatment. Since gp120 had activated p38 MAPK and JNK in the squid axoplasm, and it is known that p38 MAPK and JNK phosphorylate KHC's to release kinesin from microtubules (Morfini et al., 2006; Morfini, 2013 (submitted)), it was surprising that we did not see a significant decrease in kinesin binding to microtubules. The microtubule binding assay may not have been sensitive enough to detect changes. Also, although multiple treatment times were tested, the appropriate timing and/or concentration of gp120 may not have been used. Future studies to directly examine phosphorylation of kinesin in response to gp120 treatment would be beneficial.

The phosphoregulation of CDyn is still little understood. In one study, increased phosphorylation of DHC and DIC in rat hepatocytes inhibited CDyn ATPase activity (Runnegar et al., 1999). However, it has also been demonstrated that the PKC catalytic subunit actually enhances CDyn-mediated FAT, which can

be deleterious to neuronal function by depleting synaptic vesicles from presynaptic terminals (Morfini et al., 2007). Therefore, phosphorylation of CDyn might impair FAT by either activating or inhibiting CDyn functions. Intriguingly, it was recently found that the kinase CK2 causes uncoupling of DHC from DIC, as shown in microtubule binding assays in which CK2 caused DIC to be released from the microtubule pellet, although DHC remained in the microtubule pellet (unpublished data, Brady lab). It is still not known how CDyn is inhibited by gp120 treatment, but examination of the uncoupling of DIC to DHC might shed some light on the direct effects on CDyn. The inhibition of retrograde FAT seen by gp120 could be either a direct or indirect response to gp120 treatment. For example, the monoclonal antibody H2 that inhibits kinesin can also decrease retrograde FAT (Brady et al., 1990), demonstrating that retrograde transport can be decreased in response to inhibited anterograde transport. An alternative possibility is that IKK-2 or phosphorylated IκBα might regulate CDyn-mediated transport. Future experiments need to be done to parse out the role of dysregulation of CDyn in gp120-mediated FAT inhibition.

5. Implications for the role of gp120 in Distal Sensory Polyneuropathy

We have described a novel direct pathway of neurotoxicity for gp120. Gp120 is internalized by neurons, then localized and transported in their axons. The close proximity of gp120 to critical components of the FAT machinery places gp120 at the optimal subcellular location to interfere with phosphorylation processes regulating FAT. In fact, intra-axonal gp120 directly impairs FAT

through alteration of regulatory signaling cascades. As impaired FAT leads to dying-back neuropathies, this model explains the dying-back neurodegeneration seen in DSP as well as the timing of DSP, because impaired FAT can take decades to progress to symptoms of dying-back neuropathies. However, this direct effect of gp120 does not exclude the possibility of indirect actions as well. In fact, it is quite possible that multiple actions of gp120 synergize to harm DRG neurons. For example, the activation of CXCR4 by gp120 that leads to p38 MAPK activation might exacerbate the p38 MAPK activation caused by intra-axonal gp120. Additionally, TNF-α has been strongly implicated in the inflammatory response in the indirect pathway for DSP (Herzberg and Sagen, 2001; Keswani et al., 2003; Zheng et al., 2011). Intriguingly, TNF-α activates Tak-1 to activate the NF-kB pathway, which is the same pathway that we have found activated by intra-axonal gp120. These multiple mechanisms leading to activation of Tak-1 could very well synergize with each other. We propose, however, that the impairment of FAT by gp120 is a critical step in the pathway to the development of DSP, making DSP a member of the class of dysferopathies.

Certain risk factors for DSP also provide evidence that impaired FAT is the mechanism for development of DSP. For example, one factor that is associated with DSP is taller height (Evans et al., 2011). Since the longest axons are the most vulnerable to impairments in FAT, it is plausible that taller people with longer sensory axons would be more likely to suffer from DSP. HIV patients who have diabetes mellitus (DM) are also at greater risk for developing DSP (Evans et al., 2011; Anziska et al., 2012). Sensory neuropathies that have been linked to impaired FAT also develop in DM (King, 2001). Thus, subclinical impairments of

FAT by HIV might be exacerbated by subclinical impairments in DM, leading to a higher likelihood of the development of symptomatic DSP.

The most significant risk factor for DSP is age (Ellis et al., 2010; Nakamoto et al., 2010; Evans et al., 2011; Anziska et al., 2012), which is also associated with dysferopathies. This can be explained by the fact that transport progressively declines with aging (McQuarrie et al., 1989). A model for this (Figure 18) is that during development, an abundance of FAT exists. During the aging process, FAT declines. In healthy people, this decline does not hit a threshold within their lifetimes to cause any symptoms. In dysferopathies linked to genetic mutations, patients begin life with less FAT than healthy individuals. Therefore, their decline hits a threshold earlier, leading to the development of symptoms in mid-life. In cases of insults later in life that cause dysferopathies, these might steepen the slope of decline in FAT, leading to FAT levels dropping below threshold and causing symptoms of dying-back neuropathies.

We propose that aging is a significant risk factor for DSP because HIV infection can compromise FAT and increase the rate of FAT decline. Unmyelinated DRG axons would be most at risk for dying-back degeneration, since they are more exposed to extracellular gp120 than their myelinated counterparts. Although gp120 can cause inhibition of FAT, this would not result in symptoms until transport in the patients' neurons had declined enough to cross a threshold. Since the decline of FAT is a slow process, this would also explain the preponderance of subclinical DSP. Further studies should be undertaken to define the signaling pathways that gp120 activates and the mechanisms for FAT impairment by gp120.

Figure 18

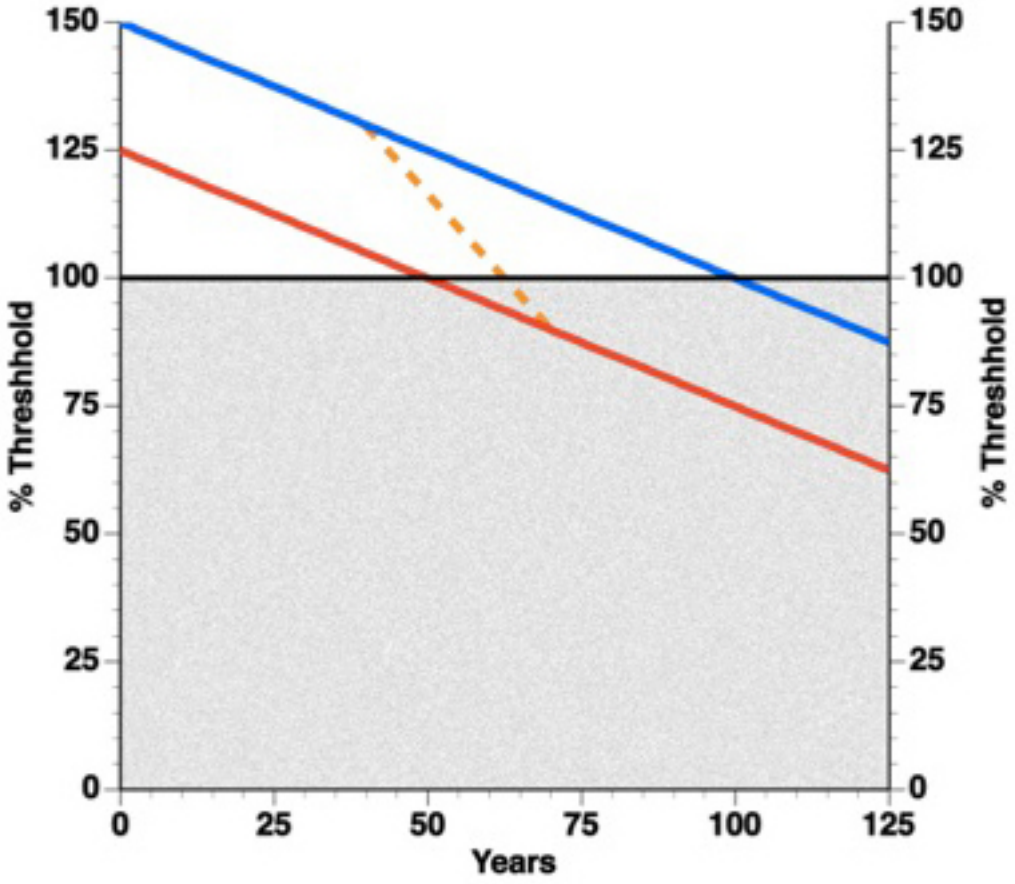

Figure 18. During development, there is an abundance of FAT. During the aging process, the amount of FAT declines (blue line). In healthy individuals, this progressive decline does not cross a threshold required for symptoms until after death. However, individuals with mutations that inhibit FAT (red line) will start out with less FAT, and the threshold at which symptoms appear will be crossed earlier, during mid-life. The slope of the blue line can also be changed due to an environmental insult (dashed yellow line), which would also cause the threshold for symptoms to be crossed earlier, leading to onset of symptoms. In the case of HIV-infected patients, this change in slope would be triggered by HIV infection. Gp120-mediated dysregulation would cause progressive decline in FAT, triggering DSP in patients after decades of infection.

CHAPTER VI

CONCLUSIONS

DSP, the most common neurological complication of HIV, causes excruciating pain for patients; yet few treatment options exist. The pain is severe enough that it is common for patients to not be able to sleep with sheets or wear socks and shoes (Dorsey and Morton, 2006). Due to improvements of HIV cART leading to increased lifespans of those infected with HIV, treatment of debilitating complications such as DSP are important to improve quality of life for these patients. Discovering new treatment targets is critical for DSP patients.

Neurons of the PNS are extremely polarized, with axons reaching up to 1 meter in length in humans. This places remarkable demands on their cell bodies, since virtually all protein synthesis occurs in the cell body, and proteins must be transported with precise timing to the appropriate location in order for axons to remain healthy. Thus, proper functioning of FAT is critical to maintain axon health and prevent dying-back neurodegeneration.

It has been determined that FAT is highly regulated by phosphotransferase activity. In fact, impairment of this kinase regulation of FAT is a common mechanism in dysferopathies, a class of dying-back neurodegenerative diseases. The similarity in DSP to these dysferopathies, including the late onset, progressive dying-back neurodegeneration of axons, and the presence of certain

risk factors indicative of impaired FAT led us to propose a novel hypothesis that dysregulation of FAT is the underlying mechanism responsible for development of DSP.

Here we showed that the neurotoxic HIV glycoprotein gp120 was internalized by F11 cells and DRG neurons, and located within axons after internalization. Internalization was partially dependent on gp120 binding to its coreceptor CXCR4, and it occurred primarily through lipid rafts with a fraction through fluid phase pinocytosis. Intra-axonal gp120 was then found to profoundly impair both anterograde and retrograde FAT. The mechanism for this inhibition of FAT was determined through kinase inhibitor studies to be through the activation of Tak-1 signaling cascade, leading to p38 MAPK and JNK activation. Both p38 MAPK and JNK kinases can directly phosphorylate kinesin and decrease FAT (Morfini et al., 2006; Morfini, 2013 (submitted)). Tak-1 activation also led to PP1 and IKK-2 activation, which is a novel regulatory pathway for FAT. Further confirming this data in mammalian cells, p38 MAPK was activated independently of CXCR4 after 30 minutes, which corresponds with gp120 internalization timing. Additionally, gp120 treatment led to release of DIC from microtubules, demonstrating that gp120 affects motor protein association with microtubules. These results have illuminated a novel mechanism for DSP (Figure 19).

The observations above suggest that abnormalities in the activities of protein kinases involved in the regulation of FAT might play a role in the pathogenesis of DSP. If the toxic effect of gp120 indeed derives, at least in part, from such alterations, then the activity of these enzymes could be corrected using

pharmacological approaches. The identification of mechanisms for gp120 internalization by sensory neurons as well as the misregulation of kinase activities relevant to FAT by intra-axonal gp120 represents a first critical step. After this, novel pharmacological inhibitors could be developed, or already existing ones applied in combination to either minimize gp120 internalization or to restore the activity of these kinases to their normal levels, without compromising their basic functions. Targeting lipid rafts by depleting cholesterol might be an effective treatment option by preventing gp120 internalization. In fact, many drugs such as statins are safe and effectively used to decrease cholesterol. Treating HIV patients with statins could target DSP and provide some relief from the pain. However, the possibility of using statins will need to be carefully examined, since certain statins have dangerous interactions with HIV protease inhibitors. Another concern would be that they may not reduce internalization sufficiently to be effective.

The development of kinase inhibitors targeting specific pools of a given protein kinase suggests that targeted inhibition of kinases relevant to FAT is not implausible (Waetzig and Herdegen, 2005). A message of hope is given by the fact that several kinase inhibitors have been already successfully tested *in vivo* in a variety of animal disease models, and some have already entered phase III in human clinical trials, including inhibitors of GSK-3 (Eldar-Finkelman and Ilouz, 2003), p38 MAPK (Munoz et al., 2007), and JNK kinases (Bogoyevitch et al., 2004), among others. Halting impairments in FAT could halt disease progression and improve disease outcomes.

This dissertation research has identified a novel mechanism for the

progression of DSP, as well as potential new treatment targets for HIV patients suffering from DSP. Further studies will be needed to explore these mechanisms and evaluate therapeutic interventions for DSP.

Figure 19

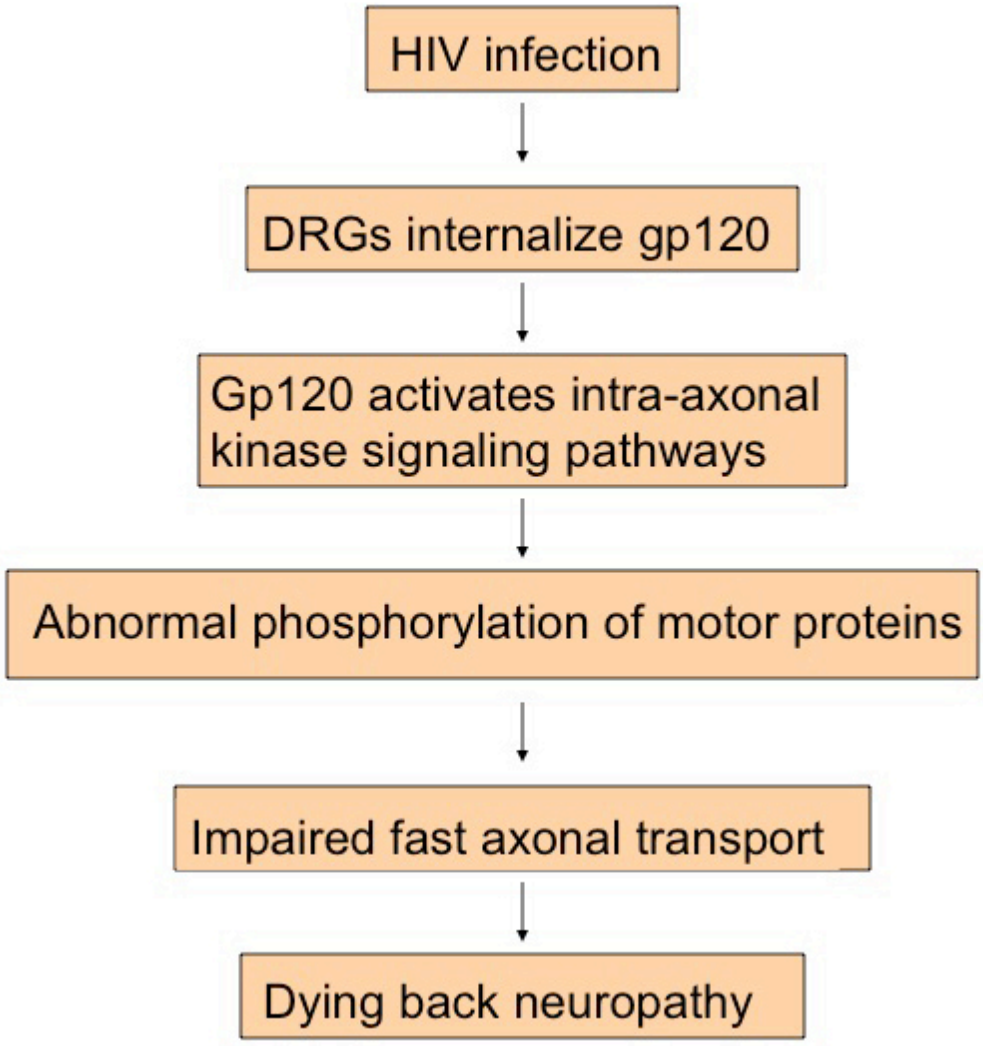

Figure 19. A model for DSP based on the results from this dissertation. In HIV infection, gp120 is internalized by sensory neurons and their axons. Intra-axonal gp120 interacts with regulatory signaling pathways for FAT, leading abnormal motor protein phosphorylation. This could lead to reduced binding to microtubules, as evidenced in the case of DIC. Ultimately, these aberrant activations of phosphotransferase activity lead to inhibited FAT. Over a period of years, the progressive decline of FAT leads to dying-back neurodegeneration of DRG axons, leading to the symptoms seen in DSP.

CITED LITERATURE

Ahmed F, MacArthur L, De Bernardi MA, Mocchetti I (2009) Retrograde and anterograde transport of HIV protein gp120 in the nervous system. Brain, behavior, and immunity 23:355-364.

Alexander M, Lynch R, Mulenga J, Allen S, Derdeyn CA, Hunter E (2010) Donor and recipient envs from heterosexual human immunodeficiency virus subtype C transmission pairs require high receptor levels for entry. J Virol 84:4100-4104.

Alirezaei M, Watry DD, Flynn CF, Kiosses WB, Masliah E, Williams BR, Kaul M, Lipton SA, Fox HS (2007) Human immunodeficiency virus-1/surface glycoprotein 120 induces apoptosis through RNA-activated protein kinase signaling in neurons. J Neurosci 27:11047-11055.

Ambrose Z, KewalRamani VN, Bieniasz PD, Hatziioannou T (2007) HIV/AIDS: in search of an animal model. Trends Biotechnol 25:333-337.

Ances BM, Letendre SL, Alexander T, Ellis RJ (2008) Role of psychiatric medications as adjunct therapy in the treatment of HIV associated neurocognitive disorders. Int Rev Psychiatry 20:89-93.

Ancuta P, Kamat A, Kunstman KJ, Kim EY, Autissier P, Wurcel A, Zaman T, Stone D, Mefford M, Morgello S, Singer EJ, Wolinsky SM, Gabuzda D (2008) Microbial translocation is associated with increased monocyte activation and dementia in AIDS patients. PLoS One 3:e2516.

Antinori A et al. (2007) Updated research nosology for HIV-associated neurocognitive disorders. Neurology 69:1789-1799.

Anziska Y, Helzner EP, Crystal H, Glesby MJ, Plankey M, Weber K, Golub E, Burian P (2012) The relationship between race and HIV-distal sensory polyneuropathy in a large cohort of US women. J Neurol Sci 315:129-132.

Apostolski S, McAlarney T, Hays AP, Latov N (1994) Complement dependent cytotoxicity of sensory ganglion neurons mediated by the gp120 glycoprotein of HIV-1. Immunol Invest 23:47-52.

Apostolski S, McAlarney T, Quattrini A, Levison SW, Rosoklija G, Lugaressi A, Corbo M, Sadiq SA, Lederman S, Hays AP, et al. (1993) The gp120 glycoprotein of human immunodeficiency virus type 1 binds to sensory ganglion neurons. Ann Neurol 34:855-863.

Arrildt KT, Joseph SB, Swanstrom R (2012) The HIV-1 env protein: a coat of many colors. Curr HIV/AIDS Rep 9:52-63.

Baas PW, Ahmad FJ (1993) The transport properties of axonal microtubules establish their polarity orientation. J Cell Biol 120:1427-1437.

Bachis A, Major EO, Mocchetti I (2003) Brain-derived neurotrophic factor inhibits human immunodeficiency virus-1/gp120-mediated cerebellar granule cell death by preventing gp120 internalization. J Neurosci 23:5715-5722.

Bachis A, Cruz MI, Mocchetti I (2010) M-tropic HIV envelope protein gp120 exhibits a different neuropathological profile than T-tropic gp120 in rat striatum. Eur J Neurosci 32:570-578.

Bachis A, Biggio F, Major EO, Mocchetti I (2009) M- and T-tropic HIVs promote apoptosis in rat neurons. J Neuroimmune Pharmacol 4:150-160.

Bachis A, Aden SA, Nosheny RL, Andrews PM, Mocchetti I (2006) Axonal transport of human immunodeficiency virus type 1 envelope protein glycoprotein 120 is found in association with neuronal apoptosis. J Neurosci 26:6771-6780.

Barre-Sinoussi F, Chermann JC, Rey F, Nugeyre MT, Chamaret S, Gruest J, Dauguet C, Axler-Blin C, Vezinet-Brun F, Rouzioux C, Rozenbaum W, Montagnier L (1983) Isolation of a T-lymphotropic retrovirus from a patient at risk for acquired immune deficiency syndrome (AIDS). Science 220:868-871.

Beffert U, Morfini G, Bock HH, Reyna H, Brady ST, Herz J (2002) Reelin-mediated signaling locally regulates protein kinase B/Akt and glycogen synthase kinase 3beta. J Biol Chem 277:49958-49964.

Ben Othmane K, Middleton LT, Loprest LJ, Wilkinson KM, Lennon F, Rozear MP, Stajich JM, Gaskell PC, Roses AD, Pericak-Vance MA, et al. (1993) Localization of a gene (CMT2A) for autosomal dominant Charcot-Marie-Tooth disease type 2 to chromosome 1p and evidence of genetic heterogeneity. Genomics 17:370-375.

Berth SH, Leopold PL, Morfini GN (2009) Virus-induced neuronal dysfunction and degeneration. Front Biosci 14:5239-5259.

Bezzi P, Domercq M, Brambilla L, Galli R, Schols D, De Clercq E, Vescovi A, Bagetta G, Kollias G, Meldolesi J, Volterra A (2001) CXCR4-activated astrocyte glutamate release via TNFalpha: amplification by microglia triggers neurotoxicity. Nat Neurosci 4:702-710.

Bhangoo SK, Ripsch MS, Buchanan DJ, Miller RJ, White FA (2009) Increased chemokine signaling in a model of HIV1-associated peripheral neuropathy. Mol Pain 5:48.

Blair MA, Ma S, Hedera P (2006) Mutation in KIF5A can also cause adult-onset hereditary spastic paraplegia. Neurogenetics 7:47-50.

Blankson JN, Persaud D, Siliciano RF (2002) The challenge of viral reservoirs in HIV-1 infection. Annu Rev Med 53:557-593.

Bloom GS, Wagner MC, Pfister KK, Brady ST (1988) Native structure and physical properties of bovine brain kinesin and identification of the ATP-binding subunit polypeptide. Biochemistry 27:3409-3416.

Blumenthal R, Durell S, Viard M (2012) HIV entry and envelope glycoprotein-mediated fusion. J Biol Chem 287:40841-40849.

Bobardt MD, Salmon P, Wang L, Esko JD, Gabuzda D, Fiala M, Trono D, Van der Schueren B, David G, Gallay PA (2004) Contribution of proteoglycans to human immunodeficiency virus type 1 brain invasion. J Virol 78:6567-6584.

Bodner A, Toth PT, Miller RJ (2004) Activation of c-Jun N-terminal kinase mediates gp120IIIB- and nucleoside analogue-induced sensory neuron toxicity. Exp Neurol 188:246-253.

Bodner A, Maroney AC, Finn JP, Ghadge G, Roos R, Miller RJ (2002) Mixed lineage kinase 3 mediates gp120IIIB-induced neurotoxicity. J Neurochem 82:1424-1434.

Bogoyevitch MA, Boehm I, Oakley A, Ketterman AJ, Barr RK (2004) Targeting the JNK MAPK cascade for inhibition: basic science and therapeutic potential. Biochim Biophys Acta 1697:89-101.

Bosch B, Grigorov B, Senserrich J, Clotet B, Darlix JL, Muriaux D, Este JA (2008) A clathrin-dynamin-dependent endocytic pathway for the uptake of HIV-1 by direct T cell-T cell transmission. Antiviral Res 80:185-193.

Bosco DA, Morfini G, Karabacak NM, Song Y, Gros-Louis F, Pasinelli P, Goolsby H, Fontaine BA, Lemay N, McKenna-Yasek D, Frosch MP, Agar JN, Julien JP, Brady ST, Brown RH, Jr. (2010) Wild-type and mutant SOD1 share an aberrant conformation and a common pathogenic pathway in ALS. Nat Neurosci 13:1396-1403.

Bradley WG, Shapshak P, Delgado S, Nagano I, Stewart R, Rocha B (1998) Morphometric analysis of the peripheral neuropathy of AIDS. Muscle Nerve 21:1188-1195.

Brady ST (1985) A novel brain ATPase with properties expected for the fast axonal transport motor. Nature 317:73-75.

Brady ST, Lasek RJ, Allen RD (1985) Video microscopy of fast axonal transport in extruded axoplasm: a new model for study of molecular mechanisms. Cell Motil 5:81-101.

Brady ST, Pfister KK, Bloom GS (1990) A monoclonal antibody against kinesin inhibits both anterograde and retrograde fast axonal transport in squid axoplasm. Proc Natl Acad Sci U S A 87:1061-1065.

Brady ST, Richards BW, Leopold PL (1993) Assay of vesicle motility in squid axoplasm. Methods Cell Biol 39:191-202.

Brady ST, Pfister, K.K., Leopold, P.L., Bloom, G.S. (1990) Fast Axonal Transport in Isolated Axoplasm. Cell Motil Cytoskeleton 17:Video Supplement 2.

Brannagan TH, 3rd, Nuovo GJ, Hays AP, Latov N (1997) Human immunodeficiency virus infection of dorsal root ganglion neurons detected by polymerase chain reaction in situ hybridization. Ann Neurol 42:368-372.

Brenneman DE, Westbrook GL, Fitzgerald SP, Ennist DL, Elkins KL, Ruff MR, Pert CB (1988) Neuronal cell killing by the envelope protein of HIV and its prevention by vasoactive intestinal peptide. Nature 335:639-642.

Brill LB, 2nd, Pfister KK (2000) Biochemical and molecular analysis of the mammalian cytoplasmic dynein intermediate chain. Methods 22:307-316.

Bruce-Keller AJ, Chauhan A, Dimayuga FO, Gee J, Keller JN, Nath A (2003) Synaptic transport of human immunodeficiency virus-Tat protein causes neurotoxicity and gliosis in rat brain. J Neurosci 23:8417-8422.

CDC (2012) Monitoring selected national HIV prevention and care objectives by using HIV surveillance data - United States and 6 U.S. dependent areas - 2010. In: HIV Surveillance Supplemental Report: Centers for Disease Control and Prevention.

Cefai D, Ferrer M, Serpente N, Idziorek T, Dautry-Varsat A, Debre P, Bismuth G (1992) Internalization of HIV glycoprotein gp120 is associated with down-modulation of membrane CD4 and p56lck together with impairment of T cell activation. J Immunol 149:285-294.

Chazal N, Gerlier D (2003) Virus entry, assembly, budding, and membrane rafts. Microbiol Mol Biol Rev 67:226-237, table of contents.

Chen P, Mayne M, Power C, Nath A (1997) The Tat protein of HIV-1 induces tumor necrosis factor-alpha production. Implications for HIV-1-associated neurological diseases. J Biol Chem 272:22385-22388.

Chi X, Amet T, Byrd D, Chang KH, Shah K, Hu N, Grantham A, Hu S, Duan J, Tao F, Nicol G, Yu Q (2011) Direct effects of HIV-1 Tat on excitability and survival of

primary dorsal root ganglion neurons: possible contribution to HIV-1-associated pain. PLoS One 6:e24412.

Chiesa R, Piccardo P, Dossena S, Nowoslawski L, Roth KA, Ghetti B, Harris DA (2005) Bax deletion prevents neuronal loss but not neurological symptoms in a transgenic model of inherited prion disease. Proc Natl Acad Sci U S A 102:238-243.

Chu Y, Morfini GA, Langhamer LB, He Y, Brady ST, Kordower JH (2012) Alterations in axonal transport motor proteins in sporadic and experimental Parkinson's disease. Brain 135:2058-2073.

Clavaguera F, Bolmont T, Crowther RA, Abramowski D, Frank S, Probst A, Fraser G, Stalder AK, Beibel M, Staufenbiel M, Jucker M, Goedert M, Tolnay M (2009) Transmission and spreading of tauopathy in transgenic mouse brain. Nature cell biology 11:909-913.

Clifford DB (2008) HIV-associated neurocognitive disease continues in the antiretroviral era. Top HIV Med 16:94-98.

Coleman M (2005) Axon degeneration mechanisms: commonality amid diversity. Nat Rev Neurosci 6:889-898.

Crepieux P, Kwon H, Leclerc N, Spencer W, Richard S, Lin R, Hiscott J (1997) I kappaB alpha physically interacts with a cytoskeleton-associated protein through its signal response domain. Mol Cell Biol 17:7375-7385.

Crublet E, Andrieu JP, Vives RR, Lortat-Jacob H (2008) The HIV-1 envelope glycoprotein gp120 features four heparan sulfate binding domains, including the co-receptor binding site. J Biol Chem 283:15193-15200.

Cyr JL, Pfister KK, Bloom GS, Slaughter CA, Brady ST (1991) Molecular genetics of kinesin light chains: generation of isoforms by alternative splicing. Proc Natl Acad Sci U S A 88:10114-10118.

Daecke J, Fackler OT, Dittmar MT, Krausslich HG (2005) Involvement of clathrin-mediated endocytosis in human immunodeficiency virus type 1 entry. J Virol 79:1581-1594.

Dash PK, Gorantla S, Gendelman HE, Knibbe J, Casale GP, Makarov E, Epstein AA, Gelbard HA, Boska MD, Poluektova LY (2011) Loss of neuronal integrity during progressive HIV-1 infection of humanized mice. J Neurosci 31:3148-3157.

Davis CB, Dikic I, Unutmaz D, Hill CM, Arthos J, Siani MA, Thompson DA, Schlessinger J, Littman DR (1997) Signal transduction due to HIV-1 envelope interactions with chemokine receptors CXCR4 or CCR5. J Exp Med 186:1793-1798.

Davis LE, Hjelle BL, Miller VE, Palmer DL, Llewellyn AL, Merlin TL, Young SA, Mills RG, Wachsman W, Wiley CA (1992) Early viral brain invasion in iatrogenic human immunodeficiency virus infection. Neurology 42:1736-1739.

De Clercq E, Yamamoto N, Pauwels R, Balzarini J, Witvrouw M, De Vreese K, Debyser Z, Rosenwirth B, Peichl P, Datema R, et al. (1994) Highly potent and selective inhibition of human immunodeficiency virus by the bicyclam derivative JM3100. Antimicrob Agents Chemother 38:668-674.

DeBoer SR, You Y, Szodorai A, Kaminska A, Pigino G, Nwabuisi E, Wang B, Estrada-Hernandez T, Kins S, Brady ST, Morfini G (2008) Conventional kinesin holoenzymes are composed of heavy and light chain homodimers. Biochemistry 47:4535-4543.

Del Real G, Jimenez-Baranda S, Lacalle RA, Mira E, Lucas P, Gomez-Mouton C, Carrera AC, Martinez AC, Manes S (2002) Blocking of HIV-1 infection by targeting CD4 to nonraft membrane domains. J Exp Med 196:293-301.

Deluca GC, Ebers GC, Esiri MM (2004) The extent of axonal loss in the long tracts in hereditary spastic paraplegia. Neuropathol Appl Neurobiol 30:576-584.

Dillman JF, 3rd, Pfister KK (1994) Differential phosphorylation in vivo of cytoplasmic dynein associated with anterogradely moving organelles. J Cell Biol 127:1671-1681.

Dillman JF, 3rd, Pfister KK (1995) Differential phosphorylation in vivo of cytoplasmic dynein in anterograde and whole cell compartments. Biophys J 68:226S.

Donelan MJ, Morfini G, Julyan R, Sommers S, Hays L, Kajio H, Briaud I, Easom RA, Molkentin JD, Brady ST, Rhodes CJ (2002) Ca2+-dependent dephosphorylation of kinesin heavy chain on beta-granules in pancreatic beta-cells. Implications for regulated beta-granule transport and insulin exocytosis. J Biol Chem 277:24232-24242.

Dong J, Xiong H (2006) Human immunodeficiency virus type 1 gp120 inhibits long-term potentiation via chemokine receptor CXCR4 in rat hippocampal slices. J Neurosci Res 83:489-496.

Donzella GA, Schols D, Lin SW, Este JA, Nagashima KA, Maddon PJ, Allaway GP, Sakmar TP, Henson G, De Clercq E, Moore JP (1998) AMD3100, a small molecule inhibitor of HIV-1 entry via the CXCR4 co-receptor. Nat Med 4:72-77.

Dorsey SG, Morton PG (2006) HIV peripheral neuropathy: pathophysiology and clinical implications. AACN clinical issues 17:30-36.

Dupuis L, Fergani A, Braunstein KE, Eschbach J, Holl N, Rene F, Gonzalez De Aguilar JL, Zoerner B, Schwalenstocker B, Ludolph AC, Loeffler JP (2009) Mice with a

mutation in the dynein heavy chain 1 gene display sensory neuropathy but lack motor neuron disease. Exp Neurol 215:146-152.

Ebbing B, Mann K, Starosta A, Jaud J, Schols L, Schule R, Woehlke G (2008) Effect of spastic paraplegia mutations in KIF5A kinesin on transport activity. Hum Mol Genet 17:1245-1252.

Eldar-Finkelman H, Ilouz R (2003) Challenges and opportunities with glycogen synthase kinase-3 inhibitors for insulin resistance and Type 2 diabetes treatment. Expert Opin Investig Drugs 12:1511-1519.

Ellis RJ, Rosario D, Clifford DB, McArthur JC, Simpson D, Alexander T, Gelman BB, Vaida F, Collier A, Marra CM, Ances B, Atkinson JH, Dworkin RH, Morgello S, Grant I (2010) Continued high prevalence and adverse clinical impact of human immunodeficiency virus-associated sensory neuropathy in the era of combination antiretroviral therapy: the CHARTER Study. Arch Neurol 67:552-558.

Erlich Y, Edvardson S, Hodges E, Zenvirt S, Thekkat P, Shaag A, Dor T, Hannon GJ, Elpeleg O (2011) Exome sequencing and disease-network analysis of a single family implicate a mutation in KIF1A in hereditary spastic paraparesis. Genome Res 21:658-664.

Evans SR, Ellis RJ, Chen H, Yeh TM, Lee AJ, Schifitto G, Wu K, Bosch RJ, McArthur JC, Simpson DM, Clifford DB (2011) Peripheral neuropathy in HIV: prevalence and risk factors. Aids 25:919-928.

Fernandes SP, Edwards TM, Ng KT, Robinson SR (2007) HIV-1 protein gp120 rapidly impairs memory in chicks by interrupting the glutamate-glutamine cycle. Neurobiol Learn Mem 87:1-8.

Fichera M, Lo Giudice M, Falco M, Sturnio M, Amata S, Calabrese O, Bigoni S, Calzolari E, Neri M (2004) Evidence of kinesin heavy chain (KIF5A) involvement in pure hereditary spastic paraplegia. Neurology 63:1108-1110.

Fischer LR, Culver DG, Tennant P, Davis AA, Wang M, Castellano-Sanchez A, Khan J, Polak MA, Glass JD (2004) Amyotrophic lateral sclerosis is a distal axonopathy: evidence in mice and man. Exp Neurol 185:232-240.

Frost B, Jacks RL, Diamond MI (2009) Propagation of tau misfolding from the outside to the inside of a cell. J Biol Chem 284:12845-12852.

Gallo KA, Johnson GL (2002) Mixed-lineage kinase control of JNK and p38 MAPK pathways. Nat Rev Mol Cell Biol 3:663-672.

Gallo RC, Salahuddin SZ, Popovic M, Shearer GM, Kaplan M, Haynes BF, Palker TJ, Redfield R, Oleske J, Safai B, et al. (1984) Frequent detection and isolation of

cytopathic retroviruses (HTLV-III) from patients with AIDS and at risk for AIDS. Science 224:500-503.

Gallo RC, Sarin PS, Gelmann EP, Robert-Guroff M, Richardson E, Kalyanaraman VS, Mann D, Sidhu GD, Stahl RE, Zolla-Pazner S, Leibowitch J, Popovic M (1983) Isolation of human T-cell leukemia virus in acquired immune deficiency syndrome (AIDS). Science 220:865-867.

Ghil SH, Kim BJ, Lee YD, Suh-Kim H (2000) Neurite outgrowth induced by cyclic AMP can be modulated by the alpha subunit of Go. J Neurochem 74:151-158.

Ghosh S, Chandran A, Jansen JP (2012) Epidemiology of HIV-related neuropathy: a systematic literature review. AIDS Res Hum Retroviruses 28:36-48.

Gilbert M, Kirihara J, Mills J (1991) Enzyme-linked immunoassay for human immunodeficiency virus type 1 envelope glycoprotein 120. J Clin Microbiol 29:142-147.

Ginty DD, Segal RA (2002) Retrograde neurotrophin signaling: Trk-ing along the axon. Curr Opin Neurobiol 12:268-274.

Giulian D, Vaca K, Noonan CA (1990) Secretion of neurotoxins by mononuclear phagocytes infected with HIV-1. Science 250:1593-1596.

Gorry PR, Bristol G, Zack JA, Ritola K, Swanstrom R, Birch CJ, Bell JE, Bannert N, Crawford K, Wang H, Schols D, De Clercq E, Kunstman K, Wolinsky SM, Gabuzda D (2001) Macrophage tropism of human immunodeficiency virus type 1 isolates from brain and lymphoid tissues predicts neurotropism independent of coreceptor specificity. J Virol 75:10073-10089.

Gould TW, Buss RR, Vinsant S, Prevette D, Sun W, Knudson CM, Milligan CE, Oppenheim RW (2006) Complete dissociation of motor neuron death from motor dysfunction by Bax deletion in a mouse model of ALS. J Neurosci 26:8774-8786.

Grafstein B, Forman DS (1980) Intracellular transport in neurons. Physiol Rev 60:1167-1283.

Greene WC (2007) A history of AIDS: looking back to see ahead. Eur J Immunol 37 Suppl 1:S94-102.

Greene WC, Peterlin BM (2002) Charting HIV's remarkable voyage through the cell: Basic science as a passport to future therapy. Nat Med 8:673-680.

Griffin JW, George, E.B., Hsieh, S., Glass, J.D. (1995) Axonal degeneration and disorders of the axonal cytoskeleton. In: The axon: structure, function and

pathophysiology (S.G. Waxman JDKPKS, ed). New York: Oxford University Press.

Ha J, Lo KW, Myers KR, Carr TM, Humsi MK, Rasoul BA, Segal RA, Pfister KK (2008) A neuron-specific cytoplasmic dynein isoform preferentially transports TrkB signaling endosomes. J Cell Biol 181:1027-1039.

Haase AT (1986) Pathogenesis of lentivirus infections. Nature 322:130-136.

Hacker H, Karin M (2006) Regulation and function of IKK and IKK-related kinases. Sci STKE 2006:re13.

Hafezparast M et al. (2003) Mutations in dynein link motor neuron degeneration to defects in retrograde transport. Science (New York, NY 300:808-812.

Hahn K, Robinson B, Anderson C, Li W, Pardo CA, Morgello S, Simpson D, Nath A (2008) Differential effects of HIV infected macrophages on dorsal root ganglia neurons and axons. Exp Neurol 210:30-40.

Hall AK (2006) Rodent sensory neuron culture and analysis. Curr Protoc Neurosci Chapter 3:Unit 3 19.

Hanna Z, Kay DG, Cool M, Jothy S, Rebai N, Jolicoeur P (1998) Transgenic mice expressing human immunodeficiency virus type 1 in immune cells develop a severe AIDS-like disease. J Virol 72:121-132.

Haughey NJ, Holden CP, Nath A, Geiger JD (1999) Involvement of inositol 1,4,5-trisphosphate-regulated stores of intracellular calcium in calcium dysregulation and neuron cell death caused by HIV-1 protein tat. J Neurochem 73:1363-1374.

Heaton RK et al. (2010) HIV-associated neurocognitive disorders persist in the era of potent antiretroviral therapy: CHARTER Study. Neurology 75:2087-2096.

Heerssen HM, Pazyra MF, Segal RA (2004) Dynein motors transport activated Trks to promote survival of target-dependent neurons. Nat Neurosci 7:596-604.

Herzberg U, Sagen J (2001) Peripheral nerve exposure to HIV viral envelope protein gp120 induces neuropathic pain and spinal gliosis. J Neuroimmunol 116:29-39.

Hesselgesser J, Taub D, Baskar P, Greenberg M, Hoxie J, Kolson DL, Horuk R (1998) Neuronal apoptosis induced by HIV-1 gp120 and the chemokine SDF-1 alpha is mediated by the chemokine receptor CXCR4. Curr Biol 8:595-598.

Hirokawa N, Noda Y (2008) Intracellular transport and kinesin superfamily proteins, KIFs: structure, function, and dynamics. Physiol Rev 88:1089-1118.

Hirokawa N, Sato-Yoshitake R, Kobayashi N, Pfister KK, Bloom GS, Brady ST (1991) Kinesin associates with anterogradely transported membranous organelles in vivo. J Cell Biol 114:295-302.

Holland NR, Stocks A, Hauer P, Cornblath DR, Griffin JW, McArthur JC (1997) Intraepidermal nerve fiber density in patients with painful sensory neuropathy. Neurology 48:708-711.

Hollenbeck PJ (1993) Phosphorylation of neuronal kinesin heavy and light chains in vivo. J Neurochem 60:2265-2275.

Hu S, Sheng WS, Lokensgard JR, Peterson PK (2005) Morphine potentiates HIV-1 gp120-induced neuronal apoptosis. J Infect Dis 191:886-889.

Isaacman-Beck J, Hermann EA, Yi Y, Ratcliffe SJ, Mulenga J, Allen S, Hunter E, Derdeyn CA, Collman RG (2009) Heterosexual transmission of human immunodeficiency virus type 1 subtype C: Macrophage tropism, alternative coreceptor use, and the molecular anatomy of CCR5 utilization. J Virol 83:8208-8220.

Johnston JB, Zhang K, Silva C, Shalinsky DR, Conant K, Ni W, Corbett D, Yong VW, Power C (2001) HIV-1 Tat neurotoxicity is prevented by matrix metalloproteinase inhibitors. Ann Neurol 49:230-241.

Kamerman PR, Moss PJ, Weber J, Wallace VC, Rice AS, Huang W (2012) Pathogenesis of HIV-associated sensory neuropathy: evidence from in vivo and in vitro experimental models. J Peripher Nerv Syst 17:19-31.

Kamiyama H, Yoshii H, Tanaka Y, Sato H, Yamamoto N, Kubo Y (2009) Raft localization of CXCR4 is primarily required for X4-tropic human immunodeficiency virus type 1 infection. Virology 386:23-31.

Kan H, Xie Z, Finkel MS (2000) HIV gp120 enhances NO production by cardiac myocytes through p38 MAP kinase-mediated NF-kappaB activation. Am J Physiol Heart Circ Physiol 279:H3138-3143.

Kanaan NM, Morfini G, Pigino G, LaPointe NE, Andreadis A, Song Y, Leitman E, Binder LI, Brady ST (2012) Phosphorylation in the amino terminus of tau prevents inhibition of anterograde axonal transport. Neurobiol Aging 33:826 e815-830.

Kapasi AA, Patel G, Franki N, Singhal PC (2002) HIV-1 gp120-induced tubular epithelial cell apoptosis is mediated through p38-MAPK phosphorylation. Mol Med 8:676-685.

Karin M (1999) How NF-kappaB is activated: the role of the IkappaB kinase (IKK) complex. Oncogene 18:6867-6874.

Kaul M, Zheng J, Okamoto S, Gendelman HE, Lipton SA (2005) HIV-1 infection and AIDS: consequences for the central nervous system. Cell Death Differ 12 Suppl 1:878-892.

Kaul M, Ma Q, Medders KE, Desai MK, Lipton SA (2007) HIV-1 coreceptors CCR5 and CXCR4 both mediate neuronal cell death but CCR5 paradoxically can also contribute to protection. Cell Death Differ 14:296-305.

Keele BF et al. (2008) Identification and characterization of transmitted and early founder virus envelopes in primary HIV-1 infection. Proc Natl Acad Sci U S A 105:7552-7557.

Keswani SC, Hoke A (2003) Incidence of and risk factors for HIV-associated distal sensory polyneuropathy. Neurology 61:279; author reply 279-280.

Keswani SC, Jack C, Zhou C, Hoke A (2006) Establishment of a rodent model of HIV-associated sensory neuropathy. The Journal of neuroscience 26:10299-10304.

Keswani SC, Pardo CA, Cherry CL, Hoke A, McArthur JC (2002) HIV-associated sensory neuropathies. Aids 16:2105-2117.

Keswani SC, Polley M, Pardo CA, Griffin JW, McArthur JC, Hoke A (2003) Schwann cell chemokine receptors mediate HIV-1 gp120 toxicity to sensory neurons. Ann Neurol 54:287-296.

Khan MZ, Brandimarti R, Patel JP, Huynh N, Wang J, Huang Z, Fatatis A, Meucci O (2004) Apoptotic and antiapoptotic effects of CXCR4: is it a matter of intrinsic efficacy? Implications for HIV neuropathogenesis. AIDS Res Hum Retroviruses 20:1063-1071.

Kim KY, Kim BC, Xu Z, Kim SJ (2004) Mixed lineage kinase 3 (MLK3)-activated p38 MAP kinase mediates transforming growth factor-beta-induced apoptosis in hepatoma cells. J Biol Chem 279:29478-29484.

King JE, Eugenin EA, Buckner CM, Berman JW (2006) HIV tat and neurotoxicity. Microbes Infect 8:1347-1357.

King RH (2001) The role of glycation in the pathogenesis of diabetic polyneuropathy. Mol Pathol 54:400-408.

Kramer-Hammerle S, Rothenaigner I, Wolff H, Bell JE, Brack-Werner R (2005) Cells of the central nervous system as targets and reservoirs of the human immunodeficiency virus. Virus Res 111:194-213.

Kranick SM, Nath A (2012) Neurologic Complications of HIV-1 Infection and Its Treatment in the Era of Antiretroviral Therapy. Continuum (Minneap Minn) 18:1319-1337.

Krathwohl MD, Kaiser JL (2004) HIV-1 promotes quiescence in human neural progenitor cells. J Infect Dis 190:216-226.

Kreutzberg GW (1969) Neuronal dynamics and axonal flow. IV. Blockage of intra-axonal enzyme transport by colchicine. Proc Natl Acad Sci U S A 62:722-728.

Kruman, II, Nath A, Mattson MP (1998) HIV-1 protein Tat induces apoptosis of hippocampal neurons by a mechanism involving caspase activation, calcium overload, and oxidative stress. Exp Neurol 154:276-288.

Kutsch O, Oh J, Nath A, Benveniste EN (2000) Induction of the chemokines interleukin-8 and IP-10 by human immunodeficiency virus type 1 tat in astrocytes. J Virol 74:9214-9221.

Kwong PD, Wyatt R, Robinson J, Sweet RW, Sodroski J, Hendrickson WA (1998) Structure of an HIV gp120 envelope glycoprotein in complex with the CD4 receptor and a neutralizing human antibody. Nature 393:648-659.

Lajoie P, Nabi IR (2010) Lipid rafts, caveolae, and their endocytosis. Int Rev Cell Mol Biol 282:135-163.

Lannuzel A, Lledo PM, Lamghitnia HO, Vincent JD, Tardieu M (1995) HIV-1 envelope proteins gp120 and gp160 potentiate NMDA-induced [Ca2+]i increase, alter [Ca2+]i homeostasis and induce neurotoxicity in human embryonic neurons. Eur J Neurosci 7:2285-2293.

Lasek RJaB, S.T. (1982) The Structural Hypothesis of axonal transport: Two classes of moving elements. In: Axoplasmic Transport (Weiss DG, ed). Berlin/Heidelberg: Springer-Verlag.

Lazarov O, Morfini GA, Pigino G, Gadadhar A, Chen X, Robinson J, Ho H, Brady ST, Sisodia SS (2007) Impairments in fast axonal transport and motor neuron deficits in transgenic mice expressing familial Alzheimer's disease-linked mutant presenilin 1. J Neurosci 27:7011-7020.

Lehmann HC, Chen W, Borzan J, Mankowski JL, Hoke A (2011) Mitochondrial dysfunction in distal axons contributes to human immunodeficiency virus sensory neuropathy. Ann Neurol 69:100-110.

Leitner T, Kumar S, Albert J (1997) Tempo and mode of nucleotide substitutions in gag and env gene fragments in human immunodeficiency virus type 1 populations with a known transmission history. J Virol 71:4761-4770.

Leopold PL, Pfister KK (2006) Viral strategies for intracellular trafficking: motors and microtubules. Traffic 7:516-523.

Leopold PL, McDowall AW, Pfister KK, Bloom GS, Brady ST (1992) Association of kinesin with characterized membrane-bounded organelles. Cell Motil Cytoskeleton 23:19-33.

Li JY, Englund E, Holton JL, Soulet D, Hagell P, Lees AJ, Lashley T, Quinn NP, Rehncrona S, Bjorklund A, Widner H, Revesz T, Lindvall O, Brundin P (2008) Lewy bodies in grafted neurons in subjects with Parkinson's disease suggest host-to-graft disease propagation. Nat Med 14:501-503.

Li ST, Matsushita M, Moriwaki A, Saheki Y, Lu YF, Tomizawa K, Wu HY, Terada H, Matsui H (2004) HIV-1 Tat inhibits long-term potentiation and attenuates spatial learning [corrected]. Ann Neurol 55:362-371.

Li W, Galey D, Mattson MP, Nath A (2005) Molecular and cellular mechanisms of neuronal cell death in HIV dementia. Neurotox Res 8:119-134.

Liao Z, Cimakasky LM, Hampton R, Nguyen DH, Hildreth JE (2001) Lipid rafts and HIV pathogenesis: host membrane cholesterol is required for infection by HIV type 1. AIDS Res Hum Retroviruses 17:1009-1019.

Lim JP, Gleeson PA (2011) Macropinocytosis: an endocytic pathway for internalising large gulps. Immunol Cell Biol 89:836-843.

Liu J, Xu C, Chen L, Xu P, Xiong H (2012) Involvement of Kv1.3 and p38 MAPK signaling in HIV-1 glycoprotein 120-induced microglia neurotoxicity. Cell Death Dis 3:e254.

Liu NQ, Lossinsky AS, Popik W, Li X, Gujuluva C, Kriederman B, Roberts J, Pushkarsky T, Bukrinsky M, Witte M, Weinand M, Fiala M (2002) Human immunodeficiency virus type 1 enters brain microvascular endothelia by macropinocytosis dependent on lipid rafts and the mitogen-activated protein kinase signaling pathway. J Virol 76:6689-6700.

Liu Y, Jones M, Hingtgen CM, Bu G, Laribee N, Tanzi RE, Moir RD, Nath A, He JJ (2000) Uptake of HIV-1 tat protein mediated by low-density lipoprotein receptor-related protein disrupts the neuronal metabolic balance of the receptor ligands. Nat Med 6:1380-1387.

Lo Giudice M, Neri M, Falco M, Sturnio M, Calzolari E, Di Benedetto D, Fichera M (2006) A missense mutation in the coiled-coil domain of the KIF5A gene and late-onset hereditary spastic paraplegia. Arch Neurol 63:284-287.

Loberg EM, Brorson SH, Skjorten F, Torvik A (1992) Neuronal uptake of plasma proteins in cryogenic brain lesions. An immunoelectron microscopic study. Apmis 100:1033-1040.

Lucas M, Stuart LM, Zhang A, Hodivala-Dilke K, Febbraio M, Silverstein R, Savill J, Lacy-Hulbert A (2006) Requirements for apoptotic cell contact in regulation of macrophage responses. J Immunol 177:4047-4054.

Mandelkow E, Mandelkow EM (2002) Kinesin motors and disease. Trends Cell Biol 12:585-591.

Manders EMM, Verbeek, F.J., Aten, J.A. (1993) Measurement of co-localization of objects in dual-color confocal images Journal of Microscopy 169:375-382.

Manes S, del Real G, Lacalle RA, Lucas P, Gomez-Mouton C, Sanchez-Palomino S, Delgado R, Alcami J, Mira E, Martinez AC (2000) Membrane raft microdomains mediate lateral assemblies required for HIV-1 infection. EMBO Rep 1:190-196.

Marcondes MC, Burudi EM, Huitron-Resendiz S, Sanchez-Alavez M, Watry D, Zandonatti M, Henriksen SJ, Fox HS (2001) Highly activated CD8(+) T cells in the brain correlate with early central nervous system dysfunction in simian immunodeficiency virus infection. J Immunol 167:5429-5438.

Masliah E, Heaton RK, Marcotte TD, Ellis RJ, Wiley CA, Mallory M, Achim CL, McCutchan JA, Nelson JA, Atkinson JH, Grant I (1997) Dendritic injury is a pathological substrate for human immunodeficiency virus-related cognitive disorders. HNRC Group. The HIV Neurobehavioral Research Center. Ann Neurol 42:963-972.

Maung R, Medders KE, Sejbuk NE, Desai MK, Russo R, Kaul M (2012) Genetic knockouts suggest a critical role for HIV co-receptors in models of HIV gp120-induced brain injury. J Neuroimmune Pharmacol 7:306-318.

McArthur JC (2004) HIV dementia: an evolving disease. J Neuroimmunol 157:3-10.

McArthur JC, Brew BJ, Nath A (2005) Neurological complications of HIV infection. Lancet Neurol 4:543-555.

McQuarrie IG, Brady ST, Lasek RJ (1989) Retardation in the slow axonal transport of cytoskeletal elements during maturation and aging. Neurobiol Aging 10:359-365.

Medders KE, Sejbuk NE, Maung R, Desai MK, Kaul M (2010) Activation of p38 MAPK is required in monocytic and neuronal cells for HIV glycoprotein 120-induced neurotoxicity. J Immunol 185:4883-4895.

Medina I, Ghose S, Ben-Ari Y (1999) Mobilization of intracellular calcium stores participates in the rise of [Ca2+]i and the toxic actions of the HIV coat protein GP120. Eur J Neurosci 11:1167-1178.

Melli G, Keswani SC, Fischer A, Chen W, Hoke A (2006) Spatially distinct and functionally independent mechanisms of axonal degeneration in a model of HIV-associated sensory neuropathy. Brain 129:1330-1338.

Meucci O, Miller RJ (1996) gp120-induced neurotoxicity in hippocampal pyramidal neuron cultures: protective action of TGF-beta1. J Neurosci 16:4080-4088.

Meucci O, Fatatis A, Simen AA, Bushell TJ, Gray PW, Miller RJ (1998) Chemokines regulate hippocampal neuronal signaling and gp120 neurotoxicity. Proc Natl Acad Sci U S A 95:14500-14505.

Michalak Z, Lebrun A, Di Miceli M, Rousset MC, Crespel A, Coubes P, Henshall DC, Lerner-Natoli M, Rigau V (2012) IgG leakage may contribute to neuronal dysfunction in drug-refractory epilepsies with blood-brain barrier disruption. J Neuropathol Exp Neurol 71:826-838.

Michaud J, Fajardo R, Charron G, Sauvageau A, Berrada F, Ramla D, Dilhuydy H, Robitaille Y, Kessous-Elbaz A (2001) Neuropathology of NFHgp160 transgenic mice expressing HIV-1 env protein in neurons. J Neuropathol Exp Neurol 60:574-587.

Millan J, Cerny J, Horejsi V, Alonso MA (1999) CD4 segregates into specific detergent-resistant T-cell membrane microdomains. Tissue Antigens 53:33-40.

Milligan ED, Mehmert KK, Hinde JL, Harvey LO, Martin D, Tracey KJ, Maier SF, Watkins LR (2000) Thermal hyperalgesia and mechanical allodynia produced by intrathecal administration of the human immunodeficiency virus-1 (HIV-1) envelope glycoprotein, gp120. Brain Res 861:105-116.

Milligan ED, O'Connor KA, Armstrong CB, Hansen MK, Martin D, Tracey KJ, Maier SF, Watkins LR (2001) Systemic administration of CNI-1493, a p38 mitogen-activated protein kinase inhibitor, blocks intrathecal human immunodeficiency virus-1 gp120-induced enhanced pain states in rats. J Pain 2:326-333.

Misse D, Cerutti M, Noraz N, Jourdan P, Favero J, Devauchelle G, Yssel H, Taylor N, Veas F (1999) A CD4-independent interaction of human immunodeficiency virus-1 gp120 with CXCR4 induces their cointernalization, cell signaling, and T-cell chemotaxis. Blood 93:2454-2462.

Misse D, Esteve PO, Renneboog B, Vidal M, Cerutti M, St Pierre Y, Yssel H, Parmentier M, Veas F (2001) HIV-1 glycoprotein 120 induces the MMP-9 cytopathogenic factor production that is abolished by inhibition of the p38 mitogen-activated protein kinase signaling pathway. Blood 98:541-547.

Mitsuhashi S, Shima H, Li Y, Tanuma N, Okamoto T, Kikuchi K, Ubukata M (2008) Tautomycetin suppresses the TNFalpha/NF-kappaB pathway via inhibition of IKK activation. Int J Oncol 33:1027-1035.

Miyauchi K, Kim Y, Latinovic O, Morozov V, Melikyan GB (2009) HIV enters cells via endocytosis and dynamin-dependent fusion with endosomes. Cell 137:433-444.

Mocchetti I, Campbell LA, Harry GJ, Avdoshina V (2012) When Human Immunodeficiency Virus Meets Chemokines and Microglia: Neuroprotection or Neurodegeneration? J Neuroimmune Pharmacol.

Mocchetti I, Bachis A, Avdoshina V (2012) Neurotoxicity of human immunodeficiency virus-1: viral proteins and axonal transport. Neurotox Res 21:79-89.

Mondor I, Ugolini S, Sattentau QJ (1998) Human immunodeficiency virus type 1 attachment to HeLa CD4 cells is CD4 independent and gp120 dependent and requires cell surface heparans. J Virol 72:3623-3634.

Morfini G, Pigino G, Brady ST (2005) Polyglutamine expansion diseases: failing to deliver. Trends Mol Med 11:64-70.

Morfini G, Pigino G, Brady ST (2007a) Approaches to kinesin-1 phosphorylation. Methods Mol Biol 392:51-69.

Morfini G, Szebenyi G, Richards B, Brady ST (2001) Regulation of kinesin: implications for neuronal development. Developmental neuroscience 23:364-376.

Morfini G, Pigino G, Beffert U, Busciglio J, Brady ST (2002a) Fast axonal transport misregulation and Alzheimer's disease. Neuromolecular medicine 2:89-99.

Morfini G, Szebenyi G, Elluru R, Ratner N, Brady ST (2002b) Glycogen synthase kinase 3 phosphorylates kinesin light chains and negatively regulates kinesin-based motility. Embo J 21:281-293.

Morfini G, Pigino G, Szebenyi G, You Y, Pollema S, Brady ST (2006) JNK mediates pathogenic effects of polyglutamine-expanded androgen receptor on fast axonal transport. Nat Neurosci 9:907-916.

Morfini G, Szebenyi G, Brown H, Pant HC, Pigino G, DeBoer S, Beffert U, Brady ST (2004) A novel CDK5-dependent pathway for regulating GSK3 activity and kinesin-driven motility in neurons. Embo J 23:2235-2245.

Morfini G, Pigino G, Opalach K, Serulle Y, Moreira JE, Sugimori M, Llinas RR, Brady ST (2007b) 1-Methyl-4-phenylpyridinium affects fast axonal transport by activation of caspase and protein kinase C. Proc Natl Acad Sci U S A 104:2442-2447.

Morfini G, Stenoin, D.L., Brady, S.T. (2006) Axonal Transport. In: Basic Neurochemistry Molecular, Cellular and Medical Aspects (Siegel GJ, ed). Burlington, MA: Elsevier Academic Press.

Morfini GA, You YM, Pollema SL, Kaminska A, Liu K, Yoshioka K, Bjorkblom B, Coffey ET, Bagnato C, Han D, Huang CF, Banker G, Pigino G, Brady ST (2009a) Pathogenic huntingtin inhibits fast axonal transport by activating JNK3 and phosphorylating kinesin. Nat Neurosci 12:864-871.

Morfini GA, Burns M, Binder LI, Kanaan NM, LaPointe N, Bosco DA, Brown RH, Jr., Brown H, Tiwari A, Hayward L, Edgar J, Nave KA, Garberrn J, Atagi Y, Song Y, Pigino G, Brady ST (2009b) Axonal transport defects in neurodegenerative diseases. The Journal of neuroscience 29:12776-12786.

Morfini GA, Bosco, D.A., Brown, H., Gatto, R., Kaminska, A., Song, Y., Bagnato, C., Berth, S., Marangoni, N., Molla, L., Burns, M., Tiwari, A., Hayward, L.J., Pigino, G., Watterson, D.M., Huang, C.-F., Banker, G., Brown Jr., R.H., Brady, S.T. (2013 (submitted)) Inhibition of Fast Axonal Transport by Pathogenic SOD1 Involves Activation of P38 Map Kinase. EMBO J.

Morgello S, Estanislao L, Simpson D, Geraci A, DiRocco A, Gerits P, Ryan E, Yakoushina T, Khan S, Mahboob R, Naseer M, Dorfman D, Sharp V (2004) HIV-associated distal sensory polyneuropathy in the era of highly active antiretroviral therapy: the Manhattan HIV Brain Bank. Arch Neurol 61:546-551.

Morris JR, Lasek RJ (1984) Monomer-polymer equilibria in the axon: direct measurement of tubulin and actin as polymer and monomer in axoplasm. J Cell Biol 98:2064-2076.

Moyle G (2000) Clinical manifestations and management of antiretroviral nucleoside analog-related mitochondrial toxicity. Clin Ther 22:911-936; discussion 898.

Munch C, Rosenbohm A, Sperfeld AD, Uttner I, Reske S, Krause BJ, Sedlmeier R, Meyer T, Hanemann CO, Stumm G, Ludolph AC (2005) Heterozygous R1101K mutation of the DCTN1 gene in a family with ALS and FTD. Ann Neurol 58:777-780.

Munoz L, Ralay Ranaivo H, Roy SM, Hu W, Craft JM, McNamara LK, Chico LW, Van Eldik LJ, Watterson DM (2007) A novel p38 alpha MAPK inhibitor suppresses brain proinflammatory cytokine up-regulation and attenuates synaptic dysfunction and behavioral deficits in an Alzheimer's disease mouse model. J Neuroinflammation 4:21.

Nagano I, Shapshak P, Yoshioka M, Xin K, Nakamura S, Bradley WG (1996) Increased NADPH-diaphorase reactivity and cytokine expression in dorsal root ganglia in acquired immunodeficiency syndrome. J Neurol Sci 136:117-128.

Nakamoto BK, McMurtray A, Davis J, Valcour V, Watters MR, Shiramizu B, Chow DC, Kallianpur K, Shikuma CM (2010) Incident neuropathy in HIV-infected patients on HAART. AIDS Res Hum Retroviruses 26:759-765.

Nath A (2002) Human immunodeficiency virus (HIV) proteins in neuropathogenesis of HIV dementia. J Infect Dis 186 Suppl 2:S193-198.

Nath BM, Schumann KE, Boyer JD (2000) The chimpanzee and other non-human-primate models in HIV-1 vaccine research. Trends Microbiol 8:426-431.

Nguyen DH, Giri B, Collins G, Taub DD (2005) Dynamic reorganization of chemokine receptors, cholesterol, lipid rafts, and adhesion molecules to sites of CD4 engagement. Exp Cell Res 304:559-569.

Oh SB, Tran PB, Gillard SE, Hurley RW, Hammond DL, Miller RJ (2001) Chemokines and glycoprotein120 produce pain hypersensitivity by directly exciting primary nociceptive neurons. The Journal of neuroscience 21:5027-5035.

Oh SK, Cruikshank WW, Raina J, Blanchard GC, Adler WH, Walker J, Kornfeld H (1992) Identification of HIV-1 envelope glycoprotein in the serum of AIDS and ARC patients. J Acquir Immune Defic Syndr 5:251-256.

Okamoto S, Kang YJ, Brechtel CW, Siviglia E, Russo R, Clemente A, Harrop A, McKercher S, Kaul M, Lipton SA (2007) HIV/gp120 decreases adult neural progenitor cell proliferation via checkpoint kinase-mediated cell-cycle withdrawal and G1 arrest. Cell Stem Cell 1:230-236.

Pandey V, Bolsover SR (2000) Immediate and neurotoxic effects of HIV protein gp120 act through CXCR4 receptor. Biochem Biophys Res Commun 274:212-215.

Pardo CA, McArthur JC, Griffin JW (2001) HIV neuropathy: insights in the pathology of HIV peripheral nerve disease. Journal of the peripheral nervous system 6:21-27.

Parton RG, Simons K, Dotti CG (1992) Axonal and dendritic endocytic pathways in cultured neurons. J Cell Biol 119:123-137.

Paschal BM, Vallee RB (1987) Retrograde transport by the microtubule-associated protein MAP 1C. Nature 330:181-183.

Paschal BM, Shpetner HS, Vallee RB (1987) MAP 1C is a microtubule-activated ATPase which translocates microtubules in vitro and has dynein-like properties. J Cell Biol 105:1273-1282.

Peluso R, Haase A, Stowring L, Edwards M, Ventura P (1985) A Trojan Horse mechanism for the spread of visna virus in monocytes. Virology 147:231-236.

Phillips TJ, Cherry CL, Cox S, Marshall SJ, Rice AS (2010) Pharmacological treatment of painful HIV-associated sensory neuropathy: a systematic review and meta-analysis of randomised controlled trials. PLoS One 5:e14433.

Pigino G, Morfini G, Pelsman A, Mattson MP, Brady ST, Busciglio J (2003) Alzheimer's presenilin 1 mutations impair kinesin-based axonal transport. The Journal of neuroscience 23:4499-4508.

Pigino G, Morfini G, Atagi Y, Deshpande A, Yu C, Jungbauer L, LaDu M, Busciglio J, Brady S (2009) Disruption of fast axonal transport is a pathogenic mechanism for intraneuronal amyloid beta. Proc Natl Acad Sci U S A 106:5907-5912.

Politi C, Del Turco D, Sie JM, Golinski PA, Tegeder I, Deller T, Schultz C (2008) Accumulation of phosphorylated I kappaB alpha and activated IKK in nodes of Ranvier. Neuropathol Appl Neurobiol 34:357-365.

Popik W, Alce TM, Au WC (2002) Human immunodeficiency virus type 1 uses lipid raft-colocalized CD4 and chemokine receptors for productive entry into CD4(+) T cells. J Virol 76:4709-4722.

Popovic M, Sarngadharan MG, Read E, Gallo RC (1984) Detection, isolation, and continuous production of cytopathic retroviruses (HTLV-III) from patients with AIDS and pre-AIDS. Science 224:497-500.

Potash MJ, Chao W, Bentsman G, Paris N, Saini M, Nitkiewicz J, Belem P, Sharer L, Brooks AI, Volsky DJ (2005) A mouse model for study of systemic HIV-1 infection, antiviral immune responses, and neuroinvasiveness. Proc Natl Acad Sci U S A 102:3760-3765.

Pulliam L, Herndier BG, Tang NM, McGrath MS (1991) Human immunodeficiency virus-infected macrophages produce soluble factors that cause histological and neurochemical alterations in cultured human brains. J Clin Invest 87:503-512.

Pulliam L, Gascon R, Stubblebine M, McGuire D, McGrath MS (1997) Unique monocyte subset in patients with AIDS dementia. Lancet 349:692-695.

Puls I, Jonnakuty C, LaMonte BH, Holzbaur EL, Tokito M, Mann E, Floeter MK, Bidus K, Drayna D, Oh SJ, Brown RH, Jr., Ludlow CL, Fischbeck KH (2003) Mutant dynactin in motor neuron disease. Nat Genet 33:455-456.

Puls I, Oh SJ, Sumner CJ, Wallace KE, Floeter MK, Mann EA, Kennedy WR, Wendelschafer-Crabb G, Vortmeyer A, Powers R, Finnegan K, Holzbaur EL, Fischbeck KH, Ludlow CL (2005) Distal spinal and bulbar muscular atrophy caused by dynactin mutation. Ann Neurol 57:687-694.

Rance NE, McArthur JC, Cornblath DR, Landstrom DL, Griffin JW, Price DL (1988) Gracile tract degeneration in patients with sensory neuropathy and AIDS. Neurology 38:265-271.

Rao JS, Kim HW, Kellom M, Greenstein D, Chen M, Kraft AD, Harry GJ, Rapoport SI, Basselin M (2011) Increased neuroinflammatory and arachidonic acid cascade

markers, and reduced synaptic proteins, in brain of HIV-1 transgenic rats. J Neuroinflammation 8:101.

Reid E, Kloos M, Ashley-Koch A, Hughes L, Bevan S, Svenson IK, Graham FL, Gaskell PC, Dearlove A, Pericak-Vance MA, Rubinsztein DC, Marchuk DA (2002) A kinesin heavy chain (KIF5A) mutation in hereditary spastic paraplegia (SPG10). Am J Hum Genet 71:1189-1194.

Reid W et al. (2001) An HIV-1 transgenic rat that develops HIV-related pathology and immunologic dysfunction. Proc Natl Acad Sci U S A 98:9271-9276.

Ren PH, Lauckner JE, Kachirskaia I, Heuser JE, Melki R, Kopito RR (2009) Cytoplasmic penetration and persistent infection of mammalian cells by polyglutamine aggregates. Nature cell biology 11:219-225.

Rigau V, Morin M, Rousset MC, de Bock F, Lebrun A, Coubes P, Picot MC, Baldy-Moulinier M, Bockaert J, Crespel A, Lerner-Natoli M (2007) Angiogenesis is associated with blood-brain barrier permeability in temporal lobe epilepsy. Brain 130:1942-1956.

Riviere JB et al. (2011) KIF1A, an axonal transporter of synaptic vesicles, is mutated in hereditary sensory and autonomic neuropathy type 2. Am J Hum Genet 89:219-230.

Robinson B, Li Z, Nath A (2007) Nucleoside reverse transcriptase inhibitors and human immunodeficiency virus proteins cause axonal injury in human dorsal root ganglia cultures. J Neurovirol 13:160-167.

Roy S, Zhang B, Lee VM, Trojanowski JQ (2005) Axonal transport defects: a common theme in neurodegenerative diseases. Acta Neuropathol 109:5-13.

Runnegar MT, Wei X, Hamm-Alvarez SF (1999) Increased protein phosphorylation of cytoplasmic dynein results in impaired motor function. Biochem J 342 (Pt 1):1-6.

Ryan LA, Zheng J, Brester M, Bohac D, Hahn F, Anderson J, Ratanasuwan W, Gendelman HE, Swindells S (2001) Plasma levels of soluble CD14 and tumor necrosis factor-alpha type II receptor correlate with cognitive dysfunction during human immunodeficiency virus type 1 infection. J Infect Dis 184:699-706.

Sagot Y, Vejsada R, Kato AC (1997) Clinical and molecular aspects of motoneurone diseases: animal models, neurotrophic factors and Bcl-2 oncoprotein. Trends Pharmacol Sci 18:330-337.

Sakurai H (2012) Targeting of TAK1 in inflammatory disorders and cancer. Trends Pharmacol Sci 33:522-530.

Salata MW, Dillman JF, 3rd, Lye RJ, Pfister KK (2001) Growth factor regulation of cytoplasmic dynein intermediate chain subunit expression preceding neurite extension. J Neurosci Res 65:408-416.

Sanchez-Alavez M, Criado J, Gomez-Chavarin M, Jimenez-Anguiano A, Navarro L, Diaz-Ruiz O, Galicia O, Sanchez-Narvaez F, Murillo-Rodriguez E, Henriksen SJ, Elder JH, Prospero-Garcia O (2000) HIV- and FIV-derived gp120 alter spatial memory, LTP, and sleep in rats. Neurobiol Dis 7:384-394.

Schifitto G, McDermott MP, McArthur JC, Marder K, Sacktor N, McClernon DR, Conant K, Cohen B, Epstein LG, Kieburtz K (2005) Markers of immune activation and viral load in HIV-associated sensory neuropathy. Neurology 64:842-848.

Schneider J, Kaaden O, Copeland TD, Oroszlan S, Hunsmann G (1986) Shedding and interspecies type sero-reactivity of the envelope glycopolypeptide gp120 of the human immunodeficiency virus. J Gen Virol 67 (Pt 11):2533-2538.

Schroer TA (2004) Dynactin. Annu Rev Cell Dev Biol 20:759-779.

Schultz C, Konig HG, Del Turco D, Politi C, Eckert GP, Ghebremedhin E, Prehn JH, Kogel D, Deller T (2006) Coincident enrichment of phosphorylated IkappaBalpha, activated IKK, and phosphorylated p65 in the axon initial segment of neurons. Mol Cell Neurosci 33:68-80.

Schupbach J, Popovic M, Gilden RV, Gonda MA, Sarngadharan MG, Gallo RC (1984) Serological analysis of a subgroup of human T-lymphotropic retroviruses (HTLV-III) associated with AIDS. Science 224:503-505.

Serulle Y, Morfini G, Pigino G, Moreira JE, Sugimori M, Brady ST, Llinas RR (2007) 1-Methyl-4-phenylpyridinium induces synaptic dysfunction through a pathway involving caspase and PKCdelta enzymatic activities. Proc Natl Acad Sci U S A 104:2437-2441.

Simons K, Ikonen E (1997) Functional rafts in cell membranes. Nature 387:569-572.

Simpson DM, Haidich AB, Schifitto G, Yiannoutsos CT, Geraci AP, McArthur JC, Katzenstein DA (2002) Severity of HIV-associated neuropathy is associated with plasma HIV-1 RNA levels. Aids 16:407-412.

Singh IN, El-Hage N, Campbell ME, Lutz SE, Knapp PE, Nath A, Hauser KF (2005) Differential involvement of p38 and JNK MAP kinases in HIV-1 Tat and gp120-induced apoptosis and neurite degeneration in striatal neurons. Neuroscience 135:781-790.

Singh IN, Goody RJ, Dean C, Ahmad NM, Lutz SE, Knapp PE, Nath A, Hauser KF (2004) Apoptotic death of striatal neurons induced by human immunodeficiency

virus-1 Tat and gp120: Differential involvement of caspase-3 and endonuclease G. J Neurovirol 10:141-151.

Song H, Endow SA (1998) Decoupling of nucleotide- and microtubule-binding sites in a kinesin mutant. Nature 396:587-590.

Stein BS, Gowda SD, Lifson JD, Penhallow RC, Bensch KG, Engleman EG (1987) pH-independent HIV entry into CD4-positive T cells via virus envelope fusion to the plasma membrane. Cell 49:659-668.

Stenoien DL, Brady ST (1997) Immunochemical analysis of kinesin light chain function. Mol Biol Cell 8:675-689.

Susalka SJ, Pfister KK (2000) Cytoplasmic dynein subunit heterogeneity: implications for axonal transport. J Neurocytol 29:819-829.

Susalka SJ, Hancock WO, Pfister KK (2000) Distinct cytoplasmic dynein complexes are transported by different mechanisms in axons. Biochim Biophys Acta 1496:76-88.

Szebenyi G, Morfini GA, Babcock A, Gould M, Selkoe K, Stenoien DL, Young M, Faber PW, MacDonald ME, McPhaul MJ, Brady ST (2003) Neuropathogenic forms of huntingtin and androgen receptor inhibit fast axonal transport. Neuron 40:41-52.

Tai HC, Schuman EM (2008) Ubiquitin, the proteasome and protein degradation in neuronal function and dysfunction. Nat Rev Neurosci 9:826-838.

Takekawa M, Tatebayashi K, Saito H (2005) Conserved docking site is essential for activation of mammalian MAP kinase kinases by specific MAP kinase kinase kinases. Mol Cell 18:295-306.

Tan IL, McArthur JC (2012) HIV-associated neurological disorders: a guide to pharmacotherapy. CNS Drugs 26:123-134.

Thomas ER, Dunfee RL, Stanton J, Bogdan D, Taylor J, Kunstman K, Bell JE, Wolinsky SM, Gabuzda D (2007) Macrophage entry mediated by HIV Envs from brain and lymphoid tissues is determined by the capacity to use low CD4 levels and overall efficiency of fusion. Virology 360:105-119.

Toggas SM, Masliah E, Rockenstein EM, Rall GF, Abraham CR, Mucke L (1994) Central nervous system damage produced by expression of the HIV-1 coat protein gp120 in transgenic mice. Nature 367:188-193.

Trushin SA, Algeciras-Schimnich A, Vlahakis SR, Bren GD, Warren S, Schnepple DJ, Badley AD (2007) Glycoprotein 120 binding to CXCR4 causes p38-dependent primary T cell death that is facilitated by, but does not require cell-associated CD4. J Immunol 178:4846-4853.

Tsai MY, Morfini G, Szebenyi G, Brady ST (2000) Release of kinesin from vesicles by hsc70 and regulation of fast axonal transport. Mol Biol Cell 11:2161-2173.

Ugolini S, Mondor I, Sattentau QJ (1999) HIV-1 attachment: another look. Trends Microbiol 7:144-149.

Vallee RB, Wall JS, Paschal BM, Shpetner HS (1988) Microtubule-associated protein 1C from brain is a two-headed cytosolic dynein. Nature 332:561-563.

Van Duyne R, Pedati C, Guendel I, Carpio L, Kehn-Hall K, Saifuddin M, Kashanchi F (2009) The utilization of humanized mouse models for the study of human retroviral infections. Retrovirology 6:76.

Viard M, Parolini I, Sargiacomo M, Fecchi K, Ramoni C, Ablan S, Ruscetti FW, Wang JM, Blumenthal R (2002) Role of cholesterol in human immunodeficiency virus type 1 envelope protein-mediated fusion with host cells. J Virol 76:11584-11595.

Vidricaire G, Gauthier S, Tremblay MJ (2007) HIV-1 infection of trophoblasts is independent of gp120/CD4 Interactions but relies on heparan sulfate proteoglycans. J Infect Dis 195:1461-1471.

Vivithanaporn P, Heo G, Gamble J, Krentz HB, Hoke A, Gill MJ, Power C (2010) Neurologic disease burden in treated HIV/AIDS predicts survival: a population-based study. Neurology 75:1150-1158.

Waetzig V, Herdegen T (2005) Context-specific inhibition of JNKs: overcoming the dilemma of protection and damage. Trends Pharmacol Sci 26:455-461.

Wagner MC, Pfister KK, Bloom GS, Brady ST (1989) Copurification of kinesin polypeptides with microtubule-stimulated Mg-ATPase activity and kinetic analysis of enzymatic properties. Cell Motil Cytoskeleton 12:195-215.

Wallace VC, Blackbeard J, Pheby T, Segerdahl AR, Davies M, Hasnie F, Hall S, McMahon SB, Rice AS (2007) Pharmacological, behavioural and mechanistic analysis of HIV-1 gp120 induced painful neuropathy. Pain 133:47-63.

Weedon MN, Hastings R, Caswell R, Xie W, Paszkiewicz K, Antoniadi T, Williams M, King C, Greenhalgh L, Newbury-Ecob R, Ellard S (2011) Exome sequencing identifies a DYNC1H1 mutation in a large pedigree with dominant axonal Charcot-Marie-Tooth disease. Am J Hum Genet 89:308-312.

WHO/UNAIDS/UNICEF (2011) GLOBAL HIV/AIDS RESPONSE: Epidemic update and health sector progress towards Universal Access Progress report 2011. In.

Wilkerson JL, Gentry KR, Dengler EC, Wallace JA, Kerwin AA, Armijo LM, Kuhn MN, Thakur GA, Makriyannis A, Milligan ED (2012) Intrathecal cannabilactone

CB(2)R agonist, AM1710, controls pathological pain and restores basal cytokine levels. Pain 153:1091-1106.

Wozniak MJ, Allan VJ (2006) Cargo selection by specific kinesin light chain 1 isoforms. Embo J 25:5457-5468.

Xu H, Bae M, Tovar-y-Romo LB, Patel N, Bandaru VV, Pomerantz D, Steiner JP, Haughey NJ (2011) The human immunodeficiency virus coat protein gp120 promotes forward trafficking and surface clustering of NMDA receptors in membrane microdomains. J Neurosci 31:17074-17090.

Yi Y, Lee C, Liu QH, Freedman BD, Collman RG (2004) Chemokine receptor utilization and macrophage signaling by human immunodeficiency virus type 1 gp120: Implications for neuropathogenesis. J Neurovirol 10 Suppl 1:91-96.

Yong VW, Rivest S (2009) Taking advantage of the systemic immune system to cure brain diseases. Neuron 64:55-60.

Yoshimi K, Woo M, Son Y, Baudry M, Thompson RF (2002) IgG-immunostaining in the intact rabbit brain: variable but significant staining of hippocampal and cerebellar neurons with anti-IgG. Brain Res 956:53-66.

Yoshioka M, Shapshak P, Srivastava AK, Stewart RV, Nelson SJ, Bradley WG, Berger JR, Rhodes RH, Sun NC, Nakamura S (1994) Expression of HIV-1 and interleukin-6 in lumbosacral dorsal root ganglia of patients with AIDS. Neurology 44:1120-1130.

Zhang Y, Foudi A, Geay JF, Berthebaud M, Buet D, Jarrier P, Jalil A, Vainchenker W, Louache F (2004) Intracellular localization and constitutive endocytosis of CXCR4 in human CD34+ hematopoietic progenitor cells. Stem Cells 22:1015-1029.

Zhao C, Takita J, Tanaka Y, Setou M, Nakagawa T, Takeda S, Yang HW, Terada S, Nakata T, Takei Y, Saito M, Tsuji S, Hayashi Y, Hirokawa N (2001) Charcot-Marie-Tooth disease type 2A caused by mutation in a microtubule motor KIF1Bbeta. Cell 105:587-597.

Zheng J, Ghorpade A, Niemann D, Cotter RL, Thylin MR, Epstein L, Swartz JM, Shepard RB, Liu X, Nukuna A, Gendelman HE (1999) Lymphotropic virions affect chemokine receptor-mediated neural signaling and apoptosis: implications for human immunodeficiency virus type 1-associated dementia. J Virol 73:8256-8267.

Zheng W, Ouyang H, Zheng X, Liu S, Mata M, Fink DJ, Hao S (2011) Glial TNFalpha in the spinal cord regulates neuropathic pain induced by HIV gp120 application in rats. Mol Pain 7:40.

VITA

Sarah Berth

Address:
Department of Anatomy and Cell Biology
University of Illinois at Chicago
808 S. Wood St. M/C512 Chicago, IL 60612
312-413-8581

EDUCATION:

B.A., Northwestern University, Evanston, IL 2004
Biological sciences, emphasis in neurobiology

M.D., Ph.D., University of Illinois at Chicago, Chicago, IL 2015
Neuroscience program
Department of Anatomy and Cell Biology
Dissertation: Mechanisms of Fast Axonal Transport Impairment by the HIV Glycoprotein gp120

PROFESSIONAL EXPERIENCE:

Lab Aide 2001-2004
Lab of Aryeh Routtenberg
Dept. of Psychology
Northwestern University

Hospital Volunteer 2003
Evanston Northwestern Hospital
fall semester

Independent Research 2003-2004
Lab of Aryeh Routtenberg
Dept. of Psychology
Northwestern University

Research technician 2004-2005
Lab of Aryeh Routtenberg
Dept. of Psychology
Northwestern University

Medical Volunteer 2006-present
Student Run Free Clinic at Community Health
University of Illinois at Chicago
College of Medicine

Monthly volunteer from 2007-2010 for
Clinical Connections

Medical Scientist Training Program Student Advisory Committee 2008-2011
University of Illinois at Chicago
College of Medicine, MSTP program

Graduate Student Mentor at Brain Awareness Day 2009,2011
University of Illinois at Chicago
Neuroscience program

Fundraising Chair: MSTP Soiree & Silent Auction to benefit the Student Run Free Clinic 2010
University of Illinois at Chicago
College of Medicine, MSTP program

Medical Scientist Training Program Admissions Committee Member 2012
University of Illinois at Chicago
College of Medicine, MSTP program

HONORS AND AWARDS

Rogel Scholarship 2000
University of Michigan

National Society of Collegiate Scholars member 2001
University of Michigan

Dean's list 2003
Northwestern University, spring semester

Chi Omega Order of the Owl 2003
Award for GPA, Northwestern University

Erwin Macey Research Fellowship 2003
Research fellowship for the summer of 2003
Northwestern University

Training Grant in the Neuroscience of Mental Health T32MH067631 2008-2009
Neuroscience program
University of Illinois-Chicago

Physician Scientist Career Conference Travel Award 2009
NINDS, AUPN, ANA, and CNS
Invitation and travel award to a physician scientist mentoring workshop in Washington, D.C.

Tanja Andric Scholarship 2009
Scholarship for medical students pursuing research
University of Illinois at Chicago College of Medicine

Graduate Council Travel Award 2009-2012
University of Illinois at Chicago

Graduate College Presenter's Award 2009-2012
University of Illinois at Chicago

Young Investigator Educational Enhancement Award 2011
American Society of Neurochemistry
Travel award to present research at the ASN annual conference

Dean's Scholar Award 2011
University of Illinois at Chicago
Graduate College

Central for Clinical and Translational Science PECTS Fellow 2011-2013
Center for Clinical and Translational Science
University of Illinois-Chicago
Pre-doctoral Education for Clinical and Translational Science Fellowship

Investigator-in-Training Award 2012
International Society of Neurovirology
Travel award to present research at the ISNV annual conference

PROFESSIONAL MEMBERSHIPS

American Society for the Advancement of Science
American Society for Neurochemistry
Society for Neuroscience
American Physician Scientist Association
International Society of Neurovirology
Radiological Society of North America

ABSTRACTS

Routtenberg, A., Rekart, J.L**.**, Sandoval, J., **Hatch, S.**, Kimble, R. (2003). Rat, Yes . . . Mouse, No: water maze training leads to axonal growth in the hippocampus. *Soc. Neurosci. Abstr.* 29, Program No: 717.17

Rekart, J.L., Sandoval, J., **Hatch, S.**, Bermúdez-Rattoni, F. and Routtenberg, A. (2003) Training induces expression of a brain growth protein in dentate gyrus granule cells as well as sprouting of mossy fiber axons. *Soc. Neurosci. Abstr.* 29, Program No: 860.15

Rekart, J.L., **Hatch, S.**, Routtenberg, A. (2004). Are there two distinct hippocampal granule cell locations? Evidence from *non*-immunocolocalization of GAP-43, zinc transporter and synaptophysin in mossy fibers. *Soc. Neurosci. Abstr.* 30, Program No: 941.17

Berth, S.H., Morfini, G., Sarma, T., Brady, S.T. (2009). The HIV glycoprotein gp120 impairs fast axonal transport. *American Soc. Neurochem Abstr.* PSM01-03.

Berth, S.H., Morfini, G., Sarma, T., Brady, S.T. (2009) Axon-autonomous effects of the HIV glycoprotein gp120 on fast axonal transport. *Soc. Neurosci. Abstr.* Program No: 836.13

Berth, S.H., Morfini, G., Sarma, T., Brady, S.T. (2010). The HIV glycoprotein gp120 activates signaling pathways to impair fast axonal transport. *American Soc. Neurochem Abstr.* PSM01-14.

Berth, S.H., Morfini, G., Sarma, T., Brady, S.T. (2010). The HIV glycoprotein gp120 impairs phosphotransferase regulation of fast axonal transport. *American Soc. Clinical Investigation Abstr.*, 4.

Berth, S.H., Morfini, G., Sarma, T., Brady, S.T. (2010). The HIV glycoprotein gp120 dysregulates fast axonal transport through an axon-autonomous mechanism. *Soc. Neurosci. Abstr.* Session No: 224.

Berth, S.H., Morfini, G., Sarma, T., Brady, S.T. (2011). Axon-specific mechanisms of neurotoxicity of gp120. *American Soc. Neurochem Abstr.* PSM05-02

Berth, S.H., Morfini, G., Sarma, T., Brady, S.T. (2012). The HIV glycoprotein gp120 impairs fast axonal transport. *National Clinical and Translational Sciences Predoctoral Meeting*

Berth, S.H., Morfini, G., Sarma, T., Brady, S.T. (2012). The HIV glycoprotein

gp120 impairs fast axonal transport through an axon-autonomous mechanism. *International Soc Neurovirol Abstr*. P28.

PUBLICATIONS

Berth, S.H., Leopold, P., Morfini, G. (2009). Virus-induced neuronal dysfunction and degeneration. *Front Biosci*. 14: 5239-59.

Hennigan, R.F., Moon, C.A., Parysek, L.M., Monk, K.R., Morfini, G., **Berth, S.**, Brady, S., Ratner, N. (2012) The NF2 tumor suppressor regulates microtubule-based vesicle trafficking via a novel Rac, MLK and p38 SAPK pathway. Oncogene doi:10.1038/onc.2012.135 (2012).

G.A. Morfini, D.A. Bosco, H. Brown, R.Gatto, A. Kaminska, Y. Song, C. Bagnato, **S. Berth**, N. Marangoni, L. Molla, M. Burns, A. Tiwari, L. J. Hayward, G. Pigino., D. M. Watterson, C.-F. Huang, G. Banker, R.H. Brown Jr., and S.T. Brady (2012) Inhibition of Fast Axonal Transport by Pathogenic SOD1 Involves Activation of P38 Map Kinase. Embo J. (submitted January 2013)

Berth, S.H., Morfini, G., Brady, S.T. Mechanisms of internalization and transport of the HIV glycoprotein gp120. (in preparation)

Berth, S.H., Morfini, G., Atagi, Y., Brady, S.T. The HIV glycoprotein gp120 impairs fast axonal transport via dysregulation of regulatory signaling cascades. (in preparation)

APPENDIX

ASN Neuro Copyright Permission Statement